Exceptional Event Demonstration for Ozone Exceedances in Clark County, Nevada – June 26, 2020

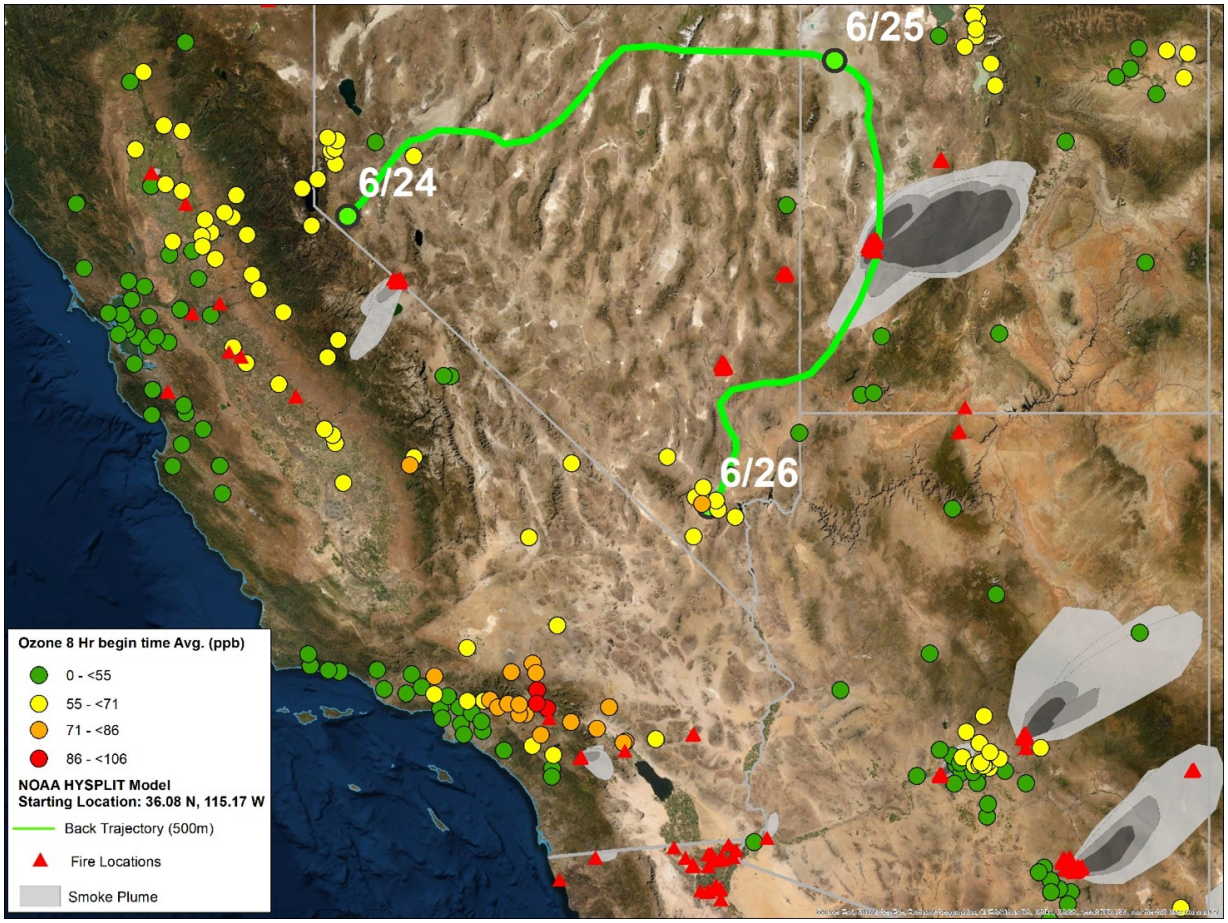

Final Report Prepared for

U.S. EPA Region 9
San Francisco, CA

July 2021

STi | Sonoma Technology

This document contains blank pages to accommodate two-sided printing.

Exceptional Event Demonstration for Ozone Exceedances in Clark County, Nevada – June 26, 2020

Prepared by

Steve Brown, PhD
Crystal McClure, PhD
Cari Gostic
David Miller, PhD
Nathan Pavlovic
Charles Scarborough

Sonoma Technology
1450 N. McDowell Blvd., Suite 200
Petaluma, CA 94954
Ph 707.665.9900 | F 707.665.9800
sonomatech.com

Prepared for

Clark County Department of Environment and Sustainability
Division of Air Quality
4701 W. Russell Road, Suite 200
Las Vegas, NV 89118
Ph 702.455.3206
www.clarkcountynv.gov

Final Report

STI-920053-7477

July 1, 2021

Cover graphic illustrates 48-hour HYSPLIT back trajectories with smoke from the Las Vegas Valley, ending on June 26, 2020. See Section 3.1.3 for more information.

Contents

Figures

Tables

Executive Summary

On June 26, 2020, Clark County experienced an atypical episode of elevated ambient ozone. During this episode, the 2015 8-hr ozone National Ambient Air Quality Standards (NAAQS) thresholds were exceeded at the Paul Meyer monitoring site. The exceedance at the Paul Meyer site could lead to an ozone nonattainment designation for the Clark County area. Air trajectory analysis and air quality modeling results show that emissions from wildfires burning in southwestern Utah and southern Nevada (north of Clark County) contributed to the transport to and formation of ozone in Clark County. The U.S. Environmental Protection Agency (EPA) Exceptional Event Rule (U.S. Environmental Protection Agency, 2016a) allows air agencies to omit air quality data from the design value calculation if it can be demonstrated that the measurement in question was caused by an exceptional event. This report describes analyses that help to establish a clear causal relationship between wildfire smoke and the June 26, 2020, ozone exceedance at the Paul Meyer monitoring site.

The analyses we conducted provide evidence supportive of wildfire smoke and impacts on ozone concentrations in Clark County. We show that (1) smoke was transported from a wildfire in southwestern Utah and from two wildfires north of Clark County in southern Nevada to the surface in the Clark County area in the hours leading up to the exceedance date; (2) wildfire smoke impacted the typical diurnal profiles of ground-level pollution measurements, including CO and $PM_{2.5}$, in the Clark County area on June 26; (3) byproducts and tracers of wildfire combustion were present and elevated at the surface in the Clark County area on the days surrounding June 26; and (4) meteorological regression modeling and similar meteorological day analysis show that ozone observations on June 26 were unusual in the historical record given the meteorological conditions. Sources of evidence used in these analyses include (1) air quality monitor data to show that supporting pollutant trends at the surface were influenced by wildfire smoke; (2) air trajectory analysis to show transport of smoke-laden air to the Clark County area; (3) media coverage of wildfires and smoke impacts; and (4) meteorological regression modeling and meteorologically similar day analysis.

EPA guidance for exceptional event demonstrations (U.S. Environmental Protection Agency, 2016b) provides a three-tiered approach; depending on the complexity of the event, increasingly involved information may be required to demonstrate a causal relationship between wildfire smoke and an exceedance. Here, we provide the results of analyses conducted to address Tier 1, Tier 2, and Tier 3 exceptional event demonstration requirements.

These analyses show that smoke was transported from a wildfire in southwestern Utah and from two wildfires north of Clark County in southern Nevada to the Clark County area over the hours leading up to June 26. Combined with additional evidence, such as meteorological regression modeling and meteorologically similar day analysis, our results provide key evidence to support smoke impacts on ozone concentrations in Clark County on June 26, 2020.

1. Overview

1.1 Introduction

2020 was an unprecedented wildfire season in California and throughout the United States (https://www.fire.ca.gov/media/4jandlhh/top20_acres.pdf; https://www.nifc.gov/fireInfo/fireInfo_statistics.html). Smoke emissions from wildfires in the western U.S. can affect downwind areas, including Clark County, Nevada. This was the case on June 26, 2020, as smoke emissions from the rapidly growing Rock Path Fire in Utah, as well as the Twin and Miller fires just north of Las Vegas, reached Clark County. On this date, one of the ozone (O_3) monitoring locations in Clark County recorded an exceedance of the 2015 National Ambient Air Quality Standard (NAAQS) for 8-hour ozone (0.070 ppm).

Emissions from wildfires can affect concentrations of ozone downwind by direct transport of both ozone and precursor gases (i.e., nitrogen oxides [NO_x] and volatile organic compounds [VOCs]). Each mechanism can enhance the overall ozone concentration and/or the amount of ozone that could be produced. For example, in an area where NO_x concentrations are high, such as an urban area like Las Vegas, Nevada, the transport of VOCs from wildfire emissions can enhance the amount of ozone that can be produced, potentially driving concentrations above the ozone standard. According to U.S. Environmental Protection Agency's (EPA) exceptional event (EE) guidance (U.S. Environmental Protection Agency, 2016), EEs such as wildfires that affect ozone concentrations can be subject to exclusion from calculations of NAAQS attainment if a clear causal relationship can be established between a specific event and the monitoring exceedance.

This report describes the clear causal relationship between the Rock Path Fire (UT), Miller Fire (NV), and Twin Fire (NV) and the exceedance of the maximum daily 8-hour ozone average (MDA8) at the Paul Meyer monitoring site in Clark County on June 26, 2020. The evidence in this report includes all three tiers of analysis required by EPA's exceptional event guidance: for Tier 1, ground and satellite-based measurement of smoke emissions, transport of smoke from the Rock Path Fire, Twin Fire, and Miller Fire to Clark County, and media coverage of the smoke event in Clark County; for Tier 2, emission vs. distance analysis, ground and satellite analysis of smoke-related pollutants, and comparison of event and non-event concentrations; and for Tier 3, meteorologically similar day analyses and statistical Generalized Additive Modeling (GAM) of the event. The wildfires that affected ozone concentrations in Clark County could not be reasonably controlled or prevented because they were caused by lightning (or an unknown source for the Twin Fire) and are unlikely to recur. Table 1-1 lists the MDA8 ozone concentrations at Paul Meyer during this event.

Table 1-1. June 26, 2020, exceptional event information. The monitoring site in Clark County that exceeded the 2015 NAAQS standard on June 26, 2020, is listed, along with the AQS Site Code, location information, and MDA8 ozone concentration.

AQS Site Code	Site Name	Latitude (degrees N)	Longitude (degrees W)	MDA8 O_3 Concentration (ppb)
320030043	Paul Meyer	36.106	-115.253	73

Concurrent with this document, Clark County is submitting documentation for other ozone EEs in 2018 and 2020 that were caused by wildfires and stratospheric intrusions. These events are mentioned throughout this report and are referred to as "proposed 2018 and 2020 exceptional events," recognizing that discussion with EPA is still pending. All proposed EEs for Clark County in 2018 and 2020 are listed in Tables 1-2 and 1-3. Wherever possible, we calculated statistics to provide context that both includes and excludes the proposed EEs from 2018 and 2020.

Table 1-2. Proposed Clark County 2018 exceptional events. For each site and date combination where the 2015 NAAQS standard was exceeded, the MDA8 ozone concentration is shown in parts per billion (ppb). Blank cells indicate that there was no exceedance on that site/date combination.

Date	Paul Meyer	Walter Johnson	Green Valley	Jerome Mack	Joe Neal	Palo Verde	Jean	Indian Springs	Apex	Boulder City
6/19/2018	72	72	77	75						
6/20/2018	71	74			72					
6/23/2018	72	76	75	72	72	71	77	73		
6/27/2018	75	76	78	76	72	72	81	78	74	72
7/14/2018	72		78	78						
7/15/2018		71	73	73	78					
7/16/2018	75	79	71	73	80	75				
7/17/2018	74	77				74				
7/25/2018	71	72	72							
7/26/2018	72	75	77	77					71	
7/27/2018	72	74			76					
7/30/2018			73	72						
7/31/2018		73			73					
8/6/2018	79	77	74	71	76	72			74	
8/7/2018	73	74	72	71	74				71	

Table 1-3. Proposed Clark County 2020 exceptional events. For each site and date combination where the 2015 NAAQS standard was exceeded, the MDA8 ozone concentration is shown in ppb. Blank cells indicate that there was no exceedance on that site/date combination.

Date	Walter Johnson	Paul Meyer	Joe Neal	Jerome Mack	Green Valley	Boulder City	Jean	Indian Springs	Apex
5/6/2020	78	77	76	73	72		75		76
5/9/2020	71	74							
5/28/2020	71	76							
6/22/2020	73	74	78						
6/26/2020		73							
8/3/2020	82	78	81		72	72	73	71	
8/7/2020	71		72					72	
8/18/2020	82	79	78						
8/19/2020	74	74	73		71				
8/20/2020			71						
8/21/2020		71							
9/2/2020	75	73							
9/26/2020	71		75						

1.2 Exceptional Event Rule Summary

The "EPA Guidance on the Preparation of Exceptional Events Demonstration for Wildfire Events that May Influence Ozone Concentrations" (U.S. Environmental Protection Agency, 2016) describes a three-tier analysis approach to determine a "clear causal relationship" for EEs demonstrations from an air agency. A summary of analysis requirements for each tier is listed in Table 1-4 and in the list below.

- Tier 1 analyses can be used when ozone exceedances are clearly influenced by a wildfire in areas of typically low ozone concentrations, are associated with ozone concentrations higher than non-event-related values, or occur outside of an area's usual ozone season.
- Tier 2 analyses are appropriate for wildfire emission cases where the impacts of the wildfire on ozone levels are less clear and require more supportive documentation than Tier 1 analyses.
- If a more complicated relationship between the wildfire and the ozone exceedance is observed, Tier 3 analyses with additional supportive documentation—such as statistical modeling of the ozone event, vertical profile analysis of smoke in the column, and meteorological analysis—should be used.

In this work, we conduct all the recommended Tier 1, Tier 2, and Tier 3 analyses.

Table 1-4. Tier 1, 2, and 3 exceptional event analysis requirements for evaluating wildfire impacts on ozone exceedances.

Tier	Requirements
1	• Comparison of fire-influenced exceedance with historical concentrations • Key factor: Evidence that fire and monitor meet one of the following criteria: – Seasonality differs from typical season, or – Ozone concentrations are 5-10 ppb higher than non-event-related concentrations • Evidence of transport of fire emissions to monitor: – Trajectories of fire emissions (reaching ground level) – Satellite images and supporting evidence from surface measurements – Media coverage and photographic evidence of smoke
2	• All Tier 1 requirements • Key Factor #1: Fire emissions and distance of fires • Key Factor #2: Comparison of the event-related ozone concentration, with non-event-related high ozone concentrations (high percentile rank over five years/seasons) – Annual and seasonal comparison • Evidence that fire emissions affected the monitor (at least one of the following): – Visibility impacts – Changes in supporting measurements – Satellite enhancements of fire-related species (i.e., NO_x, carbon monoxide [CO], aerosol optical depth [AOD], etc.) – Fire-related enhancement ratios and/or tracer species – Differences in spatial/temporal patterns
3	• All Tier 2 requirements • Evidence of fire emissions effects on monitor: – Multiple analyses from those listed for Tier 2 • Evidence of fire emissions transport to the monitor: – Trajectory or satellite plume analysis, and – Additional discussion of meteorological conditions • Additional evidence such as: – Comparison to ozone concentrations on matching (meteorologically similar) days – Statistical regression modeling – Photochemical modeling of smoke contributions to ozone concentrations

1.3 Demonstration Outline

As discussed in Section 1.2, the "clear causal relationship" analyses involve first comparing the exceedance ozone concentrations to historical values, providing evidence that the event and monitors meet the tier's key factors, providing evidence of the transport of wildfire emissions to the

monitors, and additional analyses such as ground-level measurements and various forms of modeling depending on the complexity of the event. Table 1-5 summarizes the key factors and additional supporting evidence of the tiered approach and shows the corresponding sections in this report for each analysis.

Table 1-5. Locations of Tier 1, 2, and 3 elements in this report.

Tier	Element	Section of This Report (Analysis Type)
Tier 1	Key Factor: seasonality differs from typical season and/or ozone concentrations are 5-10 ppb higher than non-event-related concentrations	Section 3.1.1 (comparison of event with historical data)
	Evidence of transport of fire emissions to monitor	Sections 3.1.2 (maps of ozone, particulate matter with a diameter less than 2.5 micrometers [$PM_{2.5}$], fire, smoke, visible satellite imagery), and 3.1.3 (Hybrid Single-Particle Lagrangian Integrated Trajectory [HYSPLIT] trajectories)
	Media coverage and photographic evidence of smoke	Section 3.1.4 (Media coverage and Images)
Tier 2	Key Factor #1: fire emissions and distance of fires	Section 3.2.1 (analysis of the relationship between fire emissions and distance [Q/d])
	Key Factor #2: comparison of event concentrations with non-event-related high ozone concentrations	Section 3.2.2 (comparison of event concentrations with non-event concentrations)
	Evidence that the fire emissions affected the monitor	Sections 3.2.3 (Satellite Retrievals of Pollutant Concentrations) and 3.2.4 (changes in supporting measurements, differences in spatial/temporal patterns, and tracer measurements)
Tier 3	Evidence of fire emissions transport to the monitor	Section 3.3.1 (trajectory or satellite plume analysis, additional discussion of meteorological conditions, comparison to ozone concentrations on matching [meteorologically similar] days)
	Meteorologically similar matching day analysis	Section 3.3.2 (methodology and analysis for meteorologically similar days)
	Additional evidence	Section 3.3.3 (statistical regression modeling)

Tier 1 analyses are shown in Section 3.1. The key factor of Tier 1 analyses is the ozone concentration's uniqueness when compared to the typical seasonality and/or levels of ozone exceedance. The EPA guidance suggests providing a time series plot of 12 months of ozone concentrations overlaying more than five years of monitored data and describing how typical seasonality differs from ozone in the demonstration (U.S. Environmental Protection Agency, 2016). In addition, trajectory analysis—produced by the HYSPLIT model, together with satellite plume imagery and ground-level measurements of plume components (e.g., $PM_{2.5}$, CO, or organic and elemental carbon)—should be used to provide evidence of wildfire emissions being transported to the monitoring sites. We demonstrate the Tier 1 analysis results for the June 26, 2020, event in Section 3.1. We address the key factors in Section 3.1.1, provide evidence of wildfire smoke transport to the Clark County monitoring sites in Sections 3.1.2 and 3.1.3, and discuss the media coverage and show ground images in Section 3.1.4.

Tier 2 analyses are shown in Section 3.2. The two key factors for Tier 2 analyses are (1) fire emissions and distance of fires to the impacted monitoring sites, and (2) comparison of event-related ozone concentrations with non-event-related high ozone values. We address the first factor in Section 3.2.1 by determining the emissions divided by distance (Q/d) relationship and address the second factor in Section 3.2.2 by comparing the six-year percentiles and yearly rank-order analysis of ozone concentrations. The Tier 2 analyses also require evidence of wildfire smoke transport to affected monitoring sites; we provide this evidence in Section 3.2.3 through satellite measurements of pollutant concentrations. In Section 3.2.4, we discuss supporting pollutant trends and diurnal patterns of $PM_{2.5}$, CO, NO_x, and total nonmethane organic compounds (TNMOC) compared with ozone concentrations and wildfire tracer measurements. The Tier 2 analyses are included in this demonstration for completeness and to inform the Tier 3 analyses but, alone, are not expected to clearly demonstrate a relationship between the wildfire emissions and the monitored exceedances (see Section 3.2). We performed Tier 3 analyses to provide clear causal weight of evidence of this relationship.

Tier 3 analyses are shown in Section 3.3. We investigated total column information and event-related meteorological conditions (Section 3.3.1) and developed a Generalized Additive Statistical Model (GAM) to estimate the wildfire's contribution to ozone concentrations (Section 3.3.2).

Following the EPA's EE guidance, we performed Tier 1, Tier 2, and Tier 3 analyses to show the "clear causal relationship" between the Rock Path, Twin, and Miller fires in Nevada and Utah and the exceedance event in Clark County on June 26, 2020. Focusing on the characterization of the meteorology, smoke, transport, and air quality on the days leading up to the event, we conducted the following specific analyses (results of these analyses are presented in Section 3):

- Developed time series plots that show the June 26 ozone concentrations at each affected monitoring site in historical context for 2020 and the previous six years
- Compiled maps of (1) ozone and $PM_{2.5}$ concentrations in the area, (2) smoke plumes, and (3) fire locations from satellite data

- Showed the transport patterns via HYSPLIT modeling, and identified where the back trajectory air mass intersected with smoke plumes or passed over or near fires
- Discussed media coverage of the June 26 event and showed ground images
- Quantified total fire emissions and calculated emissions/distance ratio (Q/d) for the fire
- Performed statistical analysis to compare event ozone concentrations to non-event concentrations
- Provided maps showing satellite retrievals of NO_x, AOD, and CO
- Developed plots to show diurnal patterns of ozone and supporting pollutants such as $PM_{2.5}$, CO, NO_x, and TNMOC
- Examined wildfire tracer species and their background concentrations vs. event concentrations
- Assessed vertical transport of smoke using satellite-observed aerosol vertical profiles and ceilometer mixing height retrievals
- Created a GAM model of MDA8 ozone concentrations to assess the enhancement of ozone concentrations due to wildfire influence

1.4 Conceptual Model

The conceptual model for the exceptional event that led to the ozone exceedances at the Paul Meyer site on June 26, 2020, is outlined in Table 1-5. We provide the analysis techniques performed and evidence for each Tier. This establishes a weight of evidence for the clear causal relationship between the wildfire emissions in southwestern Utah and southern Nevada and the June 26 exceptional ozone event. We assert that smoke from the lightning-initiated fires, which began on June 25, enhanced ozone concentrations in Clark County on June 26 and led to an exceedance at the Paul Meyer site. In support of this assertion, the key points of evidence for the conceptual model are summarized below.

1. The June 26 ozone exceedance occurred during a typical ozone season, but event concentrations at the Paul Meyer exceedance site were significantly higher than non-event concentrations. Ozone concentrations showed a high percentile rank at the Paul Meyer site when compared with the past six years and ozone seasons.
2. Satellite imagery, media reported ground images, HMS smoke, and fire detection products show the presence of wildfire smoke upwind of Clark County on June 25 and early on June 26. Radar lightning detections verified that Rock Path Fire in southwestern Utah and Miller and Twin Fires in southern Nevada were lightning initiated by 7 p.m. local time on June 25 prior to the exceedance event.

3. Back and forward trajectories from the near-surface boundary layer at Paul Meyer site at the time of maximum ozone concentration show consistent transport patterns passing over the Rock Path Fire in southwestern Utah and near the Miller and Twin Fires in southern Nevada. The combination of (1) trajectories intersecting fire locations after fire initiation times and (2) a deep mixed layer over Clark County favoring vertical mixing demonstrate that wildfire emissions were transported to the surface in Clark County on the morning of June 26.
4. Meteorological conditions on June 26 did not favor enhanced local ozone production when compared with meteorologically similar ozone season days. Average MDA8 ozone across similar days was well below the ozone NAAQS and 10 ppb lower than the June 26 exceedance at Paul Meyer.
5. GAM model predictions of MDA8 ozone at Paul Meyer on June 26 are well below the 70 ppb ozone NAAQS and 12 ppb below the observed MDA8 ozone. Using the 75^{th}-95^{th} quantile of positive residuals (observed MDA8 ozone minus GAM-predicted MDA8 ozone), we find a minimum wildfire effect on ozone of 2-7 ppb in Clark County from an atypical source, in this case, the Rock Path, Miller, and Twin Fires in Nevada and Utah. This, in addition to the meteorologically similar day conclusions in point 6 above, suggests that although Paul Meyer was the only site to experience an MDA8 ozone exceedance, ozone concentrations would likely have been ≤ 70 ppb but for smoke impacts.
6. Surface enhancements of wildfire tracers $PM_{2.5}$, CO, as well as levoglucosan above-normal ozone season concentrations and abnormal $PM_{2.5}$ and CO diurnal profiles, indicate the presence of wildfire emissions of ozone precursors at the surface in Clark County coincident with the wildfire plume arrival on June 26.

2. Historical and Non-Event Model

2.1 Regional Description

Clark County is in the southern portion of Nevada and borders California and Arizona. Clark County includes the City of Las Vegas, one of the fastest growing metropolitan areas in the United States with a population of approximately 2 million (U.S. Census Bureau, 2010). Las Vegas is located in a 1,600 km^2 desert valley basin at 500 to 900 m above sea level (Langford et al., 2015). It is surrounded by the Spring Mountains to the west (3,000 m elevation) and the Sheep Mountain Range to the north (2,500 m elevation). Three mountain ranges comprise the southern end of the valley. The valley floor slopes downward from west to east, which influences surface wind, temperature, precipitation, and runoff patterns. The Cajon Pass and I-15 corridor to the west is an important atmospheric transport pathway from the Los Angeles Basin into the Las Vegas Valley (Langford et al., 2015). **Figures 2-1 and 2-2** show the topography of the Clark County area and surrounding areas.

The Las Vegas Valley climatology features abundant sunshine and hot summertime temperatures (average summer month high temperatures of 34-40°C). Because of the mountain barriers to moisture inflow, the region experiences dry conditions year-round (~107 mm annual precipitation, 22% of which occurs during the summer monsoon season in July through September). The urban heat island effect in Las Vegas during summer leads to large temperature gradients within the valley, with generally cooler temperatures on the eastern side. During the summer season, monsoon moisture brings high humidity and thunderstorms to the region, typically in July and August (National Weather Service Forecast Office, 2020). Winds in the Las Vegas basin tend to be out of the southwest during spring and summer (Los Angeles is upwind), while winds in the fall and winter tend to be out of the northwest, with air transported between the neighboring mountain ranges and along the valley.

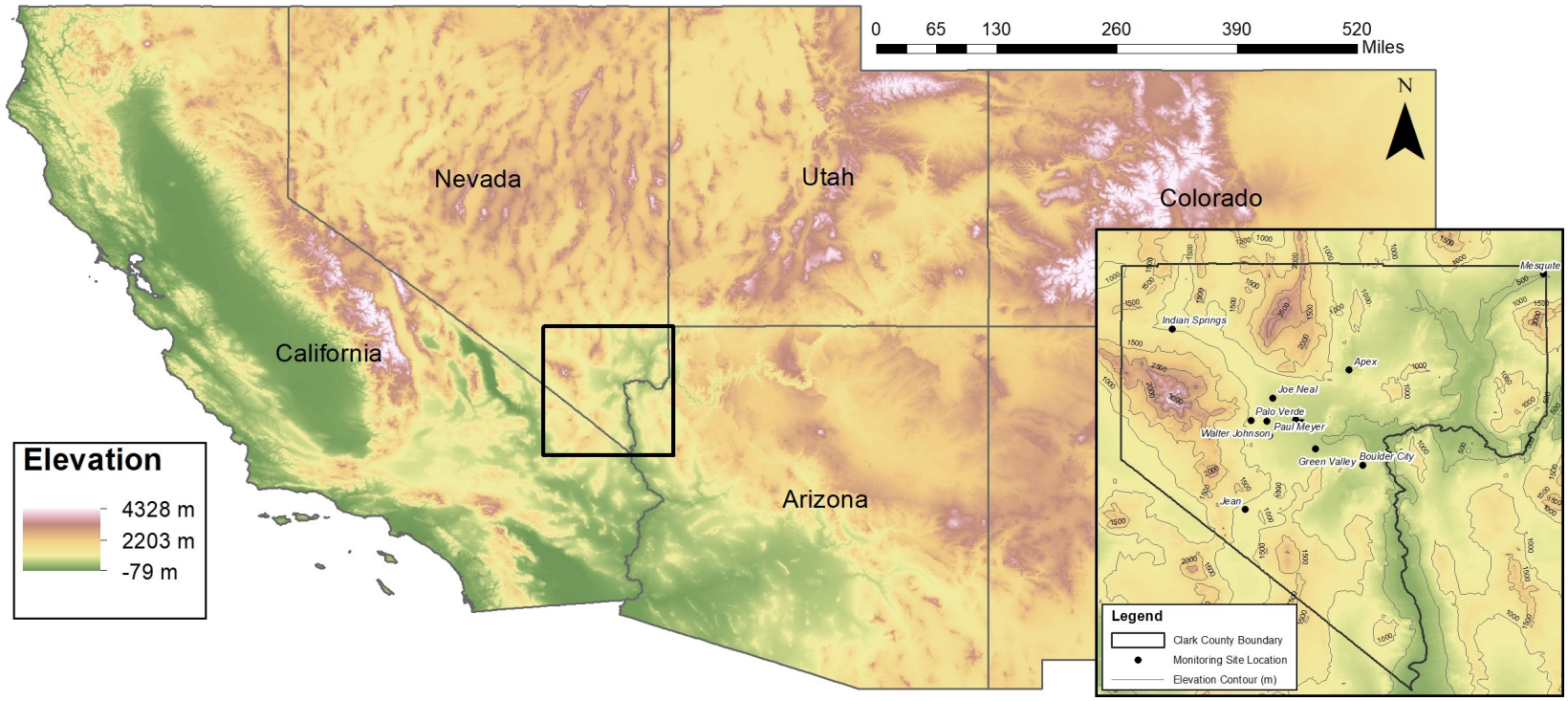

Figure 2-1. Regional topography around Clark County, with an inset showing county boundaries and the air quality monitoring sites analyzed in this report.

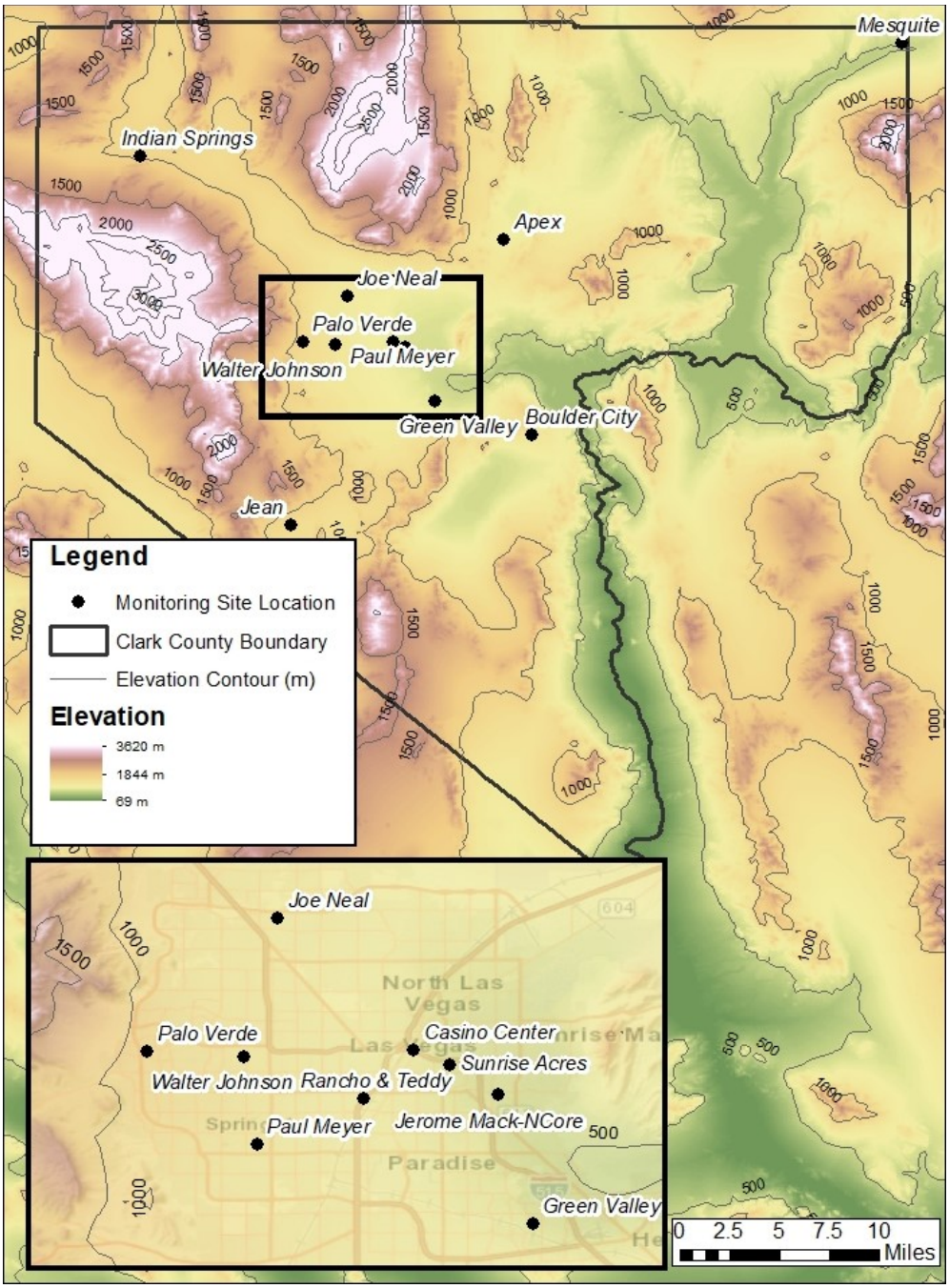

Figure 2-2. Clark County topography, with an inset showing all air quality monitoring sites in the Clark County area.

2.2 Overview of Monitoring Network

The Clark County Department of Environment and Sustainability, Division of Air Quality (DAQ) operated 14 ambient air monitoring sites in the region during 2020 (Figure 2-2). These sites measure hourly ozone, particulate matter ($PM_{2.5}$, PM_{10}), NO_x, TNMOC, and carbon monoxide (CO) concentrations along with meteorological parameters. Table 2-1 presents the monitoring data coverage across time and space for criteria pollutants and surface meteorological parameters (barometric pressure, temperature, wind speed and direction), as well as mixing height. We examined ozone and other criteria pollutants at 11 sites around Clark County to investigate the high ozone event observed on June 26, 2020. DAQ's ambient air monitoring network meets the monitoring requirements for criteria pollutants pursuant to Title 40, Part 58, of the Code of Federal Regulations (CFR), Appendix D. Data are quality-assured in accordance with 40 CFR 58 and submitted to the EPA's Air Quality System (AQS). The spatial distribution of monitoring sites characterizes the regional air quality in Las Vegas, as well as air quality upwind and downwind of the urban valley region (Figure 2-2). The Jean monitoring site along the I-15 corridor is generally upwind such that it captures atmospheric transport into the region and is least impacted by local sources (Figure 2-2).

Table 2-1. Clark County monitoring site data. The available date ranges of all parameters and monitoring sites used in this report for Clark County, Nevada, are shown. Casino Center and RT are near-road sites and are not used for the exceptional event analysis.

Site	AQS Sitecode	O_3	$PM_{2.5}$	CO	NO	NO_2	TNMOC	Temp.	Wind Speed	Wind Direction	Barom. Pressure	Mixing Height
Apex	320030022	2014-2020						2014-2020	2014-2020	2014-2020		
Boulder City	320030601	2014-2020									2014-2016	
Casino Center	320031502							2014-2020	2016-2020	2016-2020		
Green Valley	320030298	2015-2020	2014-2020	2020				2016-2020	2014-2020	2014-2020	2014-2016	
Indian Springs	320037772	2014-2020										
Jean	320031019	2014-2020	2014-2020					2014-2020	2014-2020	2014-2020	2014-2016	
Jerome Mack	320030540	2014-2020	2014-2020	2015-2020[1,2]	2015-2020	2015-2020	2020	2014-2020	2014-2020	2014-2020	2014-2020	2020
Joe Neal	320030075	2020	2018-2020	2019-2020		2015-2020		2014-2020	2014-2020	2014-2020	2014-2016	
Mesquite	320030023	2014-2020						2014-2020	2014-2020	2014-2020		
Palo Verde	320030073	2014-2020	2020					2014-2020	2014-2020	2014-2020	2014-2016	
Paul Meyer	320030043	2014-2020	2017-2020					2014-2020	2014-2020	2014-2020	2014-2016	
RT	320031501							2015-2020	2015-2020	2015-2020	2014-2016	
Sunrise Acres	320030561			2020				2014-2020	2014-2020	2014-2020	2014-2016	
Walter Johnson	320030071	2014-2020	2020					2015-2020	2015-2020	2015-2020	2014-2016	

[1] CO data invalid at Jerome Mack on Sep. 2, 2020

[2] CO data invalid at Jerome Mack Apr. 28, 2020 – May 20, 2020

2.3 Characteristics of Non-Event Historical O_3 Formation

During the ozone season (April–September) in Clark County, Nevada, ozone concentrations are typically influenced by local formation, by transport into the region, and on occasion by exceptional events such as wildfires and stratospheric intrusions. Transport from upwind source regions (e.g., Los Angeles Basin, Mojave Desert, Asia) occurs with southwesterly winds, and southerly transport dominates later in the season due to the summer monsoon (Langford et al., 2015; Zhang et al., 2020). Local precursor emissions in Clark County include mobile NO_x and VOC sources, coal and natural-gas fueled power generation NO_x sources, and biogenic VOC emissions. Based on 2017 emission inventories in Las Vegas, on a typical ozone season weekday there are 98 tons of NO_x emissions per day and 238 tons of volatile organic compound (VOC) emissions per day (Clark County Department of Environment and Sustainability, 2020). On-road mobile sources comprise 40% of NOx emissions and total mobile emissions comprise 88% of total NOx emissions during the ozone season. In contrast, 52% of VOC emissions originate from biogenic sources within Clark County. Local emissions and/or precursors transported into the region contribute to ozone formation within Clark County (Langford et al., 2015; Clark County Department of Air Quality, 2019).

In this demonstration, we discuss the impacts of wildfire smoke on ozone concentrations in Clark County on June 26, 2020. In order to fully discern the effect of wildfire smoke on ozone concentrations in Clark County on June 26, 2020, we examine the historical ozone record for all affected sites (Table 1-1). *Non-event days* refer to all days other than the June 26, 2020, event. Because percentile rankings are sensitive to including the relatively large number of potential EE days during 2018 and 2020, we also provide statistics *excluding potential EE days* (i.e., without including the 2018 and 2020 potential EE days as defined in Tables 1-2 and 1-3 in Section 1). The 8-hour ozone design value (DV) is the three-year running average of the fourth-highest daily maximum 8-hour (MDA8) ozone concentration (40 CFR Part 50, Appendix U). Within Clark County, Las Vegas is classified as an EPA Region 9 marginal nonattainment region with a 73 ppb ozone DV for 2017-2019 (U.S. Environmental Protection Agency, 2020).

We identified ozone EE days as days with significant wildfire or stratospheric intrusion influence in addition to an MDA8 concentration greater than 70 ppb. By this criterion, we identified 15 possible EE days in 2018, 13 possible EE days in 2020, and no EE days in 2019.

The June 26, 2020, exceptional event occurred early in the ozone season under meteorological conditions of hot, dry air and surface and upper-level low pressure (see Section 3.3.1). Compared with a non-event conceptual model where local precursor emissions contribute to ozone formation at ground level under similar conditions, the June 26 conditions indicate a high mixing height, enhanced vertical mixing, and northerly/northeasterly surface winds. These conditions facilitated boundary layer transport of wildfire-influenced air parcels from fires north and northeast of Las Vegas in Nevada and Utah.

Figures 2-3 and 2-4 depict the six-year historical record and seasonality of MDA8 ozone concentrations at the EE-affected monitoring site (Paul Meyer), along with the 99th percentile and NAAQS standard ozone concentrations. June 26, 2020, ranks in the top 1% for daily maximum ozone concentration in the six-year historical record at the Paul Meyer site and above the top 5% for MDA8 ozone during the ozone season. Figure 2-5 depicts a two-week ozone diurnal cycle of 1-hour ozone beginning one week before the June 26 event and ending one week after. On June 26, daily maximum 1-hour ozone concentrations were the third highest during this two-week period at the Paul Meyer monitoring site (Table 1-1).

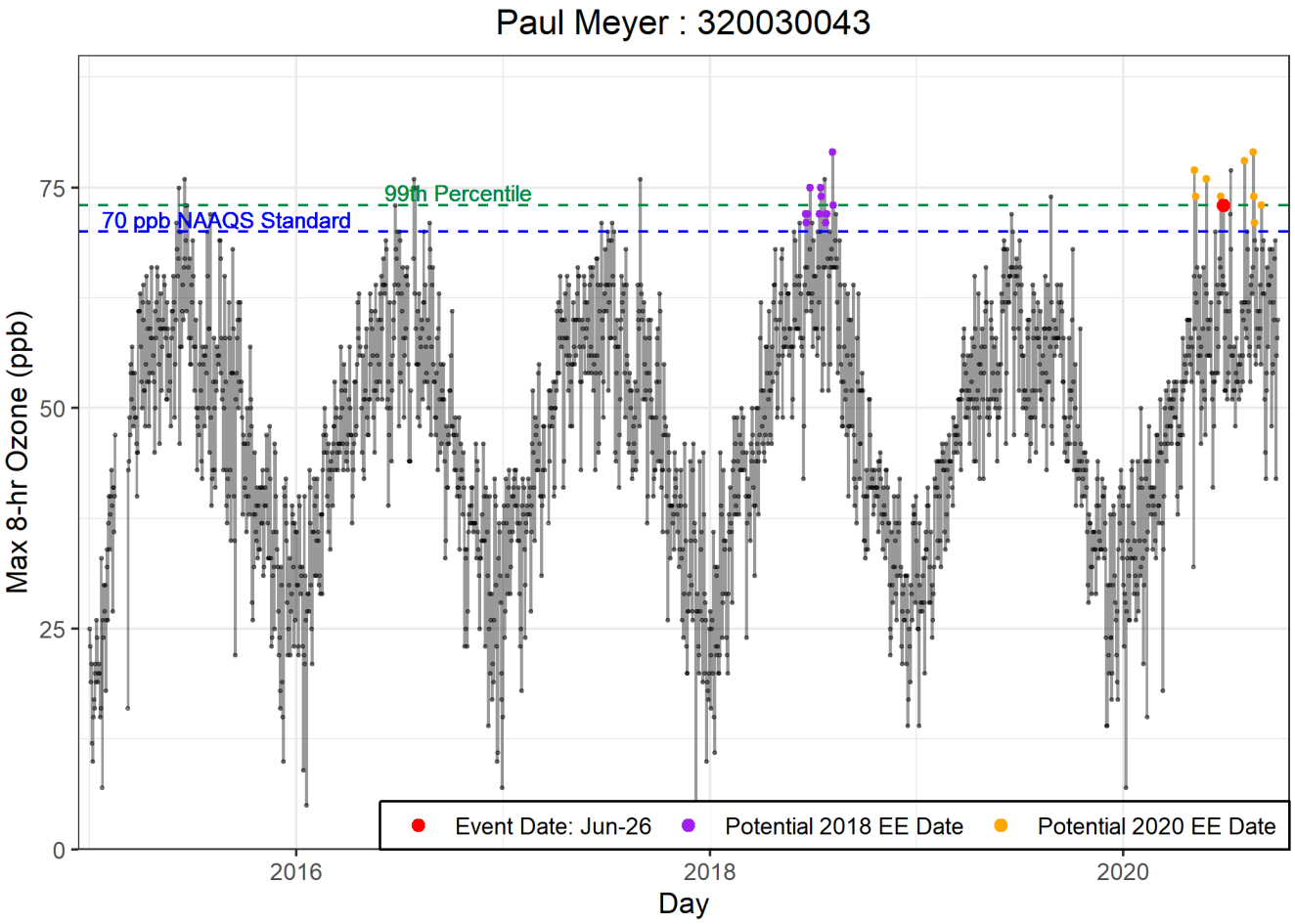

Figure 2-3. Time series of 2015-2020 ozone concentrations at Paul Meyer.

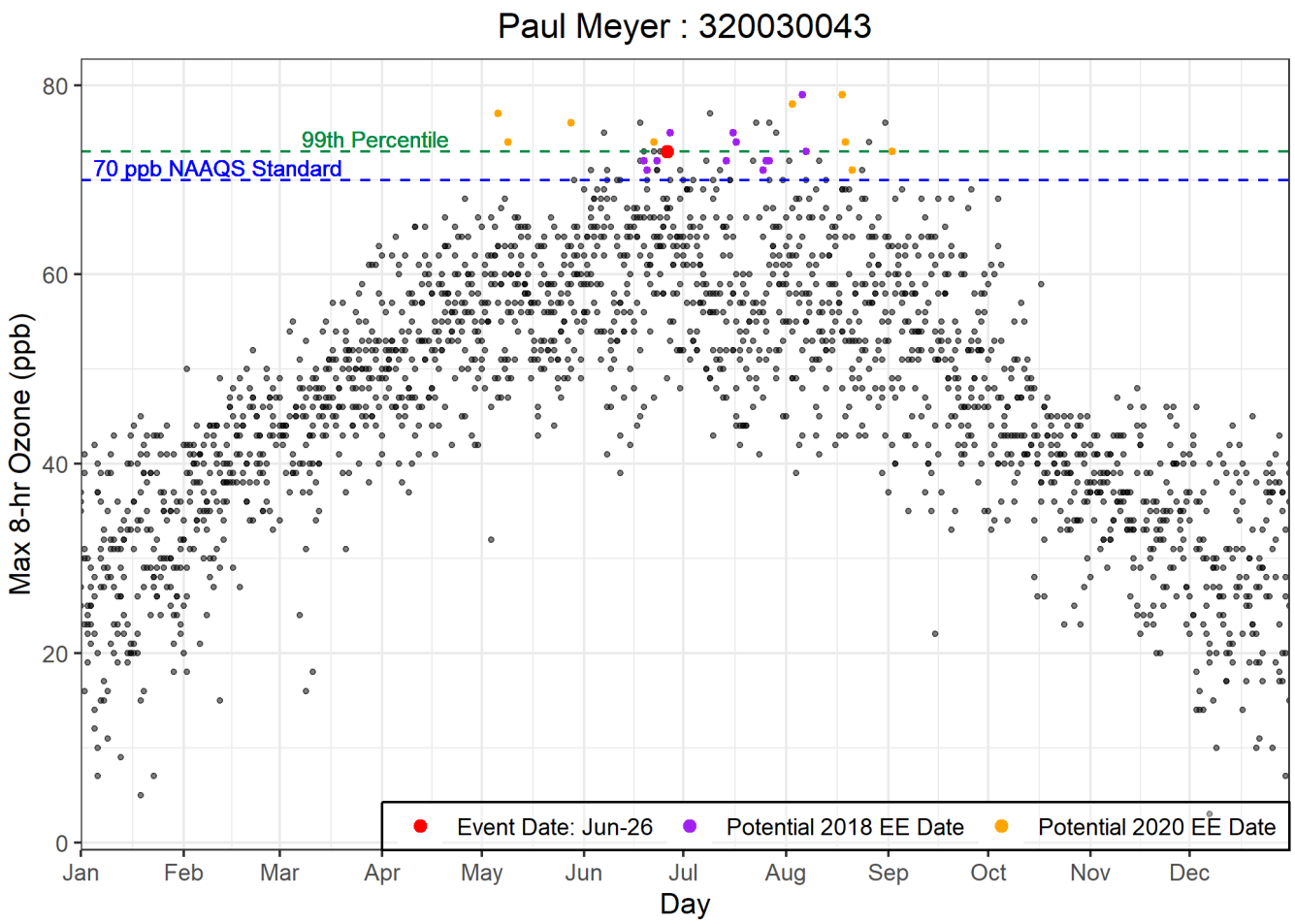

Figure 2-4. Seasonality of 2015-2020 ozone concentrations from Paul Meyer. All six years of ozone data is overlaid to create a seasonal comparison.

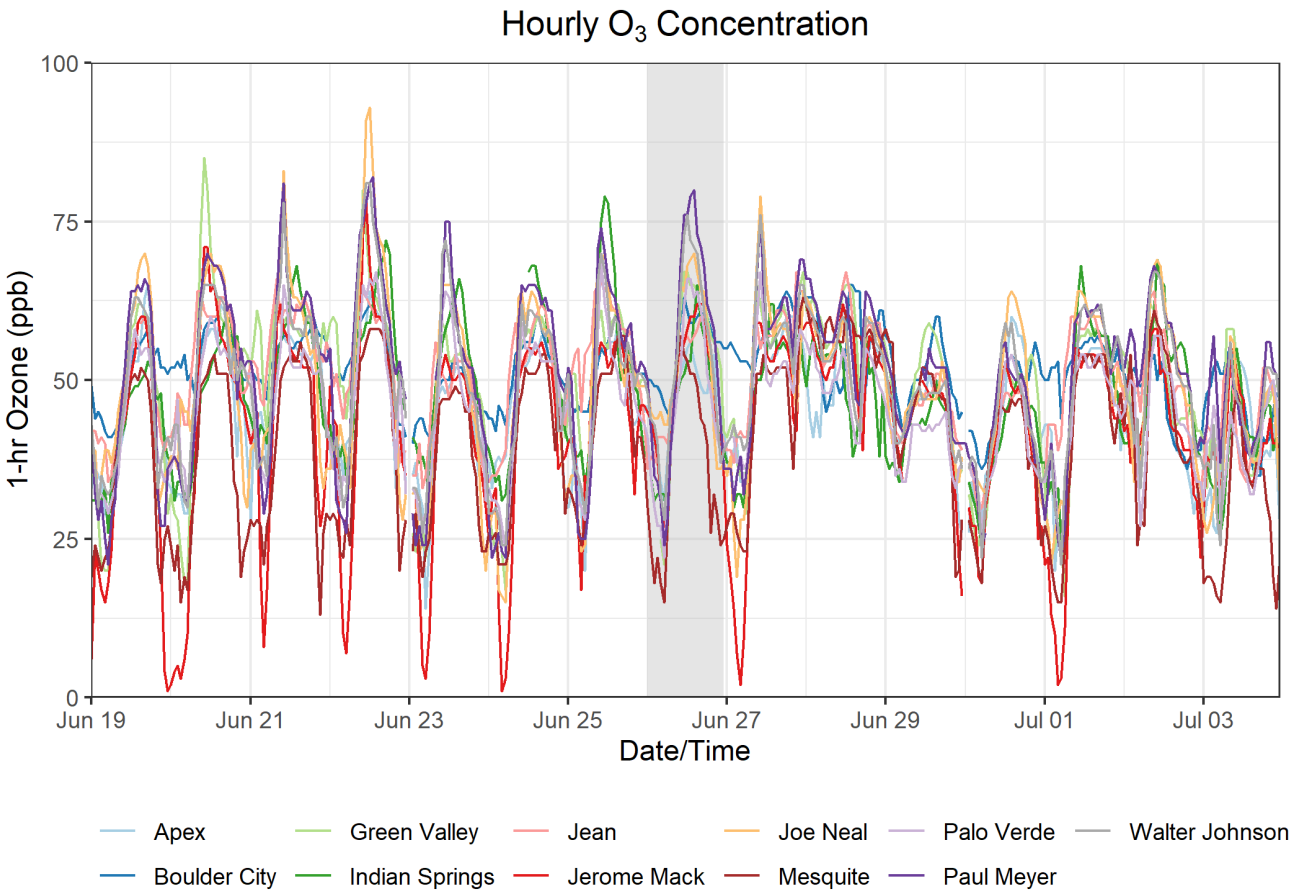

Figure 2-5. Time series of hourly ozone concentrations at Clark County monitoring sites for one week before and after the June 26 event. June 26, 2020, is shaded for reference.

3. Clear Causal Relationship Analyses

3.1 Tier 1 Analyses

3.1.1 Comparison of Event with Historical Data

To address the Tier 1 exceptional event criterion of comparison with historical ozone, we compared the June 26 exceptional event ozone concentrations at the Paul Meyer site with the 2020 ozone record, focusing mainly on the ozone season when highest ozone concentrations occur. **Figure 3-1** shows the 2020 daily maximum ozone record at the Paul Meyer site, along with the 99th percentile of previous 5-year MDA8 ozone and NAAQS criteria ozone concentrations. During 2020, June 26 ranks in the top 1% for daily maximum ozone concentration at the Paul Meyer monitoring site. When compared with daily ozone rankings on June 26 over the six-year ozone record at the Paul Meyer site (Figure 2-4), the 2020 rankings indicate that June 26, 2020, was an extreme ozone event.

The June 26, 2020, ozone exceedance occurred during a typical ozone season, but June 26 MDA8 ozone concentrations were the second highest in 2020 at Paul Meyer compared with daily ozone concentrations if potential EE days are excluded (Figure 3-1). **Table 3-1** provides historical statistics for the Paul Meyer site on June 26, 2020. The statistics shown are for May through September in 2015-2019; we do not exclude proposed 2018 EE ozone concentrations. The MDA8 ozone concentrations on June 26 were more than 10 ppb above the five-year mean and median, but only 3 ppb above the 95th percentile of ozone concentrations when compared with non-event day historical ozone concentrations at the Paul Meyer monitoring site (Table 3-1). Because June 26 is during the normal ozone season and MDA8 ozone concentrations could not be clearly distinguished from the 95th percentile ozone concentration during the non-event historical ozone season, the June 26, 2020, event does not satisfy the key factor for a Tier 1 exceptional event. Tier 2 comparisons of the event-related ozone concentrations with non-event-related high ozone concentrations (>99th percentile over five years or top four highest daily ozone measurements) are described in Section 3.2.2.

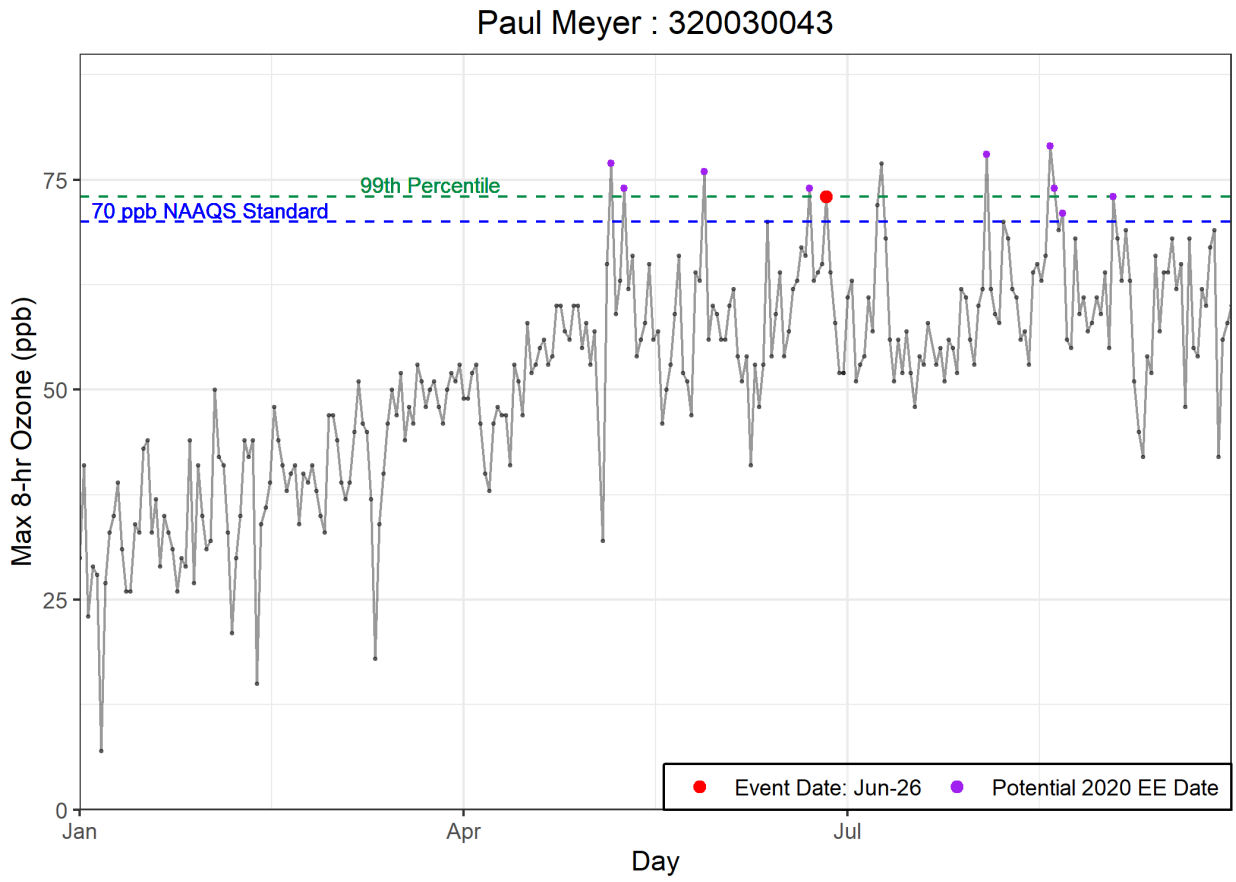

Figure 3-1. Time series of 2020 MDA8 ozone concentrations from the Paul Meyer site.

Table 3-1. Ozone season non-event comparison. June 26, 2020, MDA8 ozone concentrations are shown in the top row, and five-year (2015-2019) average MDA8 ozone statistics for May through September (ozone season) are shown in the following rows for comparison.

	Paul Meyer 320030043
Jun. 26	73
Mean	57
Median	58
Mode	58
St. Dev	8
Minimum	22
95 %ile	70
99 %ile	76
Maximum	79
Range	57
Count	911

3.1.2 Ozone, Fire, and Smoke Maps

Ozone Maps

We produced maps of ozone Air Quality Index (AQI), $PM_{2.5}$ AQI, active fire and smoke detections from satellites, and visible satellite imagery that show the transport of smoke to Clark County from the Twin and Miller fires burning in Nevada, north of Clark County, and the Rock Path Fire in Utah on June 26, 2020. These maps also show that high ozone concentrations occurred across multiple states corresponding with the presence of wildfire smoke.

From June 23 through June 26, 2020, moderate and unhealthy ground-level ozone concentrations (indicated by the yellow, orange, and red areas) were detected in the western United States (Figure 3-2), especially in California, Utah, and parts of Arizona and Nevada. On June 23, high ozone concentrations (orange and red areas) are seen in central and southern California. These high levels persist through June 24, lessening slightly on June 25, and then rebounding on June 26. Additionally, across all four days, elevated ozone levels persist over a large portion of southern Nevada, covering Clark County. On June 26, elevated ozone is present in the eastern region of Utah.

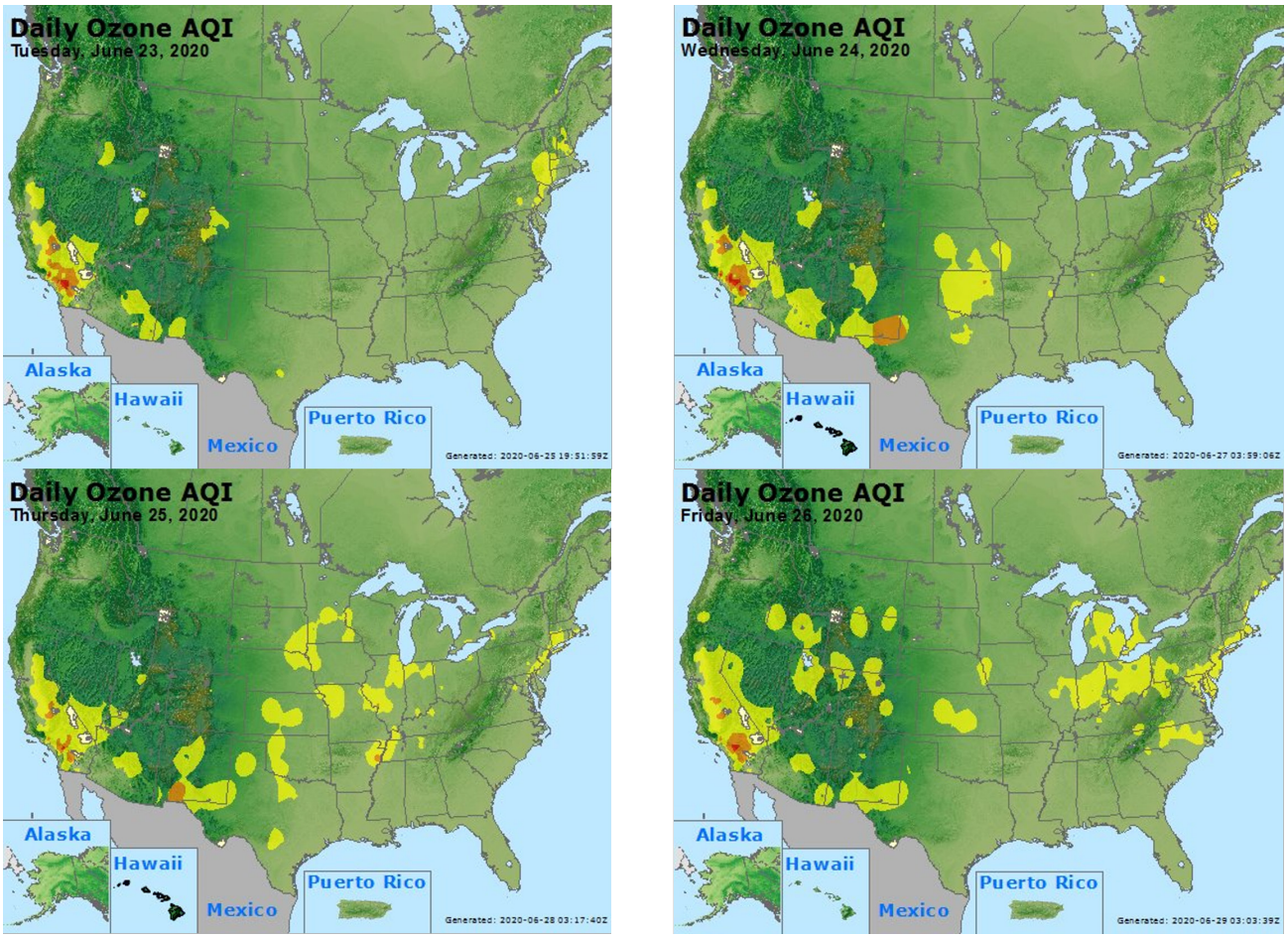

Figure 3-2. Daily ozone AQI for the three days before the June 26 event and the day of the event.

HMS Fire Detection Maps

According to EPA's guidance for Tier 1 analysis requirements (U.S. Environmental Protection Agency, 2016), the National Oceanic and Atmospheric Administration (NOAA) Hazard Mapping System (HMS) Fire and Smoke Product can be used to demonstrate the transport of fire emissions to the impacted monitors. The HMS Fire and Smoke Product consists of

1. A daily fire detection product derived from three satellite data products[1] to spatially and temporally map fire locations at 1 km grid resolution, and
2. A daily smoke product derived from visible satellite imagery[2] that consists of polygons showing regions impacted by smoke.

[1] The HMS fire detection product is developed using data from the Moderate Resolution Imaging Spectroradiometer (MODIS), Geostationary Operational Environmental Satellite system (GOES), Advanced Very High Resolution Radiometer (AVHRR) and Visible Infrared Imaging Radiometer Suite (VIIRS) satellite instruments.
[2] The HMS smoke product is derived from GOES-EAST and GOES-WEST visible satellite imagery.

The HMS smoke plume data is based on measurements from several environmental satellites and is reviewed by trained NOAA analysts to identify cases where smoke is dispersed by transport. One can download real-time HMS fire detection and smoke products and a six-month archive of the products from the NOAA Satellite and Information Service website (ospo.noaa.gov/Products/land/hms.html).

Figure 3-3 shows the HMS smoke plume and fire detection data for June 23 to June 26, 2020. There was concentrated fire activity in California, Arizona, and New Mexico. There were also several scattered fires in Nevada and Utah. On June 25, thunderstorms across eastern Nevada and western Utah resulted in lighting-induced wildfires. As a result, the Rock Path Fire in Utah ignited on June 25, and the Miller Fire in Nevada ignited on June 26, 2020. The Twin Fire also began in Nevada on June 25; however, the cause of the fire is unknown. These fires are visible in the June 26 HMS smoke maps in Figure 3-3.

The HMS smoke plume data for the days leading up to June 26 were obtained and combined with HYSPLIT back trajectories on high ozone concentration days to identify intersections and assess potential smoke impacts (Section 3.1.3). Although the maps in Figure 3-3 do not show smoke plumes directly over Clark County on the day of the ozone exceedance, the following sections provide evidence that smoke transport, based on HYSPLIT trajectories and satellite data, occurred from the Twin, Rock Path, and Miller fires to the Clark County area.

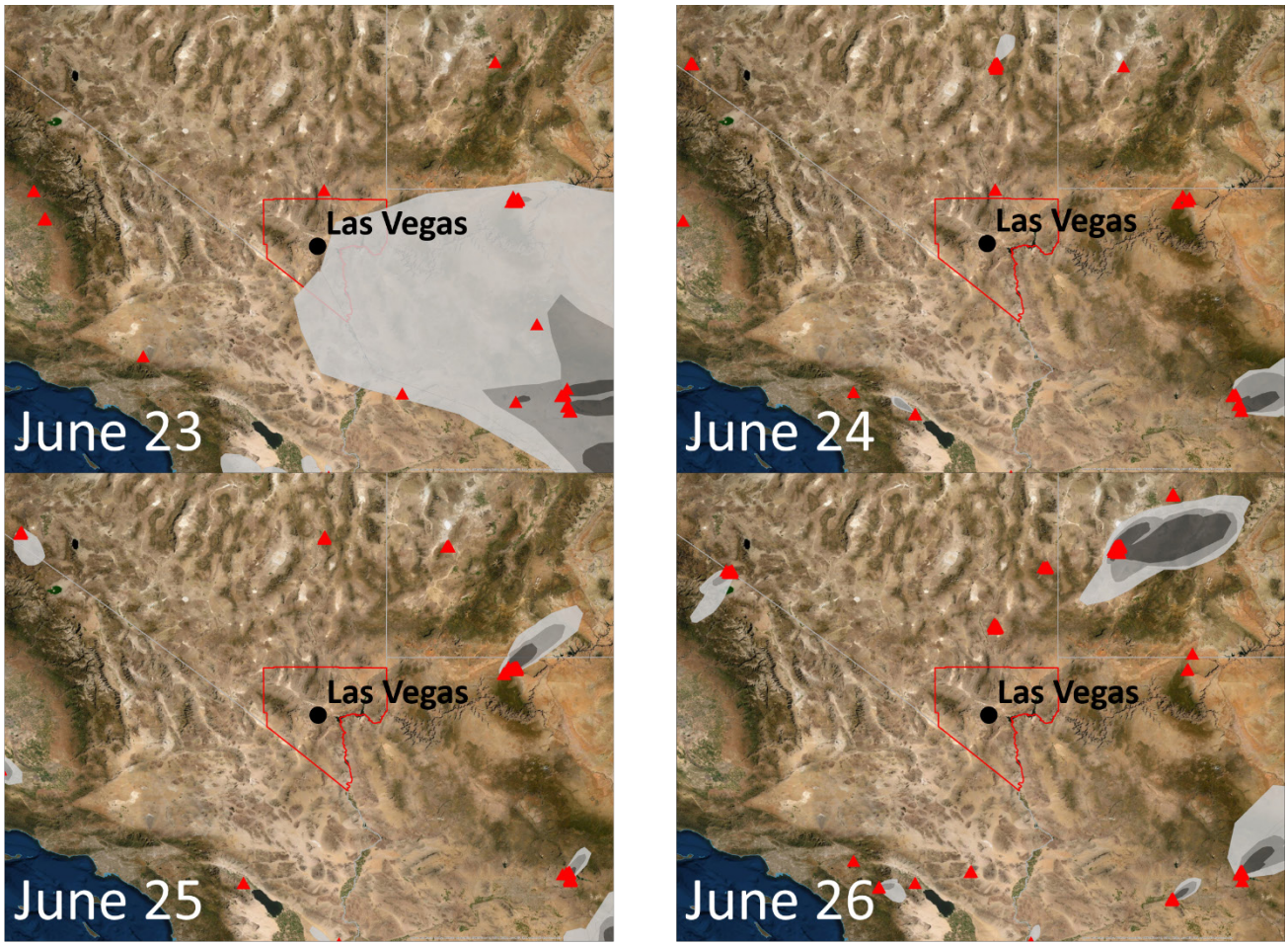

Figure 3-3. Daily HMS smoke over the United States for the three days before the June 26 event and the day of the event. Fire detections are shown as red triangles, and smoke is shown in gray.

Visible Satellite Imagery

Visible satellite imagery from the MODIS Aqua and Terra satellites on June 25 show dense clouds over the Nevada-Utah border (Figure 3-4), consistent with the thunderstorm that produced lightning strikes. The visible satellite imagery for June 26 in Figure 3-5 shows the area (circled in red) where the Rock Path, Twin, and Miller fires were burning. This is consistent with the evidence of smoke produced by the fires in the HMS maps above. The information from the visible smoke images shown here, as well as the HMS smoke maps shown above, must be combined with HYSPLIT trajectory analysis to explain the air mass movement on June 26 and corresponding elevated ozone levels observed in Clark County.

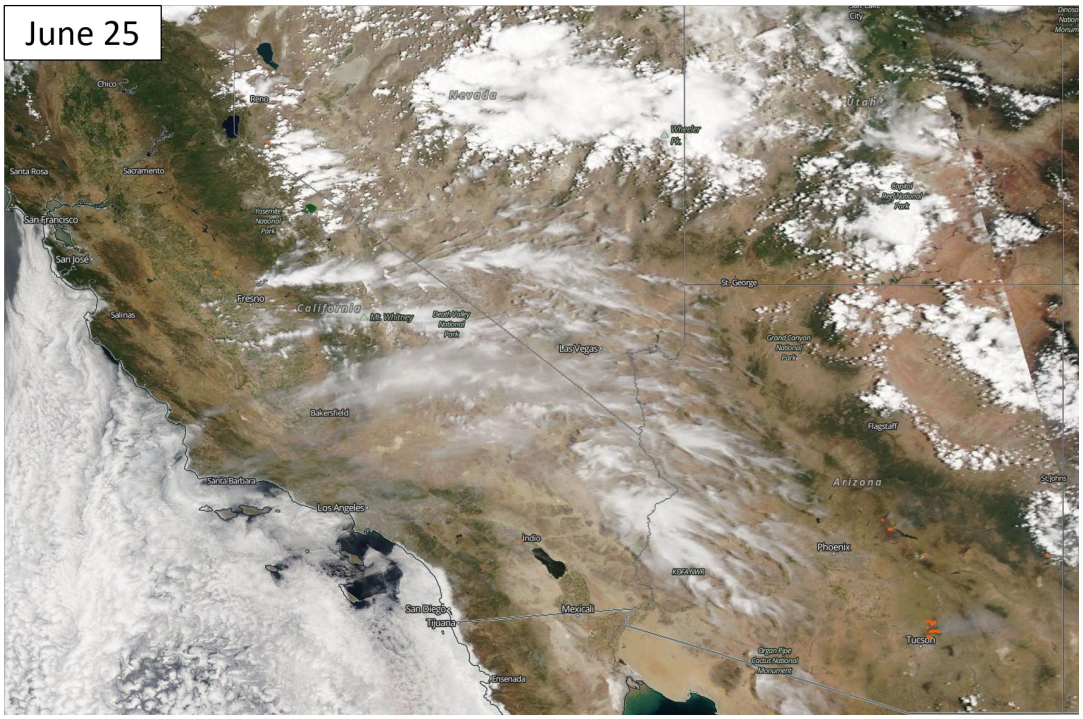

Figure 3-4. Visible satellite imagery from over southern California, Nevada, and Arizona on June 25, 2020. Source: NASA Worldview.

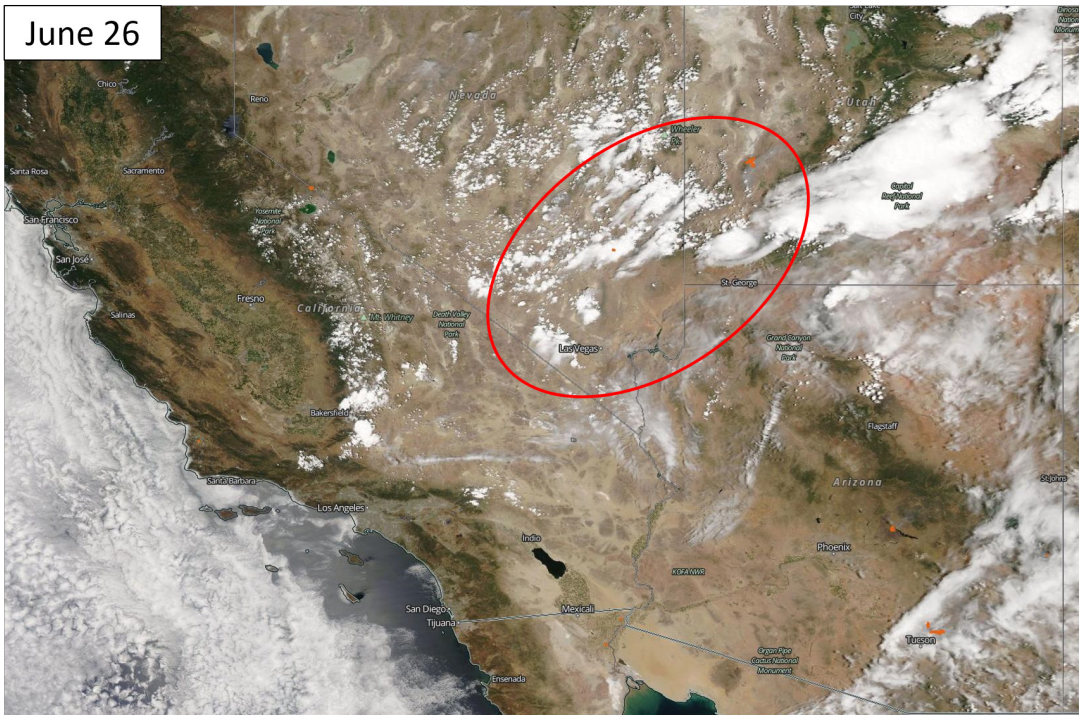

Figure 3-5. Visible satellite imagery from over southern California, Nevada, and Arizona on June 26, 2020. Source: NASA Worldview.

Radar Images

According to official fire reports, the Rock Path, Miller, and Twin fires all started on June 25-26 (see Section 3.2.1 for more details). The Rock Path and Miller fires were confirmed to be lightning-initiated; the official cause of the Twin fire is unknown according to InciWeb, although it is likely lightning-initiated due to spatial and temporal proximity to the other fires. The Rock Path fire merged with another previously burning fire (the Antelope fire) within the first 24 hours, and combined to burn a total of 42,000 acres by the end of the day on June 26. We provide radar images from June 25 in order to estimate fire initiation times for comparison with HYSPLIT back trajectories and times to initialize forward trajectories in Section 3.1.3. **Figure 3-6** shows that all fires were likely initiated no later than 6:00 p.m. PST on June 25 due to widespread thunderstorms in Nevada and Utah. High reflectivity areas are likely to include lightning strikes. The areas circled in this figure show the thunderstorms likely responsible for causing the Rock Path, Miller, and Twin fires in Nevada and Utah.

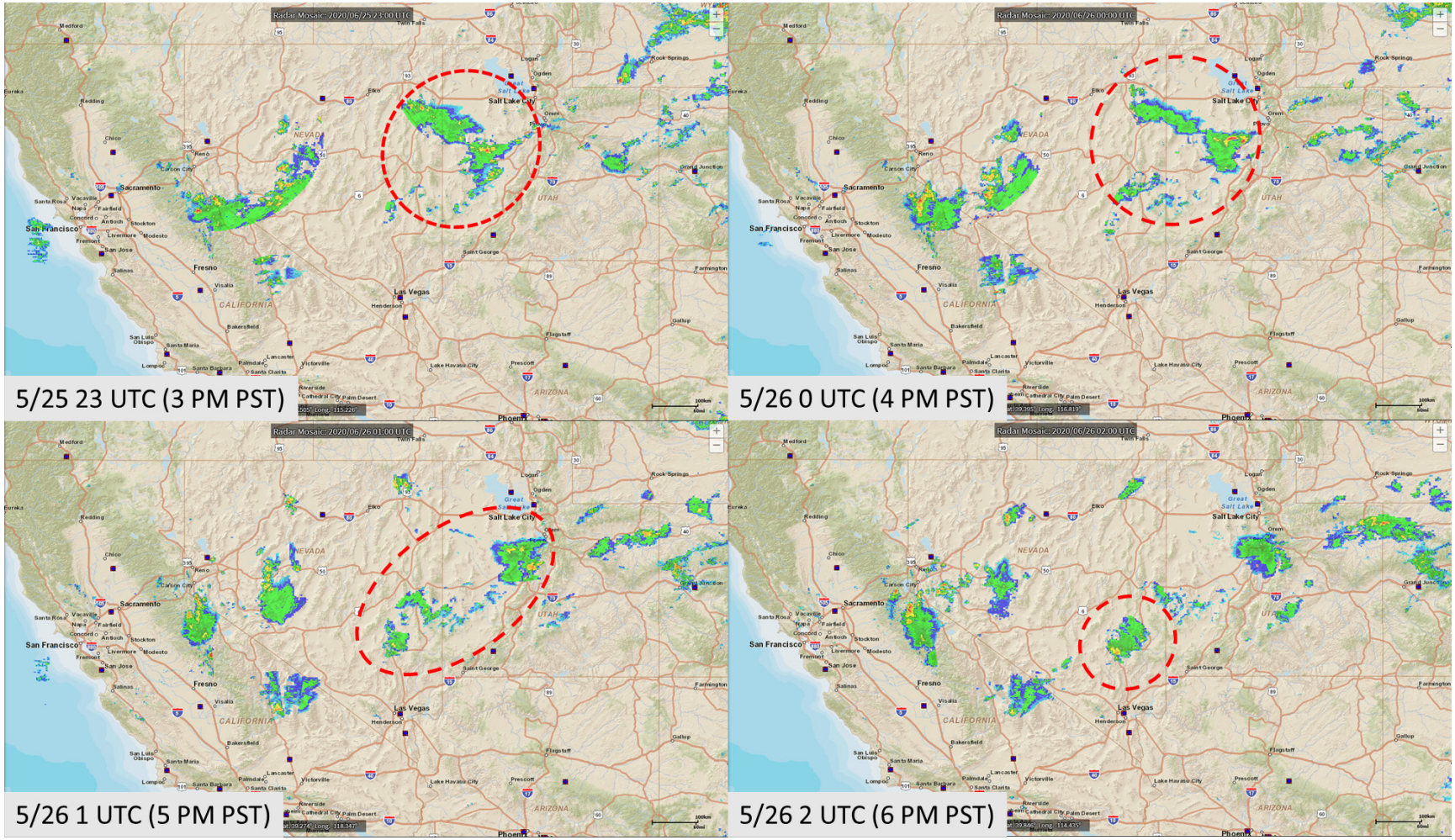

Figure 3-6. Radar images from June 25, 2020, showing the thunderstorms likely responsible for the Rock Path, Miller, and Twin fires. Red dashed areas indicate the thunderstorms near the fire locations. The images shown are radar mosaics (from multiple radar sources) and were retrieved from the NOAA National Centers for Environmental Information (NCEI): https://gis.ncdc.noaa.gov/maps/ncei/radar.

3.1.3 HYSPLIT Trajectories

HYSPLIT trajectories were run to demonstrate the transport of air parcels to Las Vegas from upwind areas and to show transport of smoke-containing air parcels from wildfires toward the affected monitors. These trajectories show that air was transported from the Rock Path Fire in western Utah and the Twin and Miller Fires to the north of Clark County to the Clark County area on the day of the event, June 26, 2020. Combined with satellite observations described in Sections 3.1.2 and 3.2.3, the trajectories demonstrate that smoke was transported from the Rock Path Fire in Utah and near the Twin and Miller fires in Nevada to Clark County.

NOAA's online HYSPLIT model tool was used for the trajectory modeling (**http://ready.arl.noaa.gov/HYSPLIT.php**). HYSPLIT is a commonly used model that calculates the path of a single air parcel from a specific location and height above the ground over a period of time; this path is the modeled trajectory. HYSPLIT trajectories can be used as evidence that fire emissions were transported to an air quality monitor. This type of analysis is important for meeting Tier 1 requirements and is required under Tier 3.

The model options used for this study are summarized in **Table 3-2**. The meteorological data from the North American Mesoscale Forecast System (NAM, 12 km resolution) and High-Resolution Rapid Refresh (HRRR, 3 km resolution) model were used (**ready.noaa.gov/archives.php**). These data are high in spatial resolution, are readily available for HYSPLIT modeling over the desired lengths of time, and are expected to capture fine-scale meteorological variability. All backward trajectory start times were selected to be in the morning (18:00 UTC or 10:00 a.m. local standard time) coinciding with the rapidly increasing ozone concentration on June 26. As suggested in the EPA's exceptional event guidance (U.S. Environmental Protection Agency, 2016), a backward trajectory length of 48 hours was selected to assess whether smoke from the current day or from the previous day may have been transported over a long distance to the monitoring sites. Trajectories were initiated at 50 m, 100 m, 500 m, and 1,000 m above ground level to capture transport throughout the mixed boundary layer, as ozone precursors may be transported aloft and influence concentrations at the surface through vertical mixing. Three backward trajectory approaches available in the HYSPLIT model were used in this analysis, including site-specific trajectories, trajectory matrix, and trajectory frequency. Site-specific back trajectories were run to show direct transport from the wildfire smoke to the affected site(s); this analysis is useful in linking smoke impacts at a single location (i.e., an air quality monitor) to wildfire smoke. Matrix back trajectories were run to show the general air parcel transport patterns from the Las Vegas area to the wildfire smoke plumes. Similarly, matrix forward trajectories were run to show air parcel transport patterns from the fires to the Las Vegas area. Matrix trajectories are useful in analyzing air transport over areas larger than a single air quality site. Trajectory frequency analysis show the frequency with which multiple trajectories initiated over multiple hours pass over a grid cell on a map. Trajectory frequencies are useful in estimating the temporal and spatial patterns of air transport from a source region to a specific air quality monitor. Together, these trajectory analyses indicate the transport patterns into Clark County on June 26, 2020.

Based on initial trajectories and satellite data, the location at which back trajectories ended was used to initiate additional back trajectories to show long-range air transport over multiple days. Additionally, forward trajectory matrices were run for the western Utah Rock Path Fire, Twin Fire, and Miller Fire locations to show transport in the direction of Clark County.

Table 3-2. HYSPLIT run configurations for each analysis type, including meteorology data set, time period of run, starting location(s), trajectory time length, starting height(s), starting time(s), vertical motion methodology, and top of model height.

HYSPLIT Parameter	Backward Trajectory Analysis – Site-Specific	Back Trajectory Analysis – Matrix	Backward Trajectory Analysis – Frequency	Forward Trajectory Analysis – Matrix
Meteorology	3-km HRRR,	12-km NAM	12-km NAM	12-km NAM
Time Period	June 24 – June 26, 2020	June 26, 2020	June 24 – June 26, 2020	June 25 – June 26, 2020
Starting Location	36.08 N, 115.17 W	Evenly spaced grid covering Las Vegas, Nevada	36.08 N, 115.17 W	Evenly spaced grids covering Rock Path Fire and Miller and Twin fires
Trajectory Time Length	24 hours, 72 hours	24 hours	24 hours, 72 hours	24 hours
Starting Heights (AGL)	50 m, 500 m, 1,000 m	100 m	100 m	100 m, 250 m, 500 m
Starting Times	18:00 UTC	18:00 UTC	18:00 UTC	03:00 UTC
Vertical Motion Method	Model Vertical Velocity	Model Vertical Velocity	Model Vertical Velocity	Model Vertical Velocity
Top of Model	10,000 m	10,000 m	10,000 m	10,000 m

Site-specific, high-resolution (3 km) backward trajectories were calculated from the Las Vegas Valley (36.08 N, 115.17 W) on June 26, 2020. 18:00 UTC (10:00 a.m. PST) was chosen as the model starting time to coincide with a rapid rise in ozone at the Paul Meyer station. The backward trajectories from

the Las Vegas Valley, together with measured ozone (8-hour begin time average) are shown in Figure 3-7 with HMS smoke plume data overlaid. The trajectory initiated at 500 m shows the air mass travelled near the Twin and Miller fires in Nevada and directly over the Rock Path Fire in Utah. The trajectory initiated at 1,000 m shows that the air mass travelled near the Twin Fire, but not the Miller or Rock Path Fires. Figure 3-7 shows that the air reaching the Las Vegas Valley on June 26 directly intersected the concentrated smoke plume generated by the Rock Path Fire in Utah and occurred on the evening of June 25 after the initiation of the Rock Path Fire (see Radar Images in Section 3.1.2). Although HMS smoke does not indicate smoke plumes for the Miller or Twin Fire, Section 3.1.4 shows media reports of smoke images and Figure 3-5 shows visible satellite imagery of smoke over southern Nevada, confirming that the Miller and Twin Fires produced smoke on June 25 and 26, 2020.

To identify variations in meteorological patterns of transported air to Las Vegas, we generated a HYSPLIT trajectory matrix. For this approach, trajectories are run in an evenly spaced grid of source locations. Figure 3-8 shows a 24-hour backward trajectory matrix with source locations encompassing Las Vegas. The backward trajectories were initiated from the morning (at 10:00 a.m. PST/18:00 UTC) of June 26, 2020, at a starting height of 100 m above ground level (AGL). As shown in the plot, consistent with the trajectories depicted in Figure 3-8, transported air from western Utah directly intersected the Rock Path Fire and progressed southwest to near where the Twin and Miller fires were burning in Nevada before intersecting Las Vegas at 100 m AGL. Figure 3-8 shows that the majority of trajectories intercepted or came near smoke from the Rock Path, Twin, and Miller fires.

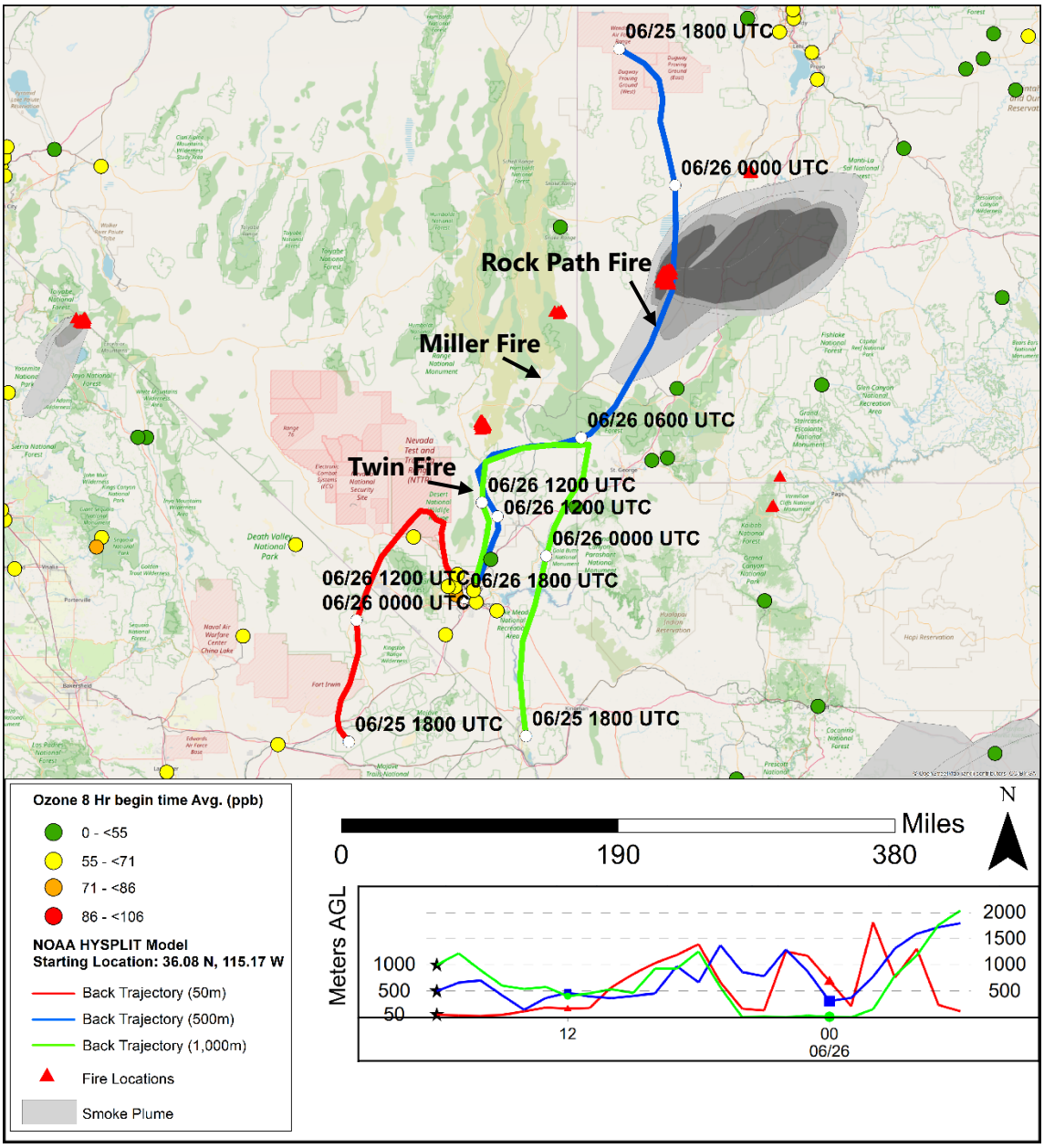

Figure 3-7. 24-hour HYSPLIT back trajectories with smoke from the Las Vegas Valley, ending on June 26, 2020, at 18:00 UTC (10:00 a.m. Local Time). HRRR 3 km back trajectories are shown for 50 m (red), 500 m (blue), and 1,000 m (green) above ground level. Eight-hour ozone averages are shown as circles (green to red), and HMS fires are shown as red triangles.

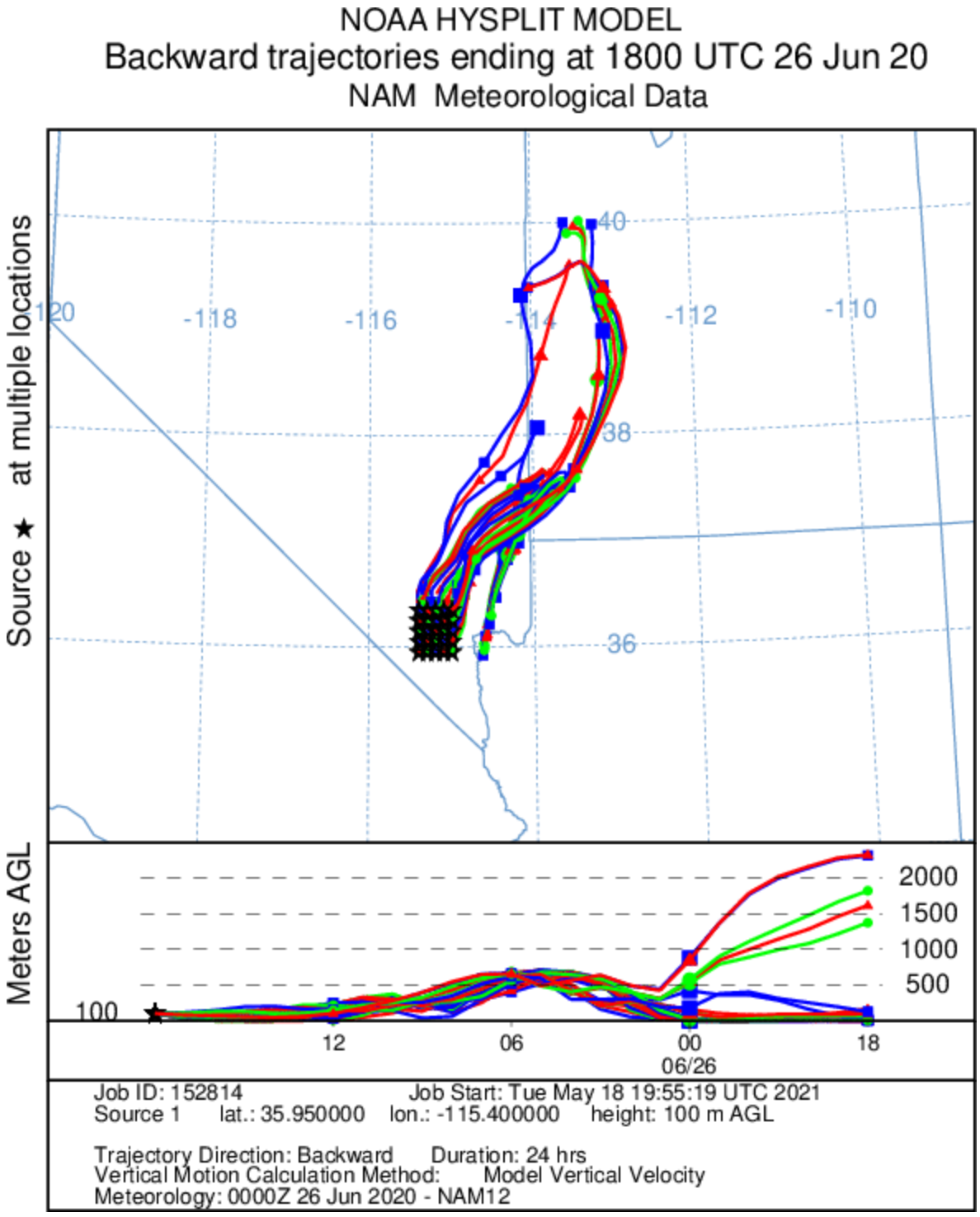

Figure 3-8. HYSPLIT back trajectory matrix. A 24-hour, NAM 12 km back trajectory matrix was initiated on June 26 at 18:00 UTC (10:00 a.m. Local Time) from Las Vegas Valley at 100 m above ground level.

The third trajectory approach used in this analysis was HYSPLIT trajectory frequency. In this option, a trajectory from a single location and height starts every three hours. Using a continuous 0.25 degree grid, the frequency of trajectories passing through each grid cell is totaled and then normalized by the total number of trajectories. **Figure 3-9** shows a 24-hour backward trajectory frequency plot starting from the Las Vegas Valley at 100 m AGL on June 26, 2020. The trajectory frequency plot yields similar results as those from the previous two approaches; transported air impacting the Las Vegas Valley on June 26, 2020, came in part from western Utah, over the Rock Path Fire and close to the two fires burning in Nevada. Air was also transported from the southeast of the Las Vegas Valley.

Forward trajectories starting on 03:00 UTC on June 26 were run for each of the three fires in question; from the Rock Path Fire location in Utah (**Figure 3-10**); from the Twin Fire in Nevada (**Figure 3-11**); and from the Miller Fire in Nevada (**Figure 3-12)**. The common initiation time of 03:00 UTC was based on archived radar images that show high reflectivity (i.e., possible lightning and thunderstorms) in the areas of the Rock Path, Twin, and Miller Fires from 20:00 UTC on June 25 to 06:00 UTC on June 26 (see Section 3.1.2 for more details). The starting heights were chosen between 100 and 500 meters to show regional transport from these fires. Vertical profiles of these fires were unknown so we chose 1,000 m for the Rock Path Fire, which was the largest fire and merged with an already burning fire on June 25 (see Section 3.2.1 for more details). Starting heights of the Twin and Miller fires at 100-250 m were estimated based on their size, biomass burned, and any images of the fire (example in Section 3.1.4). These trajectories show that air was transported from each of these three fires to Clark County throughout the day on June 26. These forward trajectories, combined with the back trajectories shown above, further support the transport of smoke from the Twin, Miller, and Rock Path fires to Clark County on June 25-26.

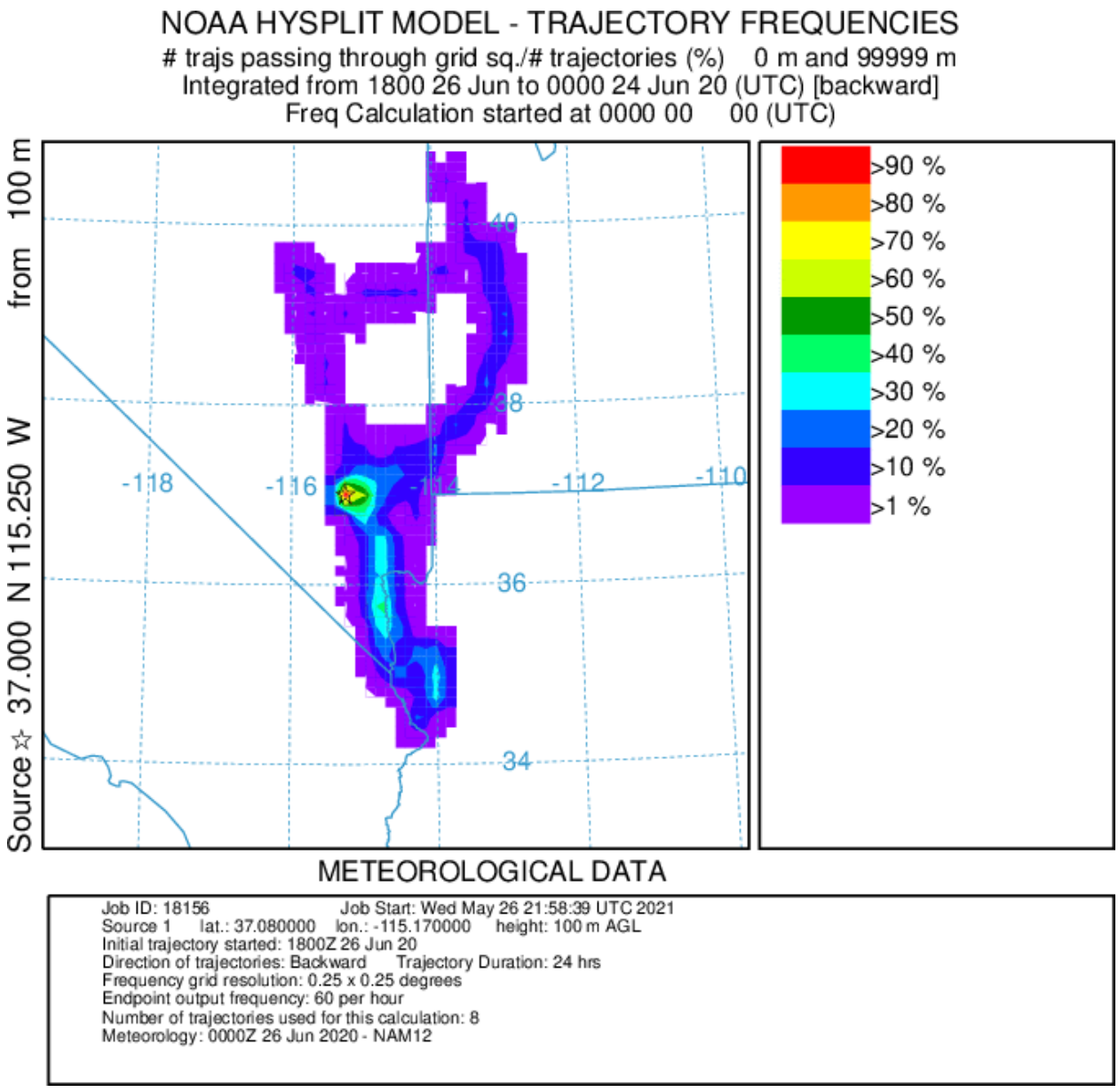

Figure 3-9. HYSPLIT back trajectory frequency. A 24-hour, NAM 12 km frequency of back trajectories was initiated on June 26 at 18:00 UTC (10:00 a.m. Local Time) from the Las Vegas Valley at 100 m above ground level. The colors within the frequency plot indicate the percentage of trajectories that pass through a grid square.

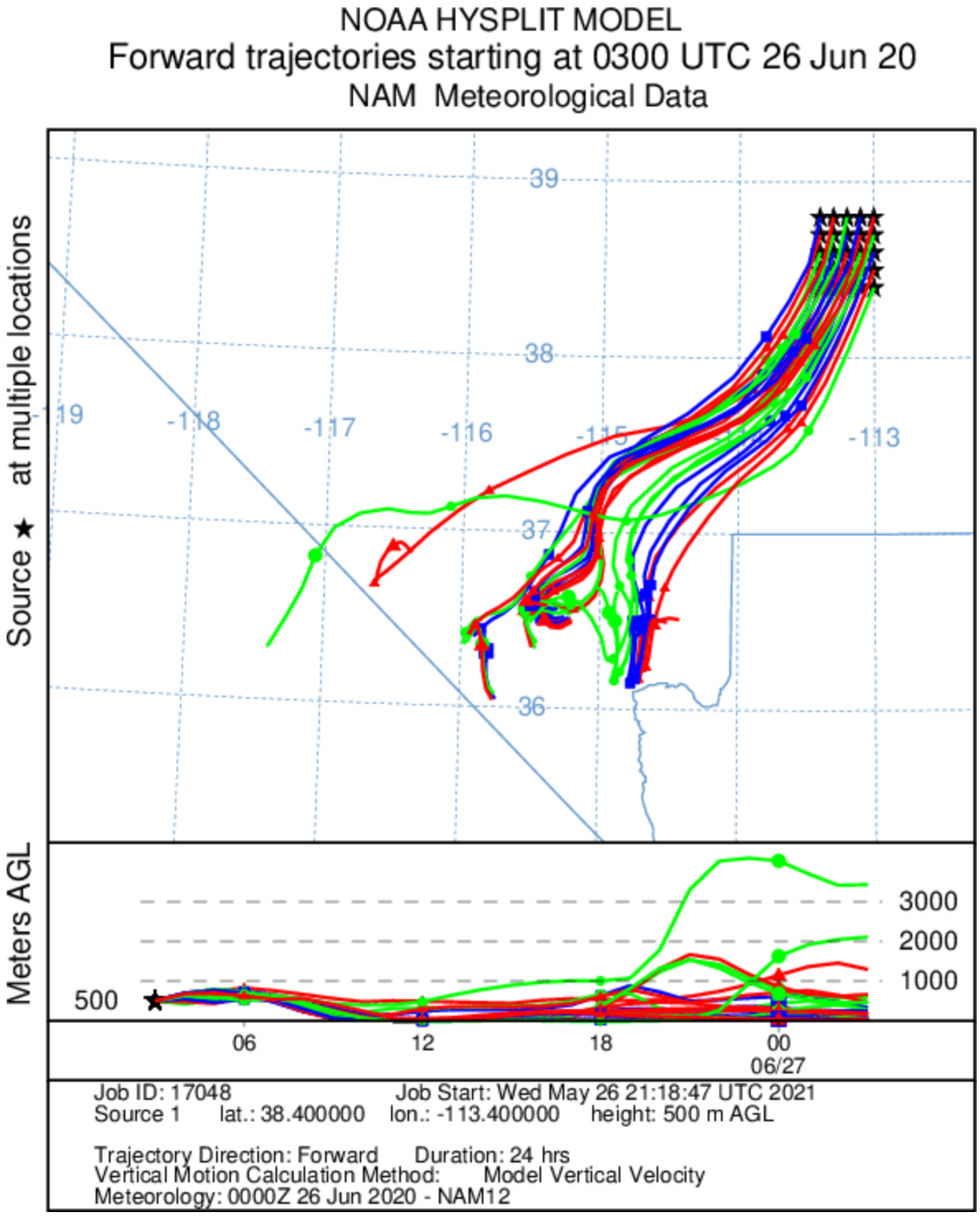

Figure 3-10. HYSPLIT forward trajectory matrix. A 24-hour, NAM 12 km forward trajectory matrix was initiated on June 26, 2020, at 03:00 UTC (7:00 p.m. June 25, local time) from the Rock Path Fire at 500 m above ground level.

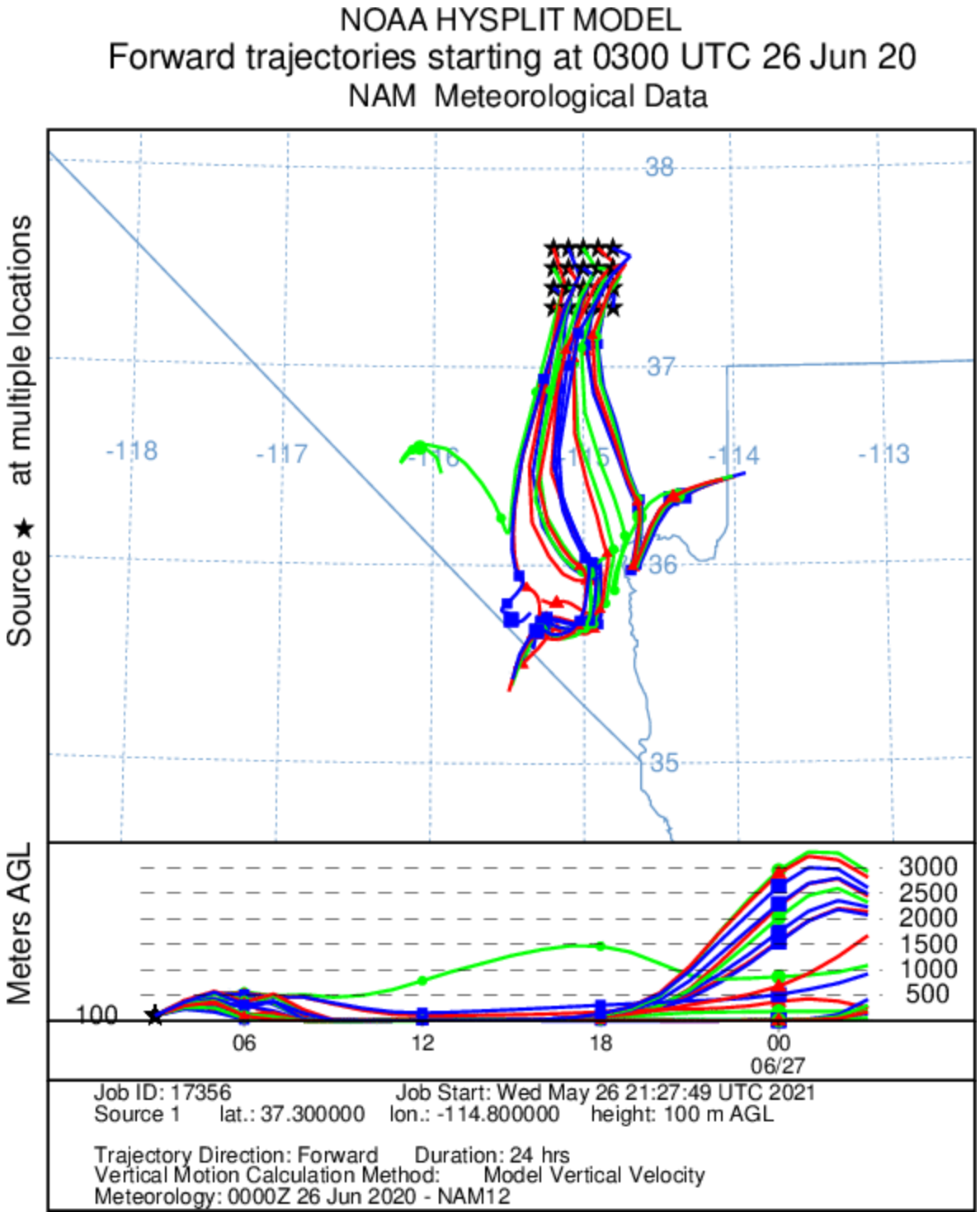

Figure 3-11. HYSPLIT forward trajectory matrix. A 24-hour, NAM 12 km forward trajectory matrix was initiated on June 26, 2020, at 03:00 UTC (7:00 p.m. June 25, local time) from the Twin Fire at 100 m above ground level.

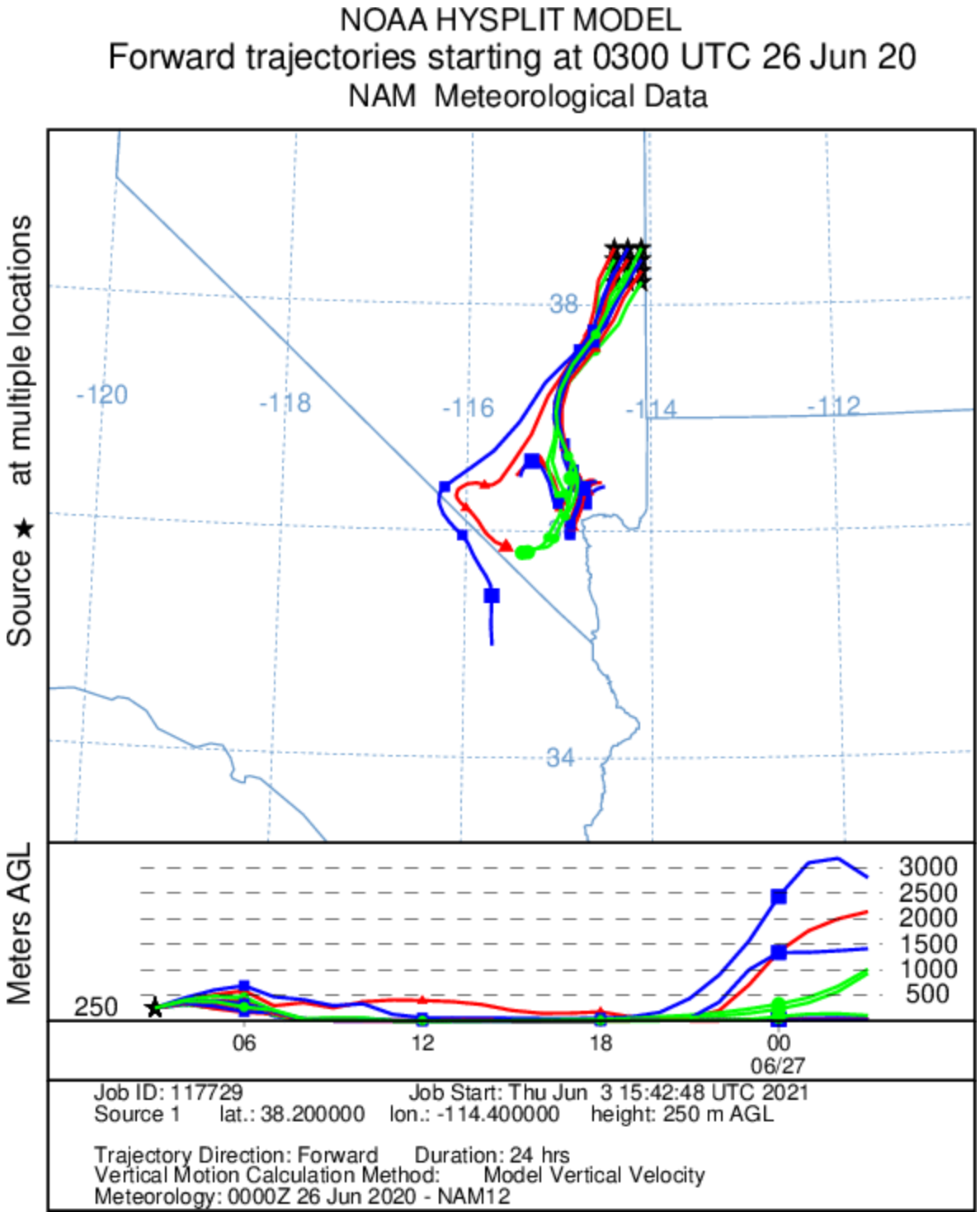

Figure 3-12. HYSPLIT forward trajectory matrix. A 24-hour, NAM 12 km forward trajectory matrix was initiated on June 26, 2020, at 03:00 UTC (7:00 p.m. June 25, local time) from the Miller Fire at 250 m above ground level.

3.1.4 Media Coverage and Ground Images

News and environmental organizations provided coverage of the fires burning in Nevada and Utah that contributed to smoky conditions on June 26. The Bureau of Land Management (BLM) in Nevada posted multiple Facebook updates, like that shown in Figure 3-13, on June 26 and 27 following the progression of the Miller Fire and the Twin Fire while they were concurrently burning across BLM-managed land in Nevada (https://www.facebook.com/BLMNevada/posts/3561289063899939, https://www.facebook.com/BLMNevada/posts/3564046753624170, https://www.facebook.com/BLMNevada/posts/3565058360189676).

Figure 3-13. Facebook post by the Bureau of Land Management (BLM), Nevada, showing a photo of the Miller Fire along with updates on the size of and weather affecting the Miller Fire and the Twin Fire burning in Nevada. The post was added on June 27, 2020.

Fire reports for the Miller Fire and the Twin Fire were also listed in the *Reno Gazette Journal*, a local news source in Nevada (https://data.rgj.com/fires/incident/6809/miller-fire/, https://data.rgj.com/fires/incident/6808/twin-fire/).

Fox13Now, a Salt Lake City news station, reported on the Rock Path Fire burning across the border near Milford, Utah (https://www.fox13now.com/news/local-news/multiple-wildfires-burning-in-central-southern-utah). At the time of the article, the fire had an "estimated size of more than 20,000 acres" and was only 25% contained.

Ground images from the Clark County Department of Environment and Sustainability DAQ's visibility cameras, located on the roof of the M Hotel in Las Vegas, show the smoky conditions that persisted on June 26 (Figure 3-14). When compared to images taken on a clear day (May 21, 2020, Figure 3-15), the June 26 images show reduced visibility and an opaque gray haze in every direction due to wildfire smoke.

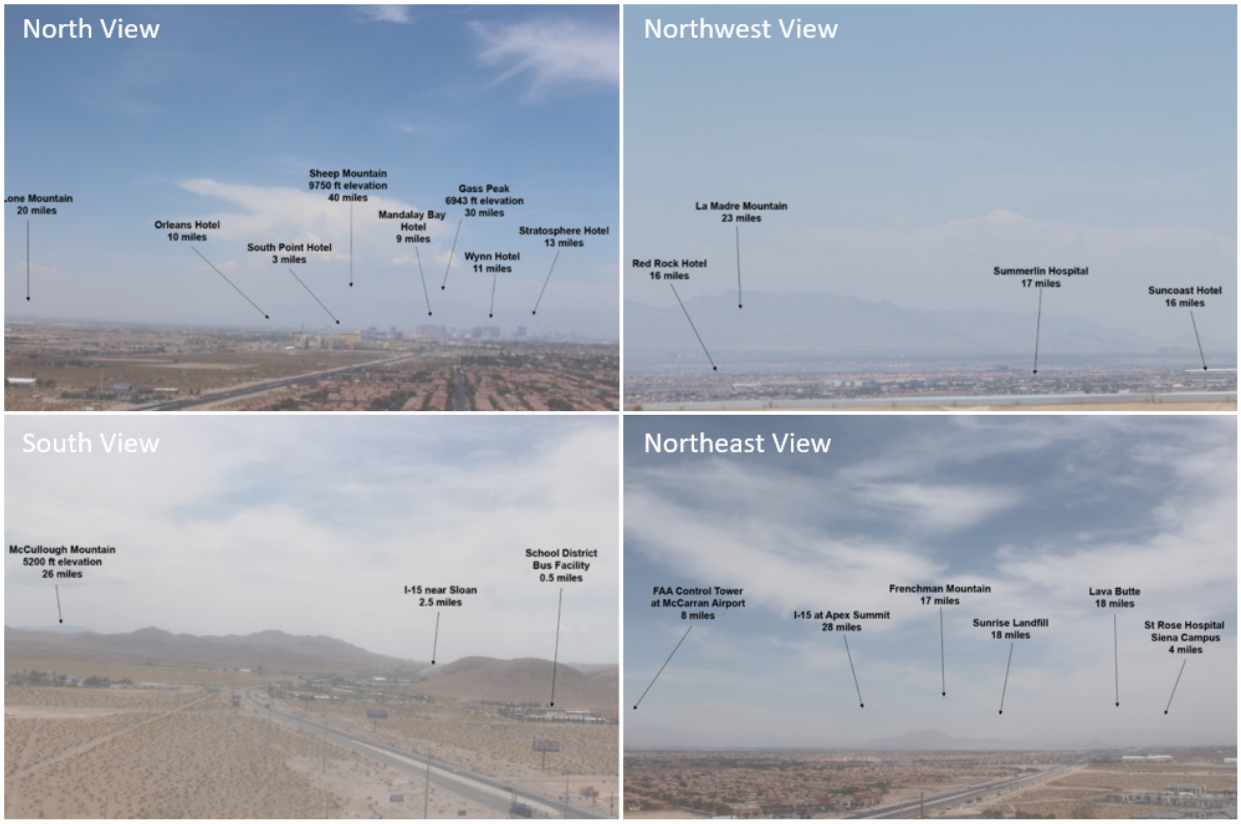

Figure 3-14. Visibility images taken on June 26, 2020, from webcams set up in Clark County. Each image is labeled with the viewing direction and landmarks.

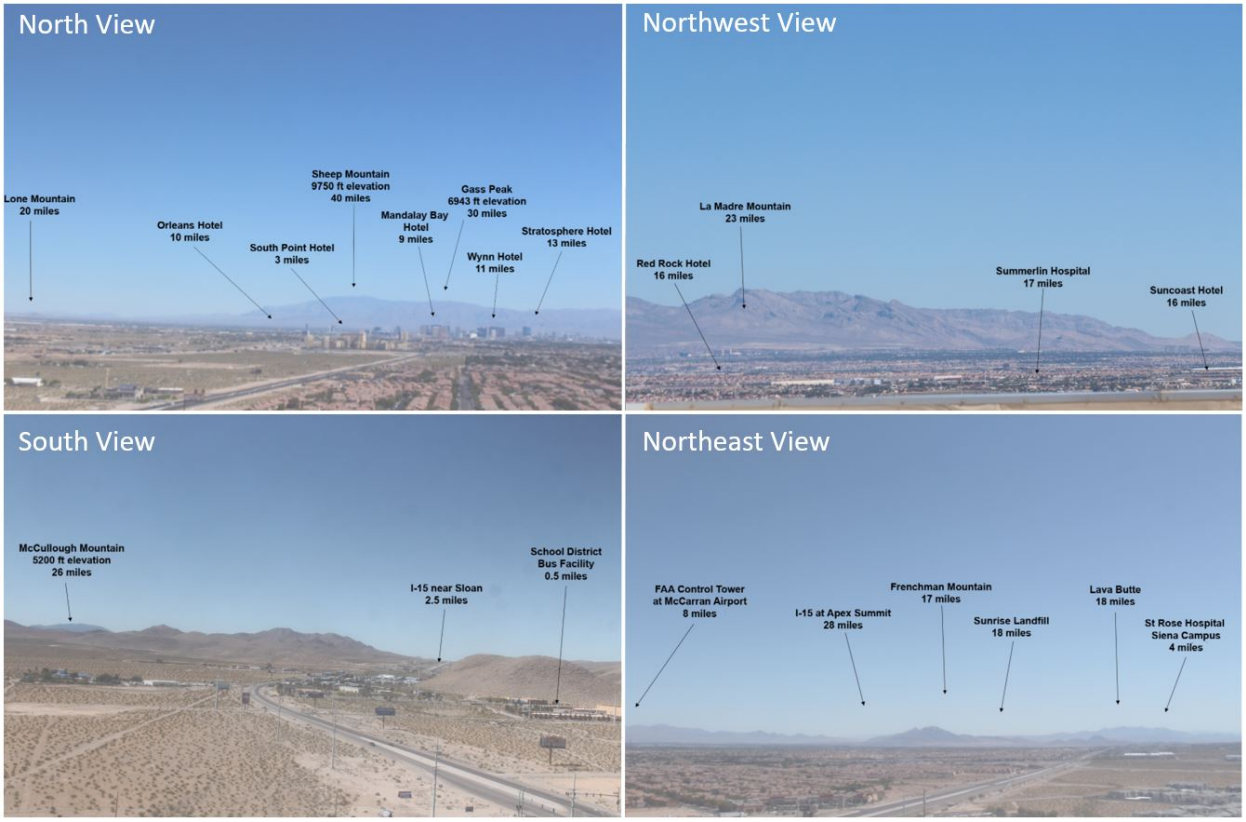

Figure 3-15. Visibility images taken on a clear day (May 21, 2020) from webcams set up in Clark County. Each image is labeled with the viewing direction and landmarks.

3.2 Tier 2 Analyses

This exceptional event demonstration meets the clear causal relationship criterion of the Exceptional Events Rule through a Tier 3 weight of evidence showing. EPA guidance says that "As part of the weight of evidence showing for the clear causal relationship rule element [for a tier 3 demonstration], air agencies should explain how the events, monitor and exceedance compare with the key factors outlined in Section 3.5.1 [Evidence that the Event, Monitor(s), and Exceedance Meet the Key Factors for Tier 2 Clear Causal Analyses]. The relationship of the event to the Tier 2 key factors may help inform the amount of additional information that will be needed to support Tier 3 analyses…") (U.S. Environmental Protection Agency, 2016). Tier 2 analyses include two key factors—Q/D analysis and comparison of event ozone concentrations with non-event concentrations—and select additional evidence to show that the fire emissions affected the monitor. This section of the demonstration presents the Tier 2 analysis results, which were used to guide the Tier 3 analyses. The Tier 2 results

are consistent with the Tier 3 analyses, and both sets of analyses contribute to the weight of evidence for the June 26 exceptional event.[3]

3.2.1 Key Factor #1: Q/d Analysis

The exceptional event guidance (U.S. Environmental Protection Agency, 2016) describes a method used to relate the quantity of smoke emissions and distance of the fire to an exceeding monitor. The resulting quantity, called Q/d, may be used to screen fires that meet a conservative threshold of air quality impacts.[4] This section provides the results of the Q/d analyses for fires that were likely to have contributed to the June 26, 2020, ozone event in Clark County.

Based on media coverage, transport analysis, and ground/satellite-based analyses described in Section 3.1, the Rock Path Fire in Utah and the Twin and Miller fires in Nevada likely caused smoky conditions and high ozone concentrations in Clark County, Nevada. **Figure 3-16** shows large fires burning near Clark County on June 26, which includes the Rock Path, Miller, and Twin fires. **Table 3-3** shows agency data available for the Nevada and Utah wildfires (as of June 2021). All three fires were reported to have started on June 25 and 26 in very dry regions and burned mostly grass, brush, and chaparral. All fires were wind-driven and expanded rapidly within the first 24 hours; the Rock Path Fire connected with the Antelope Fire and was renamed as the merged Rock Path Fire. The Rock Path Fire and the Miller Fire were caused by lightning storms, and the cause of the Twin Fire is unknown (likely also lightning storms based on meteorology and the close vicinity to the Miller Fire). Note that the Miller Fire, per InciWeb, was first reported June 26 in the afternoon, which makes it too late to effect ozone in Clark County. However, this is likely when the first incident report was created, not when the fire actually started. Because this was a lightning-initiated fire, and there were no storms in Nevada during the day on June 26, we suggest that the radar images from Section 3.1.2 provide the best estimate of when the Miller Fire actually started. For the Miller Fire to be (1) burning by 2:45 p.m. on June 26, and (2) lightning-initiated, the fire would have needed to start the night before; likely between 5-6 p.m. on June 25 based on radar reflectivity. Further information for each fire is available at the links below.

- Rock Path Fire: **https://utahfireinfo.gov/2020/06/27/rock-path-fire-update-6-27-2020/**
- Miller Fire: **https://inciweb.nwcg.gov/incident/6809/**

[3] As noted in the ozone exceptional event guidance (U.S. Environmental Protection Agency, 2016), a Tier 3 demonstration must be presented when "the relationship between the wildfire-related emissions and the monitored exceedance or violation cannot clearly be shown using Tier 1 or Tier 2 analyses." Therefore, while the analyses presented in Section 3.2 provides evidence that is supportive of a clear causal relationship between the fires identified and the monitored exceedance, these analyses alone are not expected to be sufficient to demonstrate such a relationship in the absence of the Tier 3 analyses.

[4] Specifically, fires with a Q/d value meeting the 100 tons/km threshold may qualify for a tier 2 demonstration of a clear causal relationship. However, this threshold is insufficient to identify all cases where ozone impacts from smoke may have occurred. Pages 16-17 of the guidance state "To determine an appropriate and conservative value for the Q/D threshold (below which the EPA recommends Tier 3 analyses for the clear causal relationship), the EPA conducted a review… The reviews and analyses did not conclude that particular O_3 impacts will always occur above a particular value for Q/D. For this reason, a Q/D screening step alone is not sufficient to delineate conditions where sizable O_3 impacts are likely to occur." (U.S. Environmental Protection Agency, 2016).

- Twin Fire: https://inciweb.nwcg.gov/incident/6808/

By June 26, 2020, these fires had burned approximately 42,000 acres according to the Incident Information System (InciWeb) and the Utah Fire Info estimates. The total size of the fires amounted to 50,560 acres. The Rock Path and Twin fires were reported containment by July 2020, but the Miller Fire had no containment date as of June 2021.

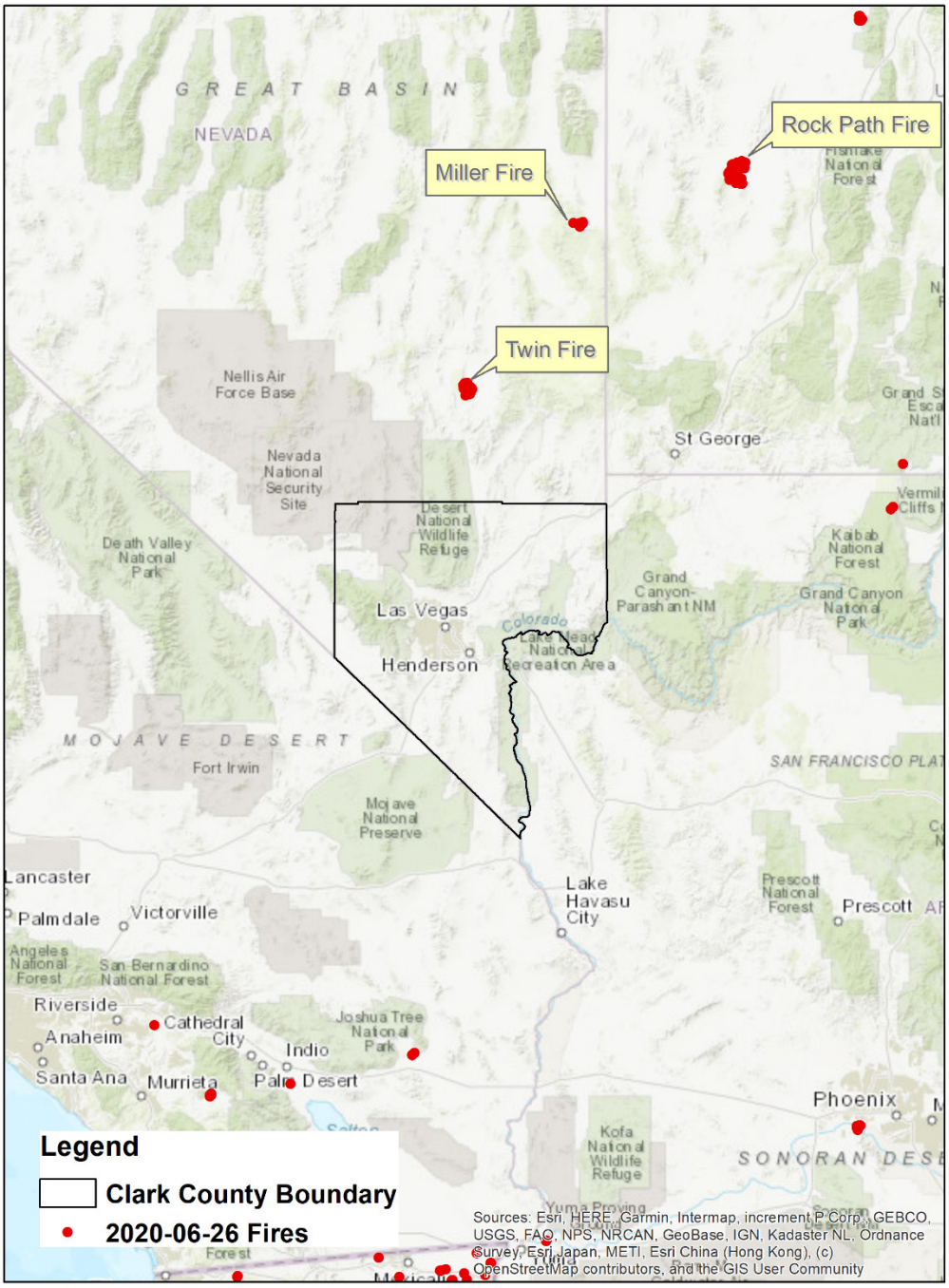

Figure 3-16. Large fires burning on June 26, 2020, in the vicinity of Clark County. The Clark County boundary is shown in black.

Table 3-3. Fire data for the Rock Path, Miller, and Twin fires associated with the June 26 exceptional event. Information includes start/containment date, cause of the fire, and the total reported acres burned. NA means a date has not officially been determined.

Fire Name	Start Date	Contained Date	Cause	Total Area Burned (acres)
Rock Path Fire	6/25/2020	7/1/2020	Lightning	20,941
Miller Fire	6/26/2020	NA	Lightning	4,519
Twin Fire	6/25/2020	7/14/2020	Unknown	25,100

Key factor #1 for a Tier 2 demonstration requires an analysis of wildfire smoke emissions from a qualifying fire and the distance of the fire to the affected monitor or monitors. To identify qualifying fires, the guidance "recommends generating 24-hour back trajectories from the affected O_3 monitoring site(s) beginning at each hour of these two or three dates" (U.S. Environmental Protection Agency, 2016). Three dates would be used only if the 8-hour averaging period for the daily maximum 8-hour ozone data includes hours falling over two dates (i.e., the 8-hour average includes at least 11 p.m. and midnight on two distinct calendar days). For this demonstration, 24-hour HYSPLIT back trajectories were generated from the monitor location starting on each hour of the day of the exceedance, as well as the day prior to the exceedance (June 25 and 26). The guidance states that "…fires that are close to any of these back trajectories" may be used to calculate Q/d (U.S. Environmental Protection Agency, 2016). To identify fires that fall near the HYSPLIT trajectories, trajectories were buffered by a distance of 25% of the distance traveled by the trajectory, which is consistent with uncertainty reported for HYSPLIT trajectory modeling (Draxler, 1991). **Figure 3-17** shows the back trajectories and buffer of uncertainty from Clark County, Nevada on June 26. All fires falling within the uncertainty buffer of one or more trajectories were considered candidates for calculating Q/d. The Twin Fire was the only candidate fire selected using the Q/d method with the HYSPLIT trajectories shown in Figure 3-17, which were generated using NAM12 12 km resolution meteorology. However, additional analyses, including HYSPLIT trajectories generated using higher resolution (3 km) meteorological data (Figure 3-7), indicate that transport from near the Rock Path and Miller fires into Clark County on May 26 as well. To investigate the emissions and transport from those fires that, we conducted an extended Q/d analysis, which is provided in **Appendix A**.

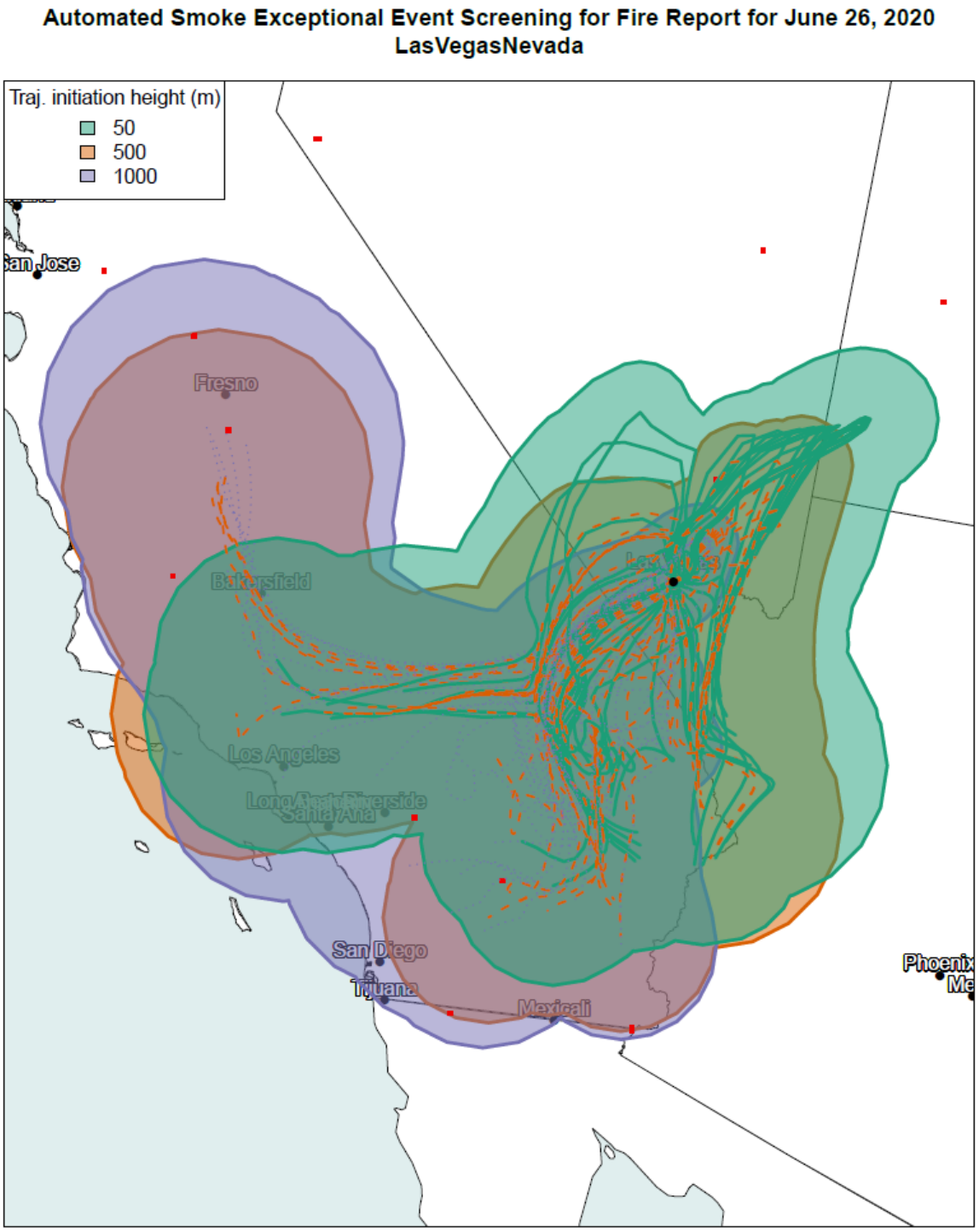

Figure 3-17. Q/d analysis. 24-hour back trajectories are shown as solid or dotted lines. The starting height of the back trajectory is indicated by the color. Uncertainty buffers, calculated as 25% of the distance traveled by the trajectory, are shown in colored polygons. Active fires on June 26 are shown as red squares. Fires falling within one or more uncertainty buffer(s) were used to calculate individual and aggregate Q/d values.

To calculate Q/d for the Twin Fire, the total daily emissions of NO_x and reactive VOCs (rVOCs) in tons is divided by the distance from the fire to impacted monitors. BlueSky Playground Version 3.0.1 (https://tools.airfire.org/playground/v3/) was used to estimate emissions of NO_x and VOCs for each fire on a daily basis for June 25 and 26. Daily fire growth was identified using agency reports or news reports citing official sources. The fire's location, as reported in InciWeb, was used to identify the distance to the impacted monitors and fuel bed type. Emissions calculations were based on very dry conditions.

EPA guidance recommends that an event may qualify for a Tier 2 demonstration if the Q/d value for a fire, or the aggregate Q/d across multiple fires, exceeds a conservative value of 100 tons/km. Daily Q/d results indicate that significant emissions of NO_x and rVOCs occurred from the Twin Fire on June 26, 2020 (Table 3-4). Furthermore, the analyses presented in Appendix A indicate substantial emissions from the Rock Path and Miller Fires. However, the emissions were not large enough to reach the Q/d threshold of 100 tons/km for a Tier 2 demonstration, and it was determined that Tier 3 analyses were needed to demonstrate a clear causal relationship.

The results of the Q/d analysis presented in this section, as well as the extended emissions transport assessment included in Appendix A, agree with and further strengthen the conceptual model and Tier 3 weight of evidence of a clear causal relationship between the identified wildfires smoke emissions and the monitored ozone exceedance identified in this demonstration.

Table 3-4. Daily growth, emissions, and Q/d for the fires with potential smoke contribution on June 26, 2020. Growth data shown were obtained from agency estimates available from InciWeb. Column "E (Tons)" represents the sum of NO_x and Reactive VOC emissions. Fire area used is based on the overnight area estimate reported on the morning of June 27, which approximately represents the total growth of the fire over June 26. Typical overnight flight times can range from 19:00 to 04:00 local time, and daily growth can only be approximated. A more conservative estimate of emissions, based on fire growth through approximately 4:00 p.m. on June 26, is presented in Appendix A, as a supplement to the Q/d value presented here in accordance with EPA guidance (U.S. Environmental Protection Agency, 2016).

Fire Name	Area (Acres)	Daily Growth (Acres)	NO_x (Tons)	VOCs (Tons)	Reactive VOCs (Tons)	E (Tons)	Distance (Km)	Q/d (Tons/km)	Fuel Loading	Fire size data source
Twin Fire	15,750	15,750	62.0	325.8	195	387.8	90	2.9	Creosote bush shrubland	https://inciweb.nwcg.gov/incident/6808/

3.2.2 Key Factor #2: Comparison of Event Concentrations with Non-Event Concentrations

Another key factor in determining whether the June 26, 2020, exceedance event is exceptional is comparison between event ozone concentrations and non-event concentrations via percentile and rank-order analysis. Table 3-5 shows June 26, 2020, concentrations as a percentile in comparison with the last six years of data (with and without the other proposed 2018 and 2020 EE days included) at each site in Clark County. For Paul Meyer, the monitoring site that showed a NAAQS standard exceedance on June 26, the ozone concentration is ranked above the 99th percentile when compared to the last six years of data, even with all other proposed 2018 and 2020 exceptional event days included. Without the other exceptional event days included, the percentile increases to 99.6. To confirm that the calculated percentiles are not biased by non-ozone season data, Table 3-6 shows the June 26 percentile ranks for Paul Meyer in comparison with the last six years of ozone season (May to September) data. With all other 2020 EE dates included, June 26 ranks in the 97th percentile when compared to other ozone seasons. With all other 2020 EE dates excluded, the percentile for June 26 increases to above the 99th percentile. The ozone season percentile rank for June 26 at Paul Meyer (with and without other EE dates) confirms that the June 26 exceptional event included unusually high concentrations of ozone when compared with the last six years of data and the last six ozone seasons.

We also compared the rank-ordered concentrations at the Paul Meyer site for 2020. As shown in Figure 2-3, 2020 did not see atypically low ozone concentrations that might bias our rank-ordered analysis for June 26. Table 3-7 shows the rank-ordered ozone concentrations for 2018 through 2020 and the design values for 2020, with the proposed 2018 and 2020 exceptional events included. With all other 2020 EE dates included, June 26 is not one of the top five highest ozone days in 2020. However, with all other 2020 EE dates excluded, June 26 is the second highest ozone day in 2020.

For further comparison with non-event ozone concentrations, Table 3-8 shows five-year (2015-2019) MDA8 ozone statistics for the week before and after June 26. This two-week window analysis at Paul Meyer shows that MDA8 ozone concentrations on June 26, 2020, were well above the average and at the 95th percentile compared with the last five years of data.

The percentile, rank-ordered analyses, and the two-week window analysis indicate that on June 26, 2020, the Paul Meyer monitoring site showed unusually high ozone concentrations compared with non-event concentrations. This conclusion supports a key factor, suggesting that June 26 was an exceptional event in Clark County, Nevada.

Table 3-5. Six-year percentile ozone. The June 26 exceptional event ozone concentration at the site is calculated as a percentile of the last six years with and without other 2018 and 2020 exceptional events included in the historical record.

AQS Site Code	Site Name	6-Year Percentile	6-Year Percentile w/o EE Dates
320030043	Paul Meyer	99.1	*99.6*

Table 3-6. Six-year, ozone-season percentile ozone. The June 26 exceptional event ozone concentration at the site is calculated as a percentile of the last six years' ozone season (May-September) with and without other 2018 and 2020 exceptional events included in the historical record.

AQS Site Code	Site Name	6-Year Percentile	6-Year Percentile w/o EE Dates
320030043	Paul Meyer	97.9	*99.1*

Table 3-7. Site-specific ozone design values for the Paul Meyer monitoring site. The top five highest ozone concentrations for 2018-2020 at Paul Meyer are shown, and proposed EE days in 2018 and 2020 are included.

Paul Meyer Rank	2018	2019	2020
Highest	79	74	79
Second Highest	76	72	78
Third Highest	75	70	77
Fourth Highest	75	69	77
Fifth Highest	74	69	76
Design Value	73		

Table 3-8. Two-week non-event comparison. MDA8 ozone concentrations at Paul Meyer on June 26, 2020, are shown in the top row. Five-year (2015-2019) average MDA8 ozone statistics for June 12 through July 10 are shown for each affected site around Clark County to compare with the event ozone concentrations.

	Paul Meyer 320030043
Jun. 26	73
Mean	63
Median	63
Mode	64
St. Dev	7
Minimum	46
95 %ile	73
99 %ile	74
Maximum	75
Range	29
Count	97

3.2.3 Satellite Retrievals of Pollutant Concentrations

Satellite retrievals of pollutants associated with wildfire smoke, such as AOD, CO, and NO_x, can provide evidence that smoke was present at a monitoring site. We examined maps of Multi-Angle Implementation of Atmospheric Correction (MAIAC) AOD from the MODIS instrument onboard the Aqua and Terra satellites, CO retrievals from the Atmospheric Infrared Sounder (AIRS) instrument onboard the Aqua satellite, and nitrogen dioxide (NO_2) retrievals from the Ozone Monitoring Instrument (OMI). AOD images did not provide conclusive evidence for this demonstration, so they have been moved to Appendix B for completeness.

CO measurements at 500 hPa from AIRS shows slightly enhanced CO concentrations at 500 hPa over southern and central Nevada by June 26 (Figure 3-18) when compared with concentrations over Las Vegas. Figure 3-19 shows a zoomed-in view of CO over Las Vegas on June 26 and slightly higher CO can be seen to the north of Clark County when compared with the Las Vegas Valley.

We additionally examined OMI retrievals of tropospheric NO_2 (Figure 3-20). Near the Twin, Miller, and Rock Path fires in Nevada and Utah, we see slightly enhanced NO_2. However, overall neither the CO nor the NO_2 satellite images provide significant evidence of smoke at 500 hPa or in the

tropospheric column. This is likely because the fires didn't inject smoke up to 500 hPa or enough emissions to impact the total column significantly.

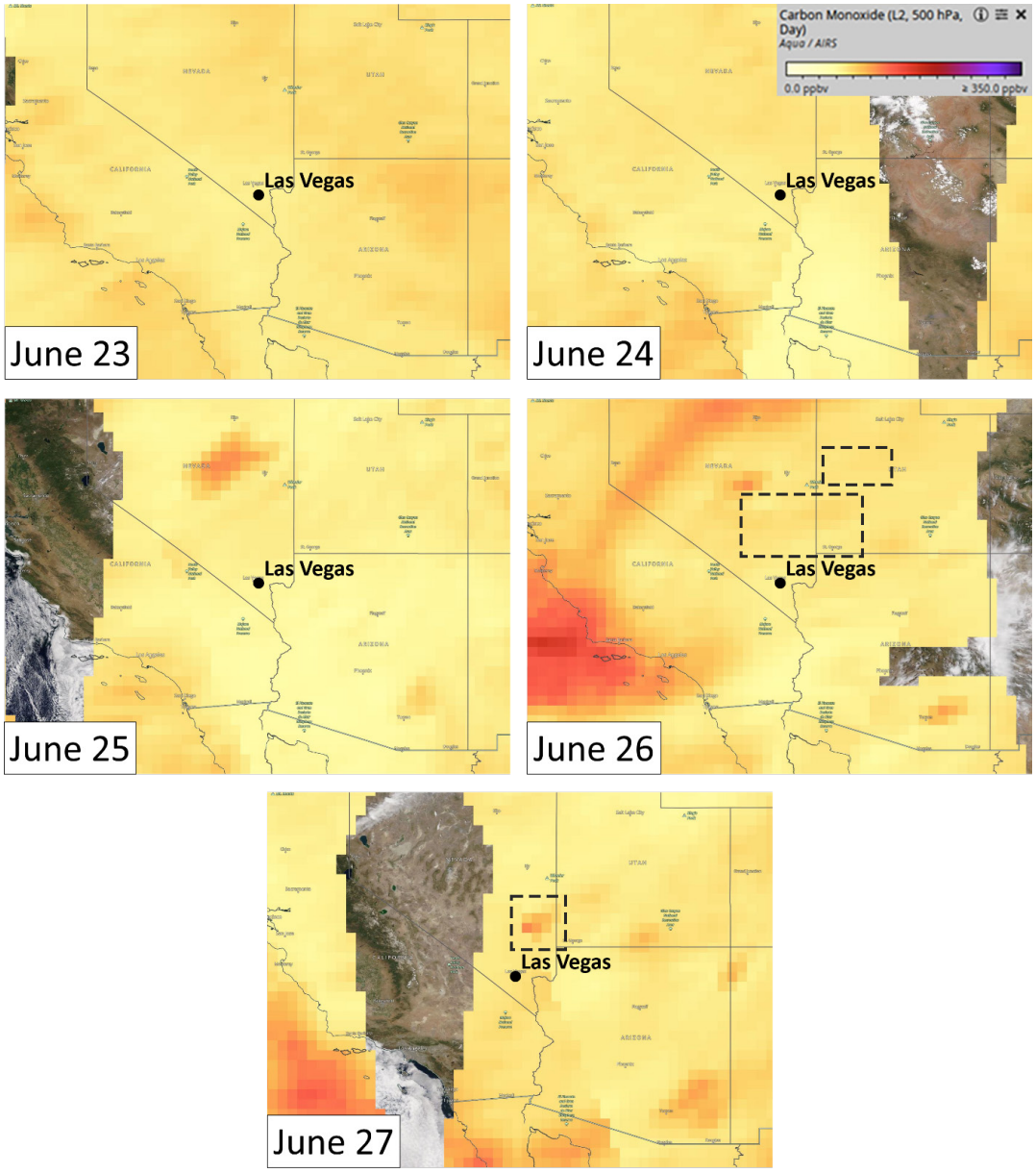

Figure 3-18. MODIS Aqua AIRS CO retrievals for June 23 – 27, 2020. These images show the retrievals for the three days before exceptional event, on the day of the exceptional event (June 26), and the day after the exceptional event. Colors range from low CO (yellow) to high CO (purple). The gray dashed boxes show possible effects from the Rock Path, Miller, or Twin fires.

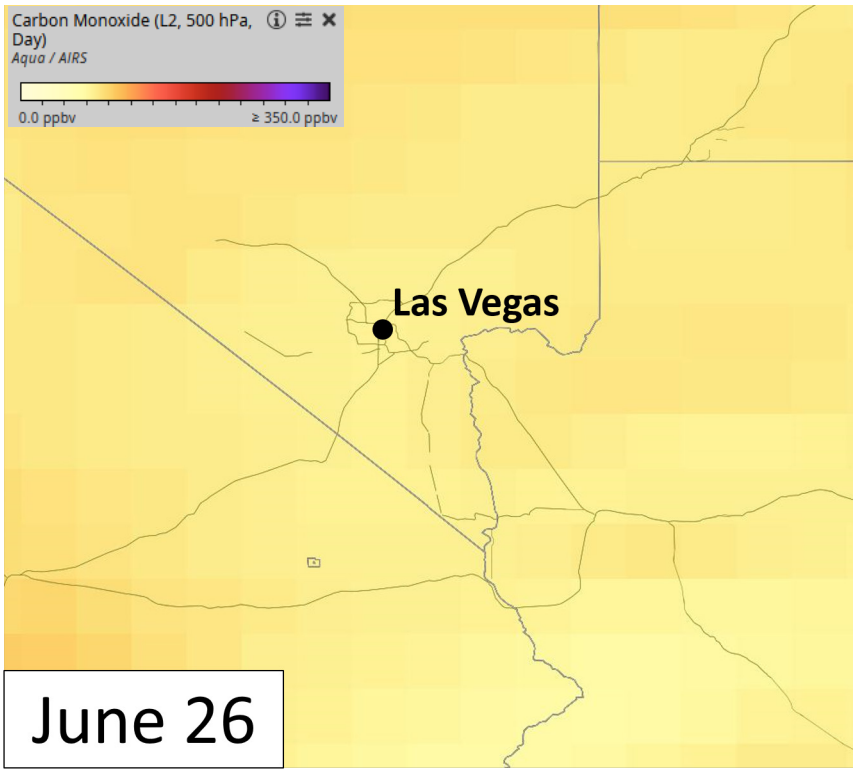

Figure 3-19. A zoomed-in view (over Clark County) of the Aqua AIRS CO retrieval during the exceptional event on June 26, 2020. Colors range from low CO (yellow) to high CO (purple).

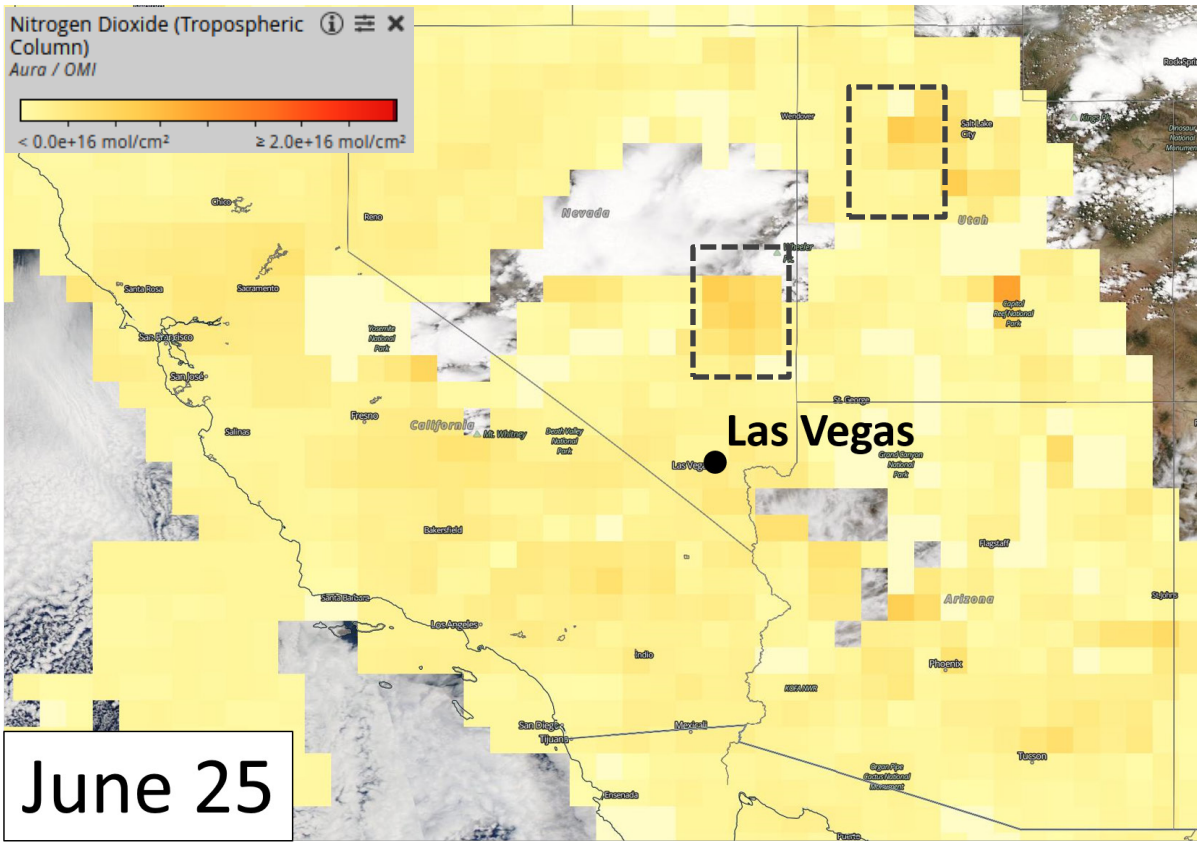

Figure 3-20. OMI Aura NO_2 retrieval for the day before the exceptional event on June 26, 2020. The gray dashed boxes show possible effects from the Rock Path, Miller, or Twin fires.

3.2.4 Supporting Pollutant Trends and Diurnal Patterns

Ground measurements of wildfire plume components (e.g., $PM_{2.5}$, CO, NO_x, and VOCs) can be used to further demonstrate that smoke impacted ground-level air quality if enhanced concentrations or unusual diurnal patterns are observed. If $PM_{2.5}$, CO, NO_x, and VOCs were enhanced at the time the smoke plume arrived in Clark County, these measurements would provide additional supporting evidence of smoke impacts in Clark County. Limited data on supporting pollutants is available from the exceedance site, Paul Meyer. We examined concentrations of $PM_{2.5}$ at the exceedance site, as well as concentrations of CO, NO, NO_2 and TNMOC at other monitoring sites in Clark County, to identify abnormally high concentrations of supporting pollutions and deviations from expected diurnal patterns during the event period.

Figure 3-21 shows an overall view of pollutants measured around Clark County in the week before and after the June 26 event. Ozone and $PM_{2.5}$ are the only pollutants with observations available at the exceedance site. On June 26, the peak daily concentrations of $PM_{2.5}$ are higher at the exceedance-affected monitoring site and other nearby sites when compared to the previous week. Similar higher spikes in $PM_{2.5}$ levels were exhibited on two days in the week following the event. This

increased concentration of $PM_{2.5}$ on the event date provides support for the presence of smoke at the surface. Observations of CO, NO, NO_2 and TNMOC are only available from non-exceedance sites, and all available data is shown in the bottom three panels of Figure 3-21. Although pollutant concentrations at the non-exceedance sites may offer information on county-wide pollutant anomalies, these sites should not be considered a direct proxy for conditions at the Paul Meyer site. CO concentrations at the Green Valley site appear elevated between June 25–27 compared to surrounding dates, and this is examined more thoroughly in the discussion below. Concentrations of NO, NO_2 and TNMOC are similar in magnitude on June 26 compared to nearby dates at all sites where data is available. The remainder of this section examines diurnal variations of supporting pollutants on a site-by-site basis to identify abnormalities in pollutant concentrations that indicate smoke influence in Clark County on June 26. Because less than one year of TNMOC data is available across sites in Clark County, this pollutant is not included in site-specific examinations below.

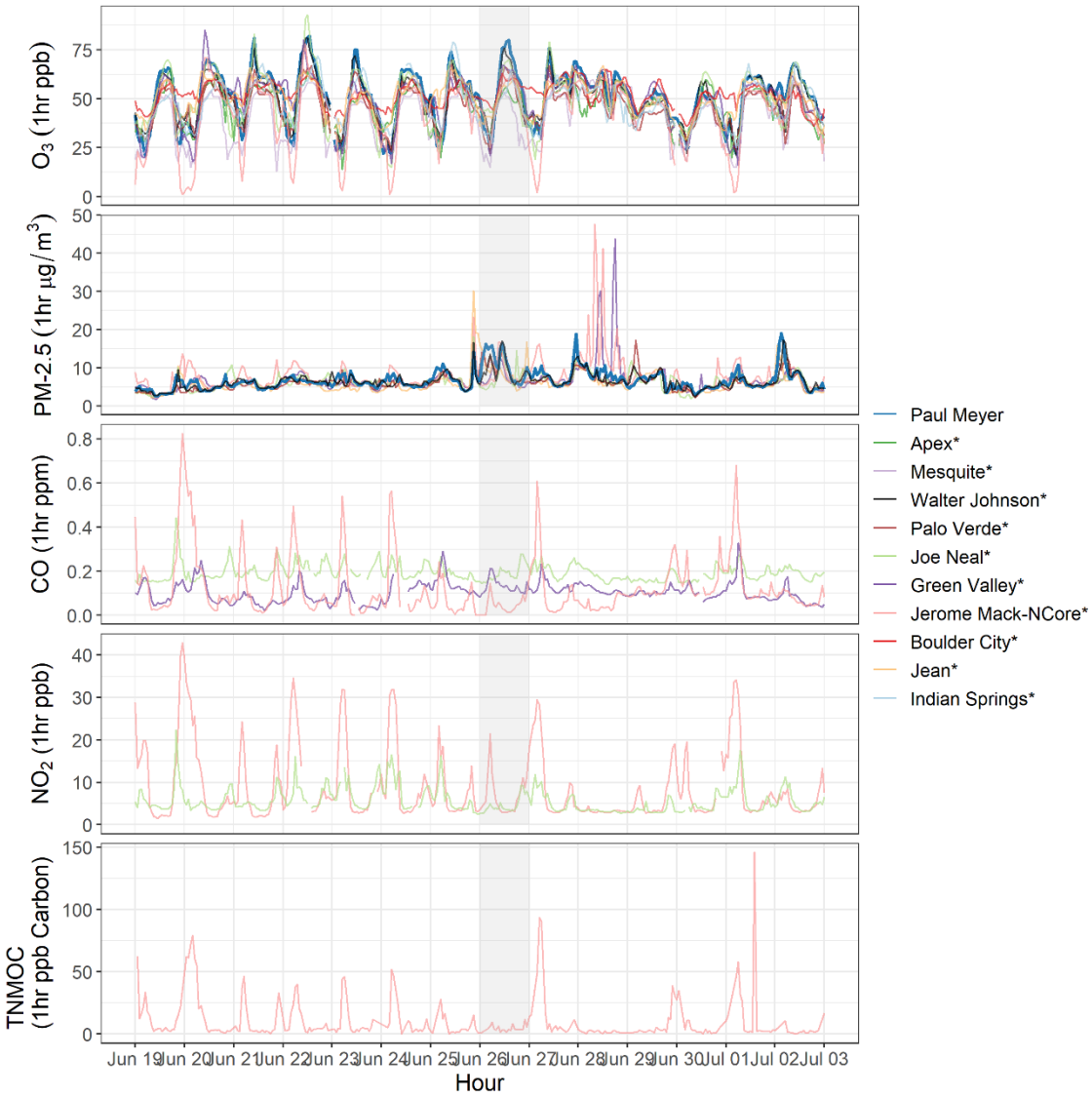

Figure 3-21. Hourly concentrations of ozone, $PM_{2.5}$, CO, NO_x, and TNMOC. The gray bar represents June 26. Paul Meyer is the only site with an ozone exceedance on June 26 (un-starred in legend). Ozone and $PM_{2.5}$ data are available at Paul Meyer. CO, NO_x and TNMOC data is available only other non-exceedance sites in Clark County.

Unusual diurnal patterns of supporting measurements can provide evidence that smoke impacted Clark County air quality. Figure 3-22 displays the diurnal profile and average seasonal diurnal profile of ozone and $PM_{2.5}$ alongside the 5th to 95th percentile range. Four years of $PM_{2.5}$ data and five years of ozone data is available at the Paul Meyer site. On a typical day, the diurnal profile of ozone shows a peak around midday and an overnight trough, while the diurnal profile of $PM_{2.5}$ has a distinct daytime trough. In contrast, $PM_{2.5}$ concentrations at the Paul Meyer site on June 26 showed an abnormal midday spike in line with the rise in ozone concentrations. The concentration of $PM_{2.5}$ at

the Paul Meyer site rose above the 95th percentile during two distinct periods on June 26, as well as on the night before the exceedance event. Ozone was well above average at its peak on June 26, and the concentration of ozone at the Paul Meyer site rose above the 95th percentile at its peak value for the day. These abnormally high $PM_{2.5}$ concentrations indicate that an unusual $PM_{2.5}$ source influenced concentrations at the Paul Meyer monitoring site on June 26. We address the source attribution of this feature in the following paragraphs.

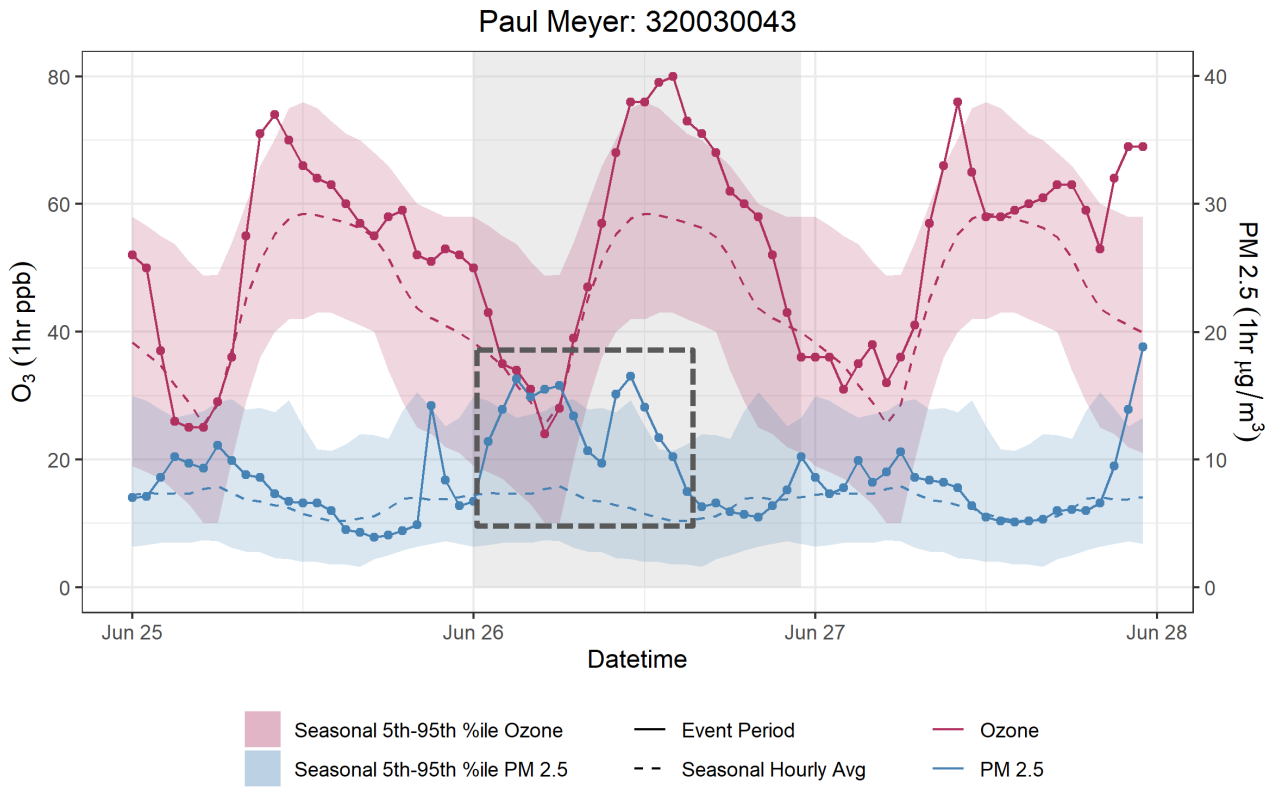

Figure 3-22. Diurnal profile of ozone (red) and $PM_{2.5}$ (blue) concentrations at Paul Meyer, including concentrations on June 26 (solid line) and the seasonal (May-Sept) average (dotted line). Shaded ribbons represent the 5th-95th percentile range. Four years of $PM_{2.5}$ data and five years of ozone data is available at Paul Meyer. We've highlighted the abnormally high $PM_{2.5}$ periods in a gray dashed box.

The ratio of PM_{10} to $PM_{2.5}$ concentrations was examined to determine if a dust event, which would have enhanced PM_{10} and $PM_{2.5}$ concentrations, was the main cause of the exceptional event. The ratio of PM_{10} to $PM_{2.5}$ was examined because a smoke event would have predominantly enhanced $PM_{2.5}$ concentrations. Figure 3-23 shows a time series of the ratio of $PM_{10}/PM_{2.5}$ concentrations from June 25 through June 28, with the five-year average ratio and 5th to 95th percentile also shown. During the June 26 event, the $PM_{10}/PM_{2.5}$ ratio rises, which—along with the increased total $PM_{2.5}$ concentrations—indicates that there was an abnormally large dust contribution to both PM_{10} and

$PM_{2.5}$ concentrations. These observations indicate that the air mass over Clark County on the night of June 25 was abnormal relative to typical local $PM_{2.5}$ and PM_{10} levels. The combination of trajectory and surface PM observations indicate that air was transported from outside of Clark County, where smoke plumes were mixed with dust from the wildfire source and desert regions within the transport footprint. HYSPLIT trajectories shown in Section 3.1.3 show that air arriving in Clark County on June 26 travelled from smoke sources in Utah and Nevada across desert regions with dust sources. This trajectory is confirmed by the arrival of dust in Clark County. A further analysis of speciation of $PM_{2.5}$ identifies biomass burning as a source of combustion that contributed to $PM_{2.5}$ concentrations in Clark County on June 26. This analysis is discussed in detail below.

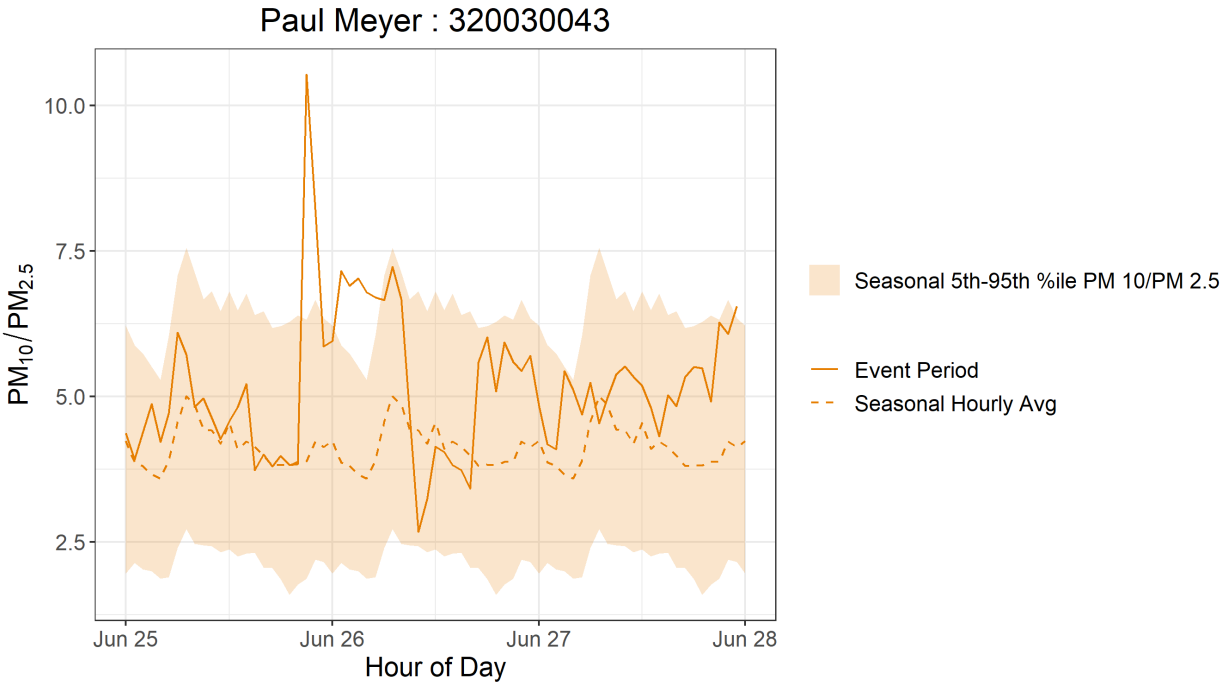

Figure 3-23. Ratio of $PM_{10}/PM_{2.5}$ concentrations at the exceedance site, Paul Meyer, during the June 26 event period. The five-year average $PM_{10}/PM_{2.5}$ ratio is displayed as a dotted line, and the 5^{th} to 95^{th} percentile range is shown as a shaded ribbon.

In **Figure 3-24**, the CO concentration recorded from June 25–27 is plotted alongside the diurnal average CO concentration and 5^{th} to 95^{th} percentile at the Green Valley monitoring site, which lies southeast of the Paul Meyer site (see Figure 2-2). One year of CO data is available at the Green Valley site. Daytime CO concentrations at Green Valley on June 25 and 26 were abnormally high compared to the expected diurnal trend, approaching the 95^{th} percentile near 1 p.m. local time on each date. Though an ozone exceedance did not occur at the Green Valley site, elevated measurements of CO on the event date supports the assertion that wildfire smoke affected the region on June 26, 2020.

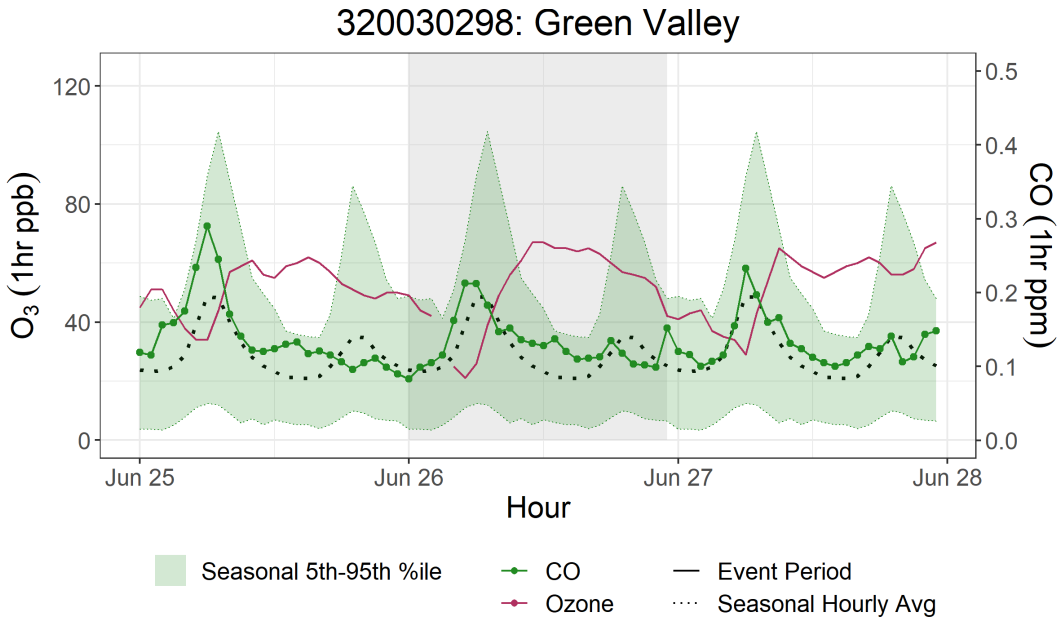

Figure 3-24. Ozone (red) and CO (green) concentrations for Green Valley on June 26. The dotted line shows the seasonal (May to Sept) average CO. The green shaded area indicates the seasonal 5th to 95th percentile values for statistical reference. One year of CO data is available at Green Valley.

Concentrations of NO_x are not available at the exceedance site, Paul Meyer. NO_x concentrations were examined at the two non-exceedance sites where data were available in Clark County on the days surrounding the June 26 event, and no significant trends were observed. Though concentrations of NO_x at these supporting sites can provide a view of abnormal concentrations on a regional scale, a lack of elevated NO_x should not be used a direct proxy for concentrations at the Paul Meyer site due to local variation. A plot of NO_x observations during the event period is included in Appendix C. Additionally, OC/EC data were inconclusive for June 26, but showed increasing values up to June 26, which could indicate wildfire influence. This analysis is also included in Appendix C.

Filter samples were also taken at the Jerome Mack (including a collocated sample) and Sunrise Acres monitoring sites in Clark County every three days during 2020. From these filter samples, concentrations of levoglucosan, a wildfire smoke tracer, were analyzed by the Desert Research Institute (DRI) via gas chromatography-mass spectroscopy (GC-MS). Levoglucosan is produced by the combustion of cellulose and is emitted during wildfire events, and can be transported downwind (Simoneit et al., 1999; Simoneit, 2002; Bhattarai et al., 2019). Levoglucosan has an atmospheric lifetime of one to four days before it is lost due to atmospheric oxidation, and it can therefore be used as a tracer of biomass burning (wildfires) far downwind from its source (Hoffmann et al., 2009; Hennigan et al., 2010; Bhattarai et al., 2019; Lai et al., 2014). In the Las Vegas region, residential wood combustion has historically not been a significant contributor to levoglucosan concentrations during the late summer timeframe (Kimbrough et al., 2016). Table 3-9 shows levoglucosan concentration,

uncertainty, and positive/negative detection certainty during the June 26 event. Table 3-9 also shows the average levoglucosan concentration from nineteen background days from 2018-2019, along with its standard deviation and propagated uncertainty at both sites for comparison. On these background days, no ozone exceedance was observed, and fire/smoke influence was minimal according to HMS. After smoke from the Rock Path, Miller, and Twin fires reached Clark County on June 26, non-zero levoglucosan concentrations and a positive detection are seen. Comparing to the average background concentrations at both sites, the 11-12 ng/m^3 of detected levoglucosan is significant, indicating that wildfire smoke was affecting the area during the period of the June 26 ozone exceedance.

Table 3-9. Levoglucosan concentrations at monitoring sites around Clark County, Nevada, during the June 26 ozone event. The average levoglucosan concentration, its standard deviation, and propagated uncertainty from background days in 2018 and 2019 for both sites are also provided for comparison. Positive or negative detection is also shown.

Sample Date	Sampling Site	Levoglucosan (ng/m^3)	Levoglucosan Uncertainty (ng/m^3)	Levoglucosan Detected?
Background days (2018-2019)	Jerome Mack	2±3	1	N/A
6/26/2020	Jerome Mack	11	1	Positive

The supporting pollutant trends and diurnal patterns, which show CO, $PM_{2.5}$ and ozone concentrations outside of their normal seasonal or yearly historical averages, provide additional proof of smoke impacts on the Clark County area during June 26, 2020. Further, levoglucosan measurements confirm that the smoke was present in Clark County during the event period. Wildfires can generate the precursors needed to create ozone, NO_x, and VOCs. While ozone concentrations can be suppressed very near a fire due to NO_x titration, downwind areas are likely to see an increase in ozone concentrations due to the presence of both precursor gases and sufficient UV radiation (i.e., when an air mass leaves an area of very thick smoke that inhibited solar radiation) (Bytnerowicz et al., 2010; Finlayson-Pitts and Pitts Jr, 1997; Jaffe et al., 2008). Ozone precursors from wildfire smoke can also be transported a significant distance downwind, and if these compounds are mixed into an urban area (such as Las Vegas), the ozone concentrations produced can be significantly higher than they would be from either the smoke plume or the urban area alone (Jaffe et al., 2013; Wigder et al., 2013; Lu et al., 2016; Brey and Fischer, 2016). Since we find evidence of smoke impacts on Clark County on June 26 via supporting pollutant measurements of $PM_{2.5}$ and CO

alongside other analyses in Sections 3.1 and 3.2, we suggest that both the direct transport of ozone and the transport of ozone precursor gases likely caused the ozone exceedance.

3.3 Tier 3 Analyses

3.3.1 Total Column & Meteorological Conditions

Supporting pollutants, satellite analyses, and HYSPLIT trajectories shown in Section 3.1-3.2 provide evidence that smoke was transported to Clark County at and before the time of the exceptional event on June 26, 2020. However, the visible true color, AOD, and CO satellite data do not provide information about the vertical distribution of visible or measured smoke components. Additionally, vertical profile measurements like the Cloud-Aerosol Light Detection and Ranging (LIDAR) and Infrared Pathfinder Satellite Observation (CALIPSO) aerosol profiler on board the CloudSat satellite also did not overpass either the Nevada and Utah fires or Clark County during any relevant dates before or after the June 26 EE. Therefore, we have moved the CALIPSO profile that was available on June 26 but too far west to profile Clark County or the fires to **Appendix D**.

The mesoscale and local meteorological conditions from June 23 to June 26 provide evidence for transport of smoke from the Rock Path Fire in Utah and the Twin and Miller fires in Nevada to Clark County, and subsequent vertical mixing of smoke from aloft to the surface. Upper-level wind barbs and geopotential heights at 500 hPa over Nevada indicate the presence of an upper troposphere low pressure system, which is associated with enhanced vertical mixing in the lower troposphere (**Figure 3-25**).

Local observations of mixing heights in the Las Vegas area on June 26 suggest that smoke was likely mixed into the lower levels of the atmosphere. Ceilometer data from the Jerome Mack site indicate mixing heights on June 26 between approximately 1,725 m and 3,250 m for several hours during the day (**Figure 3-26**). Furthermore, a low-pressure system was centered over eastern Utah on June 26. Counterclockwise winds in the lower troposphere associated with the low-pressure system transported smoke from the Rock Path Fire in Utah and the Twin and Miller fires in Nevada to Clark County, Nevada (**Figure 3-27**). Mixing height data from the ceilometer and the surface weather maps provide evidence of enhanced vertical mixing in the lower troposphere when smoke was present over Clark County.

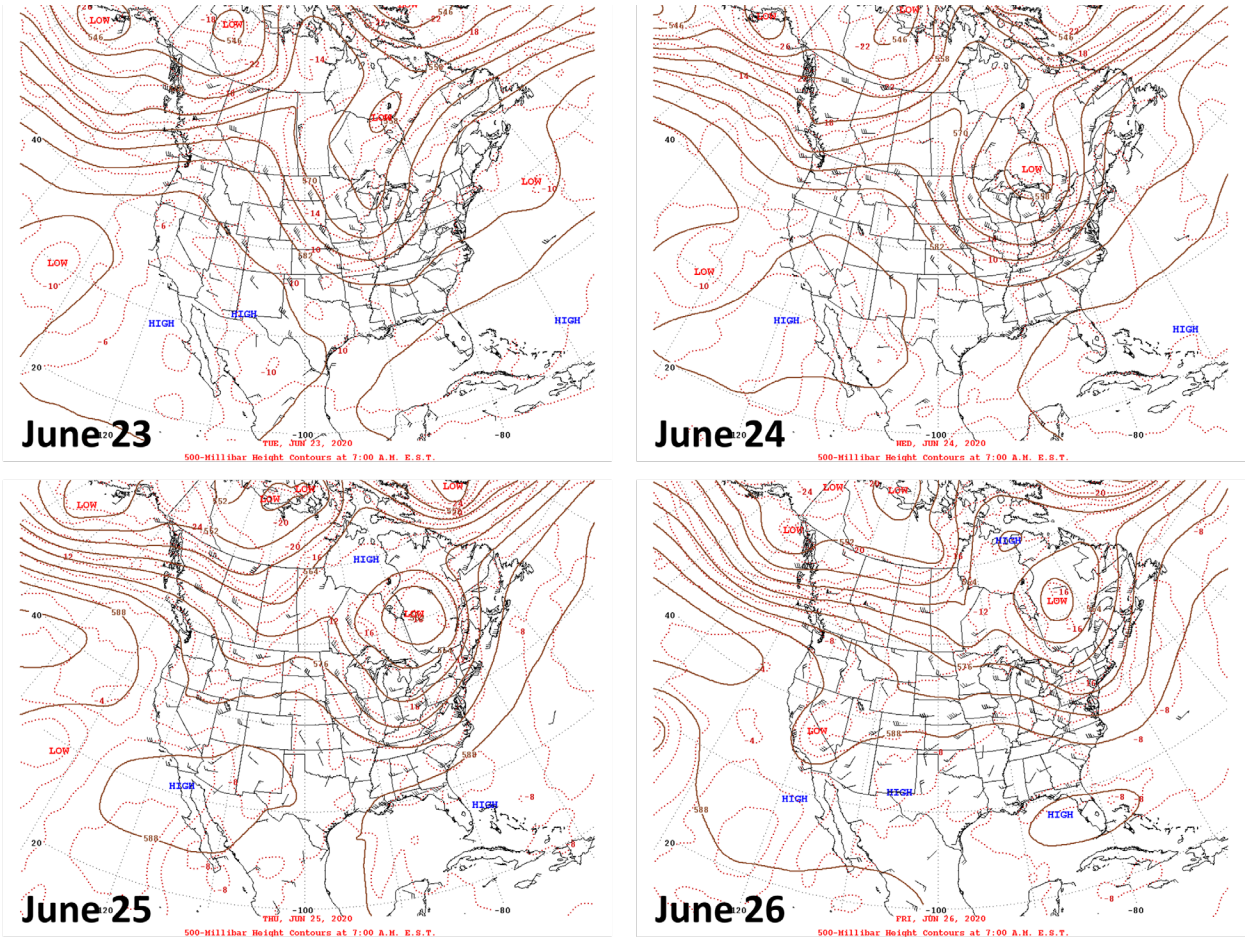

Figure 3-25. Daily upper-level meteorological maps for the three days leading up to the exceptional event and the day of the June 26 exceptional event.

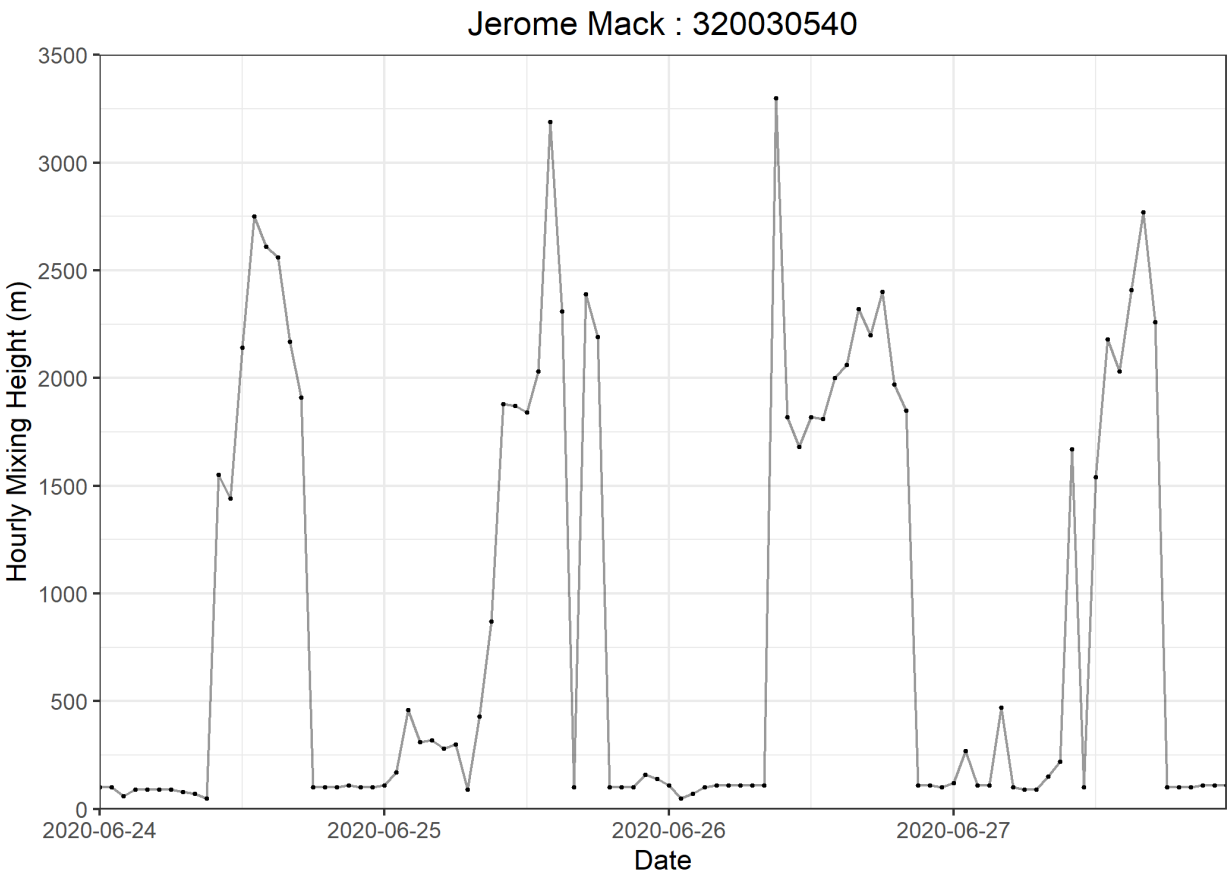

Figure 3-26. Time series of mixing heights taken from Jerome Mack (NCore site) for June 24 through 27, 2020.

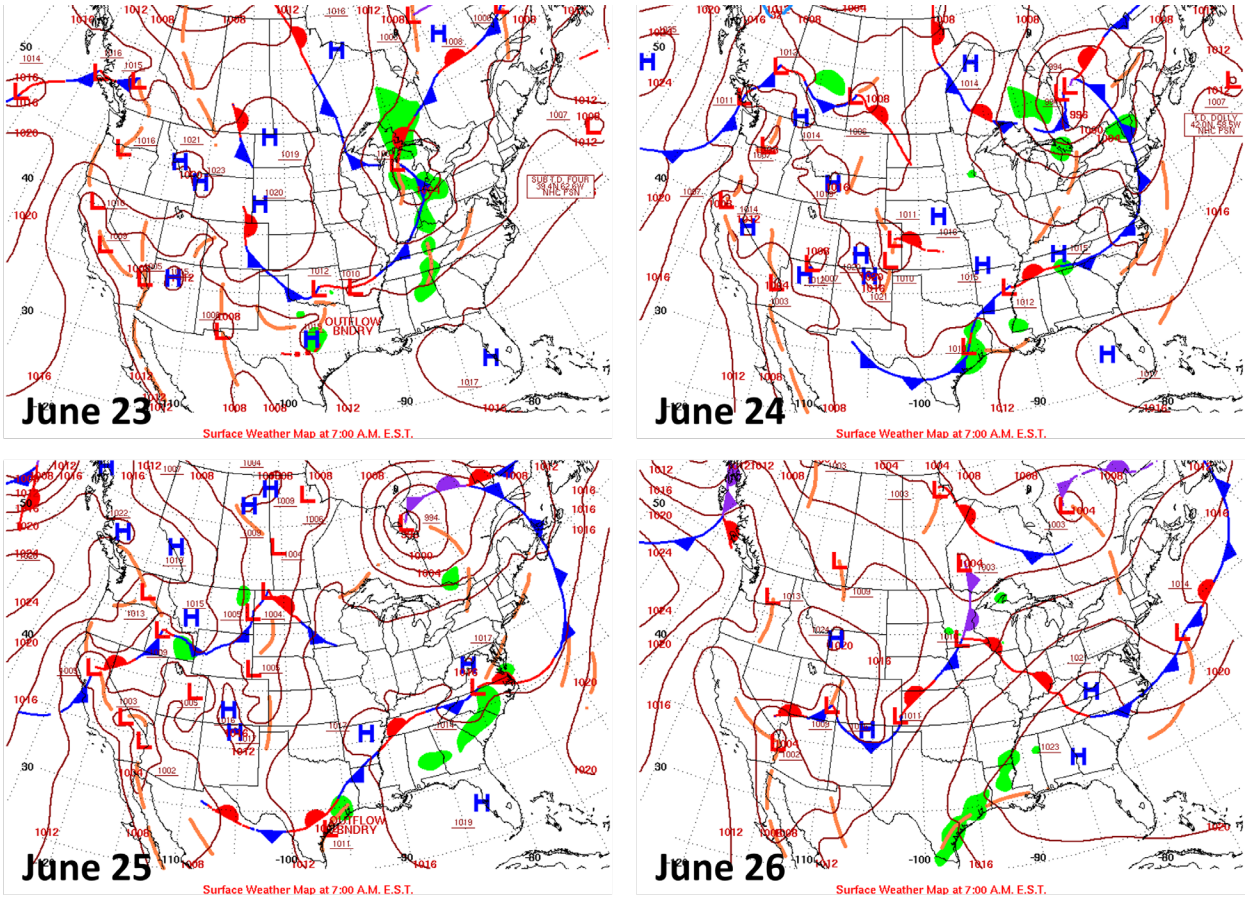

Figure 3-27. Daily surface meteorological maps for the three days leading up to the exceptional event and the day of the June 26 exceptional event.

In addition to the ceilometer-based measurements of mixing heights, vertical temperature profiles (Skew-T diagrams) can be used to estimate mixing heights. The vertical temperature profile at Las Vegas on June 26 at 12:00 UTC shows wind directions in the lower troposphere shifting from a consistently southwesterly direction to a northeasterly direction (Figures 3-28 and 3-29), indicating smoke transport in the lower levels of the atmosphere from the Rock Creek Fire and Twin and Miller fires into Clark County. Enhanced vertical mixing from June 23 and June 26 can be seen from a pronounced, very large mixed layer—as indicated by temperatures decreasing with height roughly along the dry adiabat up to at least 600 hPa—with associated warm temperatures and very dry air. The CALIPSO vertical profile of aerosols over Clark County in the morning of June 26, the upper-level weather map, the ceilometer data, the surface weather map, and the vertical temperature and wind profile suggest the existence of smoke within the mixed layer, the transport of smoke from the Rock Creek Fire and Twin and Miller fires to Clark County, and subsequent mixing in the lower troposphere.

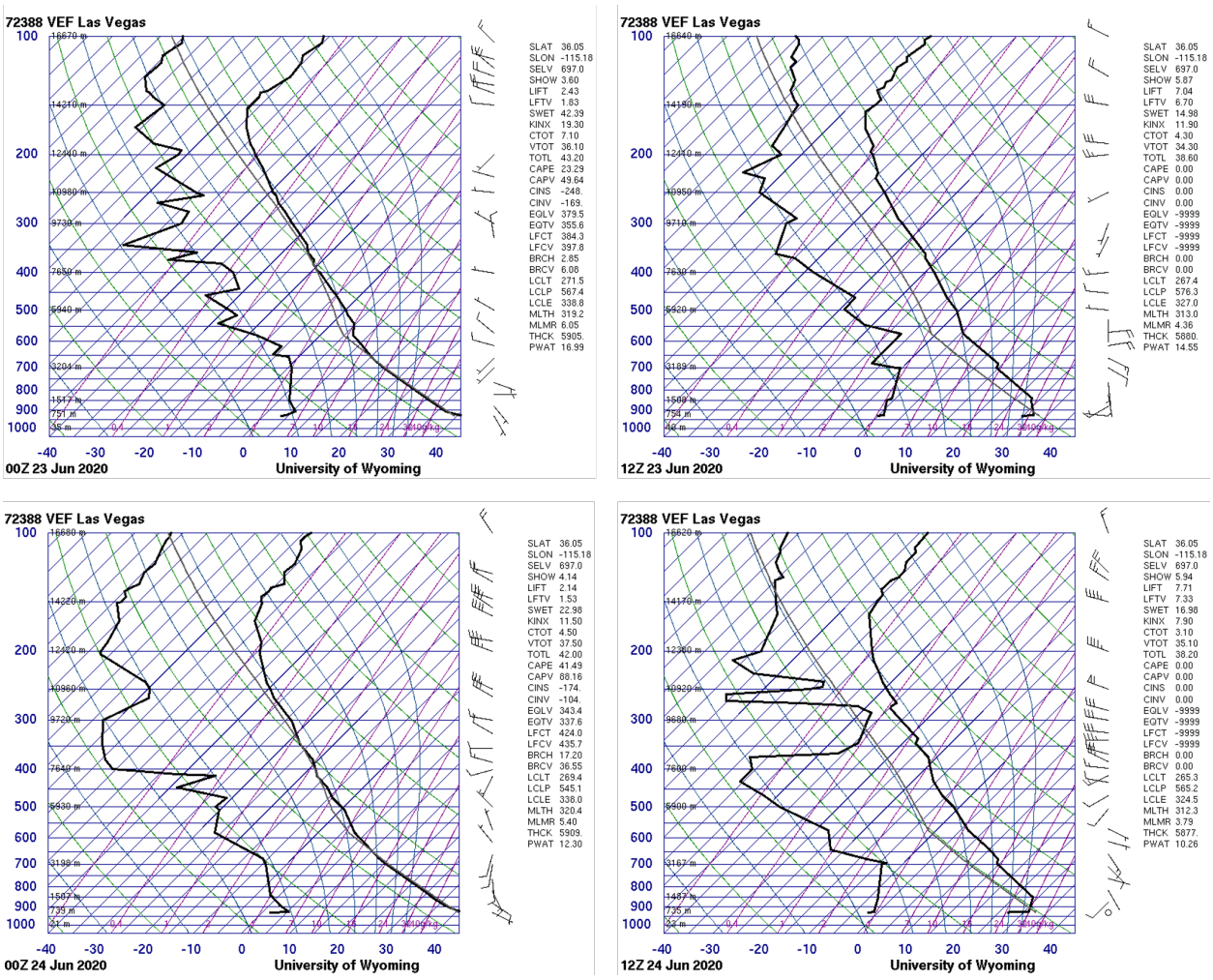

Figure 3-28. Skew-T diagrams from June 23 and 24, 2020, in Las Vegas, Nevada.

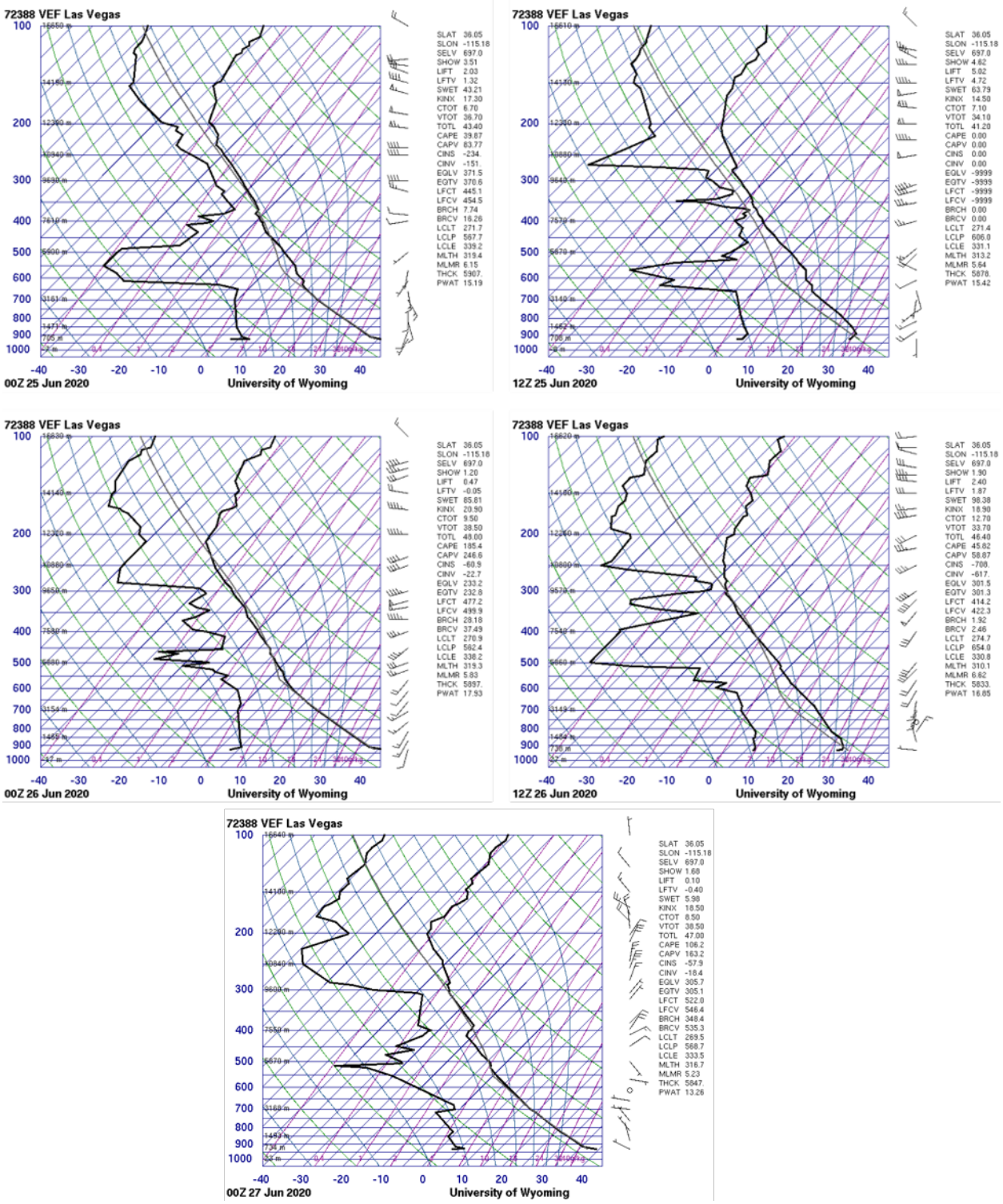

Figure 3-29. Skew-T diagrams from June 25 and 27, 2020, at 00:00 UTC (16:00 PST on June 24 through June 26), in Las Vegas, Nevada.

3.3.2 Matching Day Analysis

Ozone production and transport strongly depend on regional and local meteorological conditions. A comparison of ozone concentrations on suspected exceptional event days with non-event days that have similar meteorology can help further demonstrate that an atypical source impacted ozone in Clark County on the event day. Given that similar meteorological days are likely to have similar ozone concentrations, noticeable differences in levels of ozone between the event date and meteorologically similar days can lend evidence to a clear causal relationship between wildfire smoke and elevated ozone concentration.

Identify Meteorologically Similar Days

In order to identify the best matching meteorological days, both synoptic and local conditions were examined from ozone-season days (April 1 through September 30) between 2014 and 2020. This data set excludes days with suspected exceptional events in the 2018 and 2020 seasons, and all dates within 5 days of the current exceptional event date to ensure that lingering effects of smoke transport or stratospheric intrusion did not appear in the data.

To best represent similar air transport patterns, twice daily HYSPLIT trajectories (initiated at 18:00 and 22:00 UTC) from Clark County for 2014-2020 were clustered by total spatial variance. The calculation, based on the difference between each point along a trajectory, provides seven distinct pathways of airflow into Clark County. The cluster that best represents the trajectory on the exceptional event day was chosen, and ozone-season days within the cluster were then subset for regional meteorological comparison to the exceptional event day.

For the meteorological comparison, a correlation score was assigned to each day from the cluster subset. The National Centers for Environmental Prediction's (NCEP) reanalysis data were compiled for the ozone seasons in 2014-2020. Daily average wind speed, geopotential height, relative humidity, and temperature were considered at 1,000 mb and 500 mb. At the surface, daily average atmospheric pressure, maximum temperature, and minimum temperature were utilized. Pearson product-moment coefficient of linear correlation (pattern correlation) was calculated between the exceptional event date and each cluster-subset ozone-season day in 2014-2020 for each parameter. The pattern correlation calculates the similarity between two mapped variables at corresponding grid locations within the domain. The statistic was calculated using a regional domain of 30 °N – 45 °N latitude and 125°W - 105°W longitude. The correlation score for each day was defined as the average pattern correlation of all parameters at each height level. The correlations scores were then ranked by the highest correlation for 1,000 mb, the surface, and finally 500 mb. Dates within 5 days of the exceptional event were removed from the similar day analysis to ensure the data are mutually exclusive. 50 dates with the highest rank correlation scores were then chosen as candidate matching days for further analysis.

Local meteorological conditions for the subset of candidate matching days were then compared to conditions on June 26, and filtered to identify five or more days that best matched the event date. Meteorological maps at the surface and 500 mb, as well as local meteorological data describing temperature, wind, moisture, instability, mixing layer height, and cloud cover were examined. The data source for each parameter is summarized in Table 3-10.

Table 3-10. Local meteorological parameters and their data sources.

Meteorological Parameter	Data Source
Maximum daily temperature	Jerome Mack - NCore Monitoring Site
Average daily temperature	Jerome Mack - NCore Monitoring Site
Resultant daily wind direction	Jerome Mack - NCore Monitoring Site (calculated vector average)
Resultant daily wind speed	Jerome Mack - NCore Monitoring Site (calculated vector average)
Average daily wind speed	Jerome Mack - NCore Monitoring Site
Average daily relative humidity (RH)	Jerome Mack - NCore Monitoring Site
Precipitation	Jerome Mack - NCore Monitoring Site
Total daily global horizontal irradiance (GHI)	UNLV Measurement and Instrumentation Data Center (MIDC) in partnership with NREL (https://midcdmz.nrel.gov/apps/daily.pl?site=UNLV&start=20060318&yr=2021&mo=4&dy=29)
4:00 p.m. local standard time (LST) mixing layer mixing ratio	Upper air soundings from KVEF (http://weather.uwyo.edu/upperair/sounding.html)
4:00 p.m. LST lifted condensation level (LCL)	Upper air soundings from KVEF (http://weather.uwyo.edu/upperair/sounding.html)
4:00 p.m. LST convective available potential energy (CAPE)	Upper air soundings from KVEF (http://weather.uwyo.edu/upperair/sounding.html)
4:00 p.m. LST 1,000-500 mb thickness	Upper air soundings from KVEF (http://weather.uwyo.edu/upperair/sounding.html)
Daily surface meteorological map	NOAA's Weather Prediction Center Daily Weather Maps (https://www.wpc.ncep.noaa.gov/dailywxmap/index.html)
Daily 500 mb meteorological map	NOAA's Weather Prediction Center Daily Weather Maps (https://www.wpc.ncep.noaa.gov/dailywxmap/index.html)

Matching Day Analysis

The meteorological conditions on June 26, 2020, were not abnormal for Clark County at this time of year. Table 3-11 shows that the percentile ranking of each examined meteorological parameter at the Jerome Mack-NCore site falls within the 10th to 90th percentile range among 7 years of observations

for the period between June 11 and July 11. On June 26, CAPE was at the 76th percentile, but the measurement of 106 is not indicative of strong instability. Additionally, there was no precipitation, which is quite common for Clark County during the summer.

Table 3-12 shows a subset of seven days that best match the meteorological conditions that existed on June 26, 2020, chosen according to the above methodology, as well as the MDA8 ozone concentration on each of these dates at the Paul Meyer site. Surface and upper-level maps for June 26, 2020, and each date listed in Table 3-12 show consistent conditions. All dates show a surface low pressure system over Clark County alongside a surface high to the east. Each upper-level map shows a very low gradient of height contours over the region. Surface and upper-level maps are included in **Appendix E.**

Table 3-12 shows the average MDA8 ozone concentration across these seven days with an expected range defined by one standard deviation, a conservative estimate given the small sample size. The expected MDA8 ozone concentration at the Paul Meyer site given similar meteorological conditions as those on the exceedance date is 60 ppb, well below the 70 ppb ozone standard. Furthermore, the upper end of the provided range, 65 ppb, also falls below the ozone standard. In fact, none of these meteorologically similar days experienced an ozone exceedance at Paul Meyer. If meteorological conditions were the sole cause of the ozone exceedance on June 26, 2020, we would expect to see similarly high ozone levels on each of the similar days listed in Table 3-12, i.e., 60 +/- 5 ppb. Even those similar days with slightly higher temperatures than experienced on June 26 remained below the ozone standard. These observations lend evidence to the existence of an external source of ozone that caused ozone concentrations to rise above the 70 ppb standard on June 26.

These findings show that an atypical source contributed to the ozone exceedance on June 26, 2020. June 26 experienced normal meteorological conditions, with all examined parameters falling between the 10th and 90th percentile. Our analysis expanded on methods shown in the EPA guidance and a previously concurred exceptional event demonstration to identify six days that are meteorologically similar to September 2, 2020 (Arizona Department of Environmental Quality, 2018). No exceedances occurred on any of these seven days at the monitoring site that experienced an ozone exceedance on June 26, 2020. The expected MDA8 ozone concentration at this site is over 10 ppb below the concentration measured on June 26, 2020. Based on this evidence, it is unlikely that meteorology alone enhanced photochemical production of ozone enough to cause an exceedance on June 26, 2020. This validates the existence of an extrinsic ozone source on June 26, 2020.

Table 3-11. Percentile rank of meteorological parameters on June 26, 2020, compared to the 30-day period surrounding June 26 over seven years (June 11 through July 11, 2014-2020).

Date	Max Temp (°F)	Avg Temp (°F)	Resultant Wind Direction (°)	Resultant Wind Speed (mph)	Avg Wind Speed (mph)	Avg RH (%)	Precip (in)	Total GHI (kWh/m^2)	Mixing Layer Mixing Ratio (g/kg)	LCL (mb)	CAPE (J/kg)	500-1000 mb Thickness (m)
2020-06-26	65	64	NA	12	41	61	NA	18	64	63	76	40

Table 3-12. Top five matching meteorological days to June 26, 2020. PM refers to the Paul Meyer monitoring site. Average MDA8 ozone concentration of meteorologically similar days is shown plus-or-minus one standard deviation rounded to the nearest ppb.

Date	Max Temp (°F)	Avg Temp (°F)	Resultant Wind Direction (°)	Resultant Wind Speed (mph)	Avg Wind Speed (mph)	Avg RH (%)	Precip (in)	Total GHI (kWh/m^2)	Mixing Layer Mixing Ratio (g/kg)	LCL (mb)	CAPE (J/kg)	500-1000 mb Thickness (m)	MDA8 Ozone Concentration (ppb)
													PM
2020-06-26	**106**	**95.67**	**278.85**	**1.01**	**4.20**	**12.71**	**0**	**8.02**	**5.23**	**568**	**106**	**5,847**	**73**
2014-07-13	113	100.75	212.67	1.65	4.32	14.79	0	8.36	6.16	558	0	5,930	63
2014-07-30	106	96.04	323.97	3.73	5.01	25.17	0	7.54	7.53	615	29	5,875	60
2014-07-31	109	98.08	280.98	2.67	4.56	19.58	0	7.95	6.7	582	242	5,893	51
2015-06-26	110	100.75	253.48	1.92	3.23	7.62	0	6.63	5.5	542	2	5,932	67
2017-07-30	108	97.5	290.78	1.14	2.37	21.92	0	7.13	9.02	640	495	5,871	62
2017-09-01	108	96	347.8	2.78	3.45	17.46	0	6.78	6.89	597	119	5,870	64
2020-08-25	110	99.38	215.49	1.01	4.20	13.33	0	7.03	7.49	583	193	5,918	59
Average MDA8 Ozone Concentration of Meteorologically Similar Days													**60** ± 5

3.3.3 GAM Statistical Modeling

Generalized additive models (GAM) are a type of statistical model that allows the user to predict a response based on linear and non-linear effects from multiple variables (Wood, 2017). These models tend to provide a more robust prediction than Eulerian photochemical models or simple comparisons of similar events (Simon et al., 2012; Jaffe et al., 2013; U.S. Environmental Protection Agency, 2016). Camalier et al. (2007) successfully used GAM modeling to predict ozone concentrations across the eastern United States using meteorological variables with r^2 values of up to 0.8. Additionally, previous concurred exceptional event demonstrations and associated literature, i.e., Sacramento Metropolitan Air Quality Management District (2011), Alvarado et al. (2015), (Louisiana Department of Environmental Quality, 2018), (Arizona Department of Environmental Quality, 2016), and Pernak et al. (2019) used GAM modeling to predict ozone events that exceed the NAAQS standards, some in EE cases. By comparing the GAM-predicted ozone values to the actual measured ozone concentrations (i.e., residuals), we can determine the effect of outside influences, such as wildfires or stratospheric intrusions, on ozone concentrations each day (Jaffe et al., 2004). High, positive residuals suggest a non-typical source of ozone in the area but cannot specifically identify a source. Gong et al. (2017) and McClure and Jaffe (2018) used GAM modeling, in addition to ground and satellite measurements of wildfire pollutants, to estimate the enhancement of ozone during wildfire smoke events. Similar to other concurred EE demonstrations, we used GAM modeling of meteorological and transport variables to estimate the MDA8 ozone concentrations at multiple sites across Clark County for 2014-2020. To estimate the effect of wildfire smoke on ozone concentrations, we can couple the GAM residual results (observed MDA8 ozone–GAM-predicted MDA8 ozone) with the other analyses to confirm that the non-typical enhancement of ozone is due to wildfires on June 26, 2020.

Using the same GAM methodology as prior concurred EE demonstrations and the studies mentioned above, we examined more than 30 meteorological and transport predictor variables, and through testing, compiled the 16 most important variables to estimate MDA8 ozone each day at eight monitoring sites across Clark County, Nevada (Paul Meyer, Walter Johnson, Joe Neal, Green Valley, Boulder City, Jean, Indian Springs, and Jerome Mack). As suggested by EPA guidance (U.S. Environmental Protection Agency, 2016), we used meteorological variables measured at each station (the previous day's MDA8 ozone, daily min/max temperature, average temperature, temperature range, wind speed, wind direction, or pressure), if available (see Table 2-1). If meteorological variables were not available at a specific site, we supplemented the data with National Centers for Environmental Prediction (NCEP) reanalysis meteorological data to fill any data gaps. We also tested filling data gaps with Jerome Mack meteorological data and found results had no statistical difference. We used sounding data from KVEF (Las Vegas Airport) to provide vertical meteorological components; soundings are released at 00:00 and 12:00 UTC daily. Variables such as temperature, relative humidity, wind speed, and wind direction were averaged over the first 1000 m above the surface to provide near-surface, vertical meteorological parameters. Other sounding variables, such as Convective Available Potential Energy (CAPE), Lifting Condensation Level (LCL) pressure, mixing layer potential temperature, mixed layer mixing ratio, and 500-1,000 hPa thickness provided

additional meteorological information about the vertical column above Clark County. We also initiated HYSPLIT GDAS 1°x1° 24-hour back trajectories from downtown Las Vegas (36.173° N, -115.155° W, 500 m agl) at 18:00 and 22:00 UTC (10:00 a.m. and 2:00 p.m. local standard time) each day to provide information on morning and afternoon transport during critical ozone production hours. We clustered the twice per day back trajectories from 2014-2020 into seven clusters. Figure 3-30 shows the clusters, percentage of trajectories per cluster, and heights of each trajectory cluster. We identified a general source region for each cluster: (1) Northwest U.S., (2) Stagnant Las Vegas, (3) Central California, (4) Long-Range Transport, (5) Northern California, (6) Southern California, and (7) Baja Mexico. Within the GAM we use the cluster value to provide a factor for the distance traveled by each back trajectory. Additionally, day of year (DOY) was used in the GAM to provide information on season and weekly processes. The year (2014, 2015, etc.) was used a factor for the DOY parameter to distinguish interannual variability.

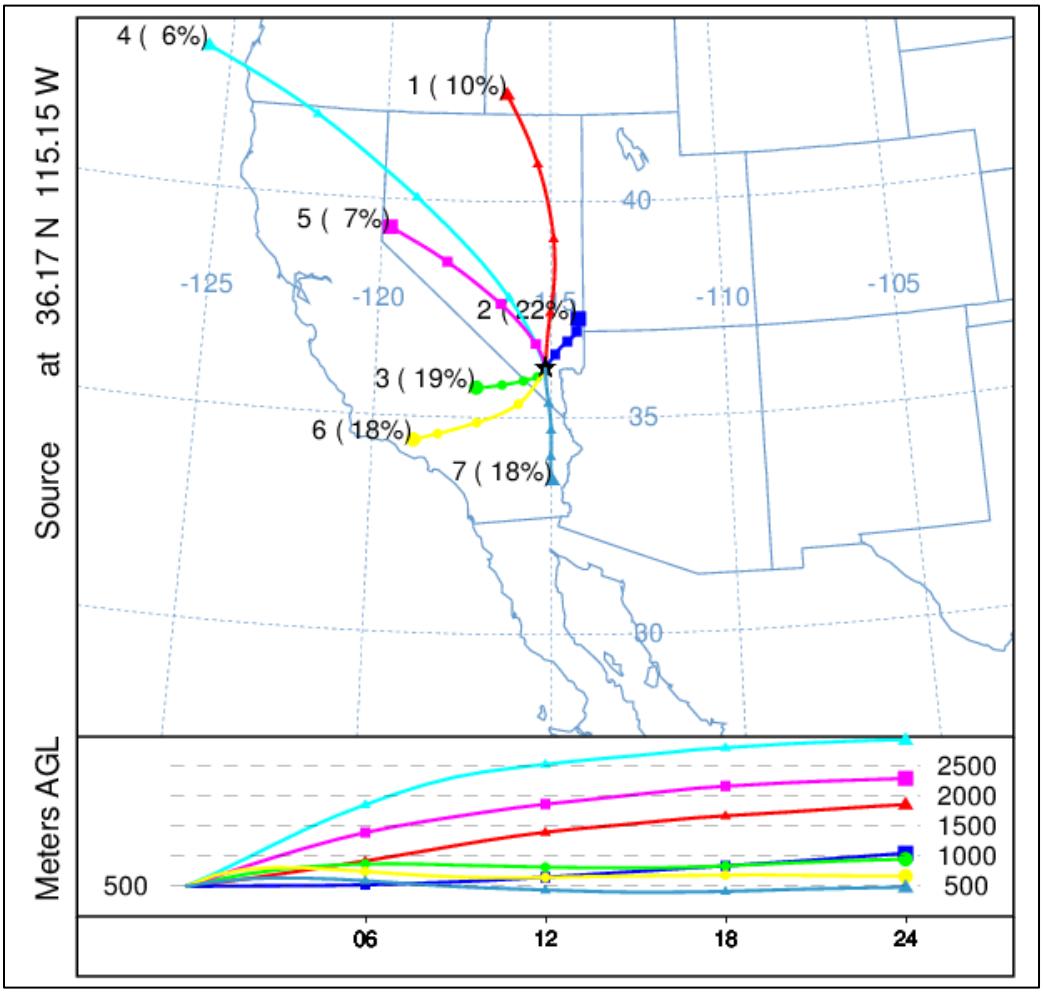

Figure 3-30 Clusters for 2014-2020 back trajectories. Seven unique clusters were identified for the twice daily (18:00 and 22:00 UTC) back-trajectories for 2014-2020 initiated in the middle of the Las Vegas Valley. The percentage of trajectories per cluster is shown next to the cluster number, and the height of each cluster is shown below the map.

Once all the meteorological and transport variables were compiled, we inserted them into the GAM equation to predict MDA8 ozone:

$$g(MDA8\ O_{3,i}) = f_1(V1_i) + f_2(V2_i) + f_3(V3_i) + \cdots + residual_i$$

where f_i are fit functions calculated from penalized cubic regression splines of observations (allowing non-linearity in the fit), Vi are the variables, and i is the daily observation. All variables were given a cubic spline basis except for wind direction, which used a cyclic cubic regression spline basis. For DOY and back trajectory distances, we used year factors (i.e., 2014-2020) and cluster factors (i.e., 1-7) to distinguish interannual variability and source region differences. The factors provide a different smooth function for each category (Wood, 2017).

For example, the GAM smooth of DOY for 2014 can be different than 2015, 2016, etc. In order to optimize the GAM, we first must adjust knots or remove any variables that are over-fitting or under-performing. We used the "mgcv" R package to summarize and check each variable for each monitoring site (Wood, 2020). A single GAM equation (using the same variables) was used for each monitoring site for consistency. During the initial optimization process, we removed the proposed 2018 and 2020 EE days from the dataset. We also ran 10 cross-validation tests by randomly splitting data 80/20 between training/testing for each monitoring site to ensure consistent results. All cross-validation tests showed statistically similar results with no large deviations for different data splits. We used data from each site during the April -September ozone seasons for 2014 through 2020, which is consistent with other papers modeling urban ozone (Solberg et al., 2018; Solberg et al., 2019; e.g., Pernak et al., 2019; McClure and Jaffe, 2018) and ozone concentrations during the periods with exceptional events are within the representative range of ozone in the GAM model.

Table 3-13 shows the variables used in the GAM and their F-value. The F-value suggests how important each variable is (higher value = more important) when predicting MDA8 ozone. Any bolded F-values had a statistically significant correlation ($p < 0.05$). R^2, the positive 95th quantile of residuals, and normalized mean square residual values for each monitoring site are listed at the bottom of the table.

Table 3-13. GAM variable results. F-values per parameter used in the GAM model are shown for each site. Units and data source for each parameter in the GAM model are shown on the right of the table. The 95th quantile, R^2, and normalized mean square residual information are shown at the bottom of the table.

Parameters	Paul Meyer	Walter Johnson	Joe Neal	Green Valley	Jerome Mack	Boulder City	Jean	Indian Springs	Unit	Source
Day of Year (DOY) factored by Year (2014-2020)	**8.11**	**7.09**	**7.65**	**11.8**	**7.94**	**7.11**	**8.68**	**7.53**	--	--
Previous Day MDA8 Ozone	**37.9**	**22.7**	**41.5**	**18.1**	**27.9**	**31.3**	**105.5**	**123.8**	ppb	Monitor Data
Average Daily Temperature	1.92	**2.90**	**4.80**	0.05	1.83	2.13	0.12	1.83	K	Monitor Data/NCEP Reanalysis
Maximum Daily Temperature	1.37	**2.74**	**2.48**	0.16	0.38	0.02	1.30	1.52	K	
Temperature Range (TMax - TMin)	**4.12**	2.13	1.38	1.74	1.77	1.51	0.50	0.54	K	
Average Daily Pressure	**5.54**	**6.42**	**6.74**	**4.64**	**2.94**	0.22	2.17	0.24	hPa	
Average Daily Wind Speed	**11.1**	**5.03**	**7.49**	**5.02**	**15.3**	0.07	0.49	2.19	knots	
Average Daily Wind Direction	0.47	**1.04**	0.24	**1.35**	**2.43**	0.69	0.11	**2.48**	deg	
18 UTC HYSPLIT Distance factored by Cluster	1.70	1.82	1.69	0.92	2.52	2.97	1.66	1.03	km	HYSPLIT Back-Trajectories
22 UTC HYSPLIT Distance factored by Cluster	1.03	0.74	1.47	1.47	1.20	1.26	1.19	0.50	km	
00 UTC Convective Available Potential Energy	3.50	0.13	0.37	1.17	1.16	0.57	**5.71**	**6.49**	J/kg	Sounding Data
00 UTC Lifting Condensation Level Pressure	1.36	**2.78**	2.29	2.41	**3.76**	0.38	1.43	0.38	hPa	
00 UTC Mixing Layer Potential Temperature	0.65	0.79	1.72	0.10	1.23	0.97	1.09	2.53	K	
00 UTC Mixed Layer Mixing Ratio	**2.10**	**2.76**	**2.85**	**3.09**	**3.07**	**2.42**	0.69	1.04	g/kg	
00 UTC 500-1000 hPa Thickness	**2.91**	0.43	1.70	1.60	1.69	**4.11**	**2.18**	1.83	m	
12 UTC 1km Average Relative Humidity	**12.4**	**14.6**	**17.8**	**21.3**	**37.5**	**26.0**	**11.1**	2.18	%	
95th Quantile of Positive Residuals (ppb)	10	10	10	10	9	9	9	10		
R^2	0.55	0.58	0.60	0.58	0.61	0.58	0.57	0.55		
Normalized Mean Square Residual	3.6E-06	7.3E-04	6.1E-05	1.3E-04	3.1E-05	1.3E-04	1.2E-04	1.5E-04		

Table 3-14 provides GAM residual and fit results for all sites for the ozone seasons of 2014 through 2020. Overall, the residuals are low for all data points, and similarly low for all non-EE days. However, the 2018 and 2020 EE day residuals are significantly higher than the non-EE day results, meaning there are large, atypical influences on these days. Figure 3-31 shows non-EE vs EE median residuals with the 95th confidence intervals denoted as notches in the boxplots. We show the data in both ways to provide specific values, as well as illustrate the difference in non-EE vs EE residuals. Since the 95th confidence intervals for median EE residuals are above and do not overlap with those for non-EE residuals at any site in Clark County, we can state that the median residuals are higher and statistically different ($p<0.025$). The R^2 for each site ranged between 0.55 and 0.61, suggesting a good fit for each monitoring site, and similar to the results in prior studies and EE demonstrations mentioned previously (r^2 range of 0.4-0.8). We also provide the positive 95th quantile MDA8 ozone concentration, which is used to estimate a "No Fire" MDA8 ozone value based on the EPA guidance (U.S. Environmental Protection Agency, 2016). We also provide the median residuals (and confidence interval) for all non-EE days with observed MDA8 at or above 60 ppb; this threshold was needed to build a sufficient sample size with a representative distribution, and derive the median and 95% confidence interval. It should be noted that four out of the seven years modeled by the GAM were high wildfire years, and these values likely include a significant amount of wildfire days. We were not able to systematically remove wildfire influence by subsetting the Clark County ozone data based on HMS smoke, HMS smoke and $PM_{2.5}$ concentrations, and low wildfire years. These methods produced a significant number of false positives and negatives, and yielded datasets that were still affected by wildfire smoke. Therefore, these values should be considered an upper estimate of residuals for high ozone days. We see that the median residuals for 2018 and 2020 EE days are significantly higher than those on non-EE high observed ozone days since their confidence intervals do not overlap (or are comparable for the Jerome Mack station). The non-EE day residuals on days where observed MDA8 was at or above 60 ppb were determined to be normally distributed with a slight positive skew (median skewness = 0.39).

Table 3-14. Overall 2014-2020 GAM median residuals and 95% confidence interval range in square brackets for each site modeled. Sample size is shown in parentheses below the residual statistics. For sample sizes of less than ten, we include a range of residuals in square brackets instead of the 95% confidence interval. Residual results are split by non-EE days and the 2018 and 2020 EE days. R^2 for each site is also shown along with the positive 95th quantile result.

Site Name	All Residuals (ppb)	Non-EE Day Residuals (ppb)	2018 & 2020 EE Day Residuals (ppb)	R^2	Positive 95th Quantile (ppb)	Non-EE Day Residuals when MDA8 ≥ 60 ppb (ppb)
Boulder City	0.22 [-0.04, 0.48] (1,132)	0.22 [-0.04, 0.48] (1,130)	12.05 [10.38-13.72] (2)	0.58	9	4.05 [3.55, 4.55] (200)
Green Valley	0.17 [-0.15, 0.48] (948)	0.10 [-0.21, 0.41] (934)	7.38 [5.40, 9.36] (14)	0.58	10	3.76 [3.28, 4.23] (271)
Indian Springs	0.13 [-0.18, 0.44] (1,014)	0.08 [-0.22, 0.38] (1,010)	12.30 [9.37-17.19] (4)	0.55	10	4.79 [4.26, 5.32] (201)
Jean	0.21 [-0.06, 0.48] (1,149)	0.20 [-0.07, 0.47] (1,146)	12.57 [9.59-13.90] (3)	0.57	9	3.40 [2.94, 3.85] (290)
Jerome Mack	0.09 [-0.19, 0.36] (1,152)	0.05 [-0.22, 0.32] (1,141)	6.83 [4.21, 9.45] (11)	0.61	9	3.83 [3.32, 4.33] (242)
Joe Neal	0.23 [-0.08, 0.54] (1,113)	0.17 [-0.13, 0.47] (1,097)	7.77 [5.79, 9.75] (16)	0.60	10	3.32 [2.92, 3.71] (377)
Paul Meyer	0.21 [-0.08, 0.50] (1,159)	0.10 [-0.19, 0.39] (1,137)	8.11 [6.34, 9.88] (22)	0.55	10	3.58 [3.19, 3.97] (388)
Walter Johnson	0.27 [-0.03, 0.57] (1,163)	0.19 [-0.10, 0.48] (1,141)	7.16 [5.11, 9.21] (22)	0.58	10	3.53 [3.13, 3.93] (379)

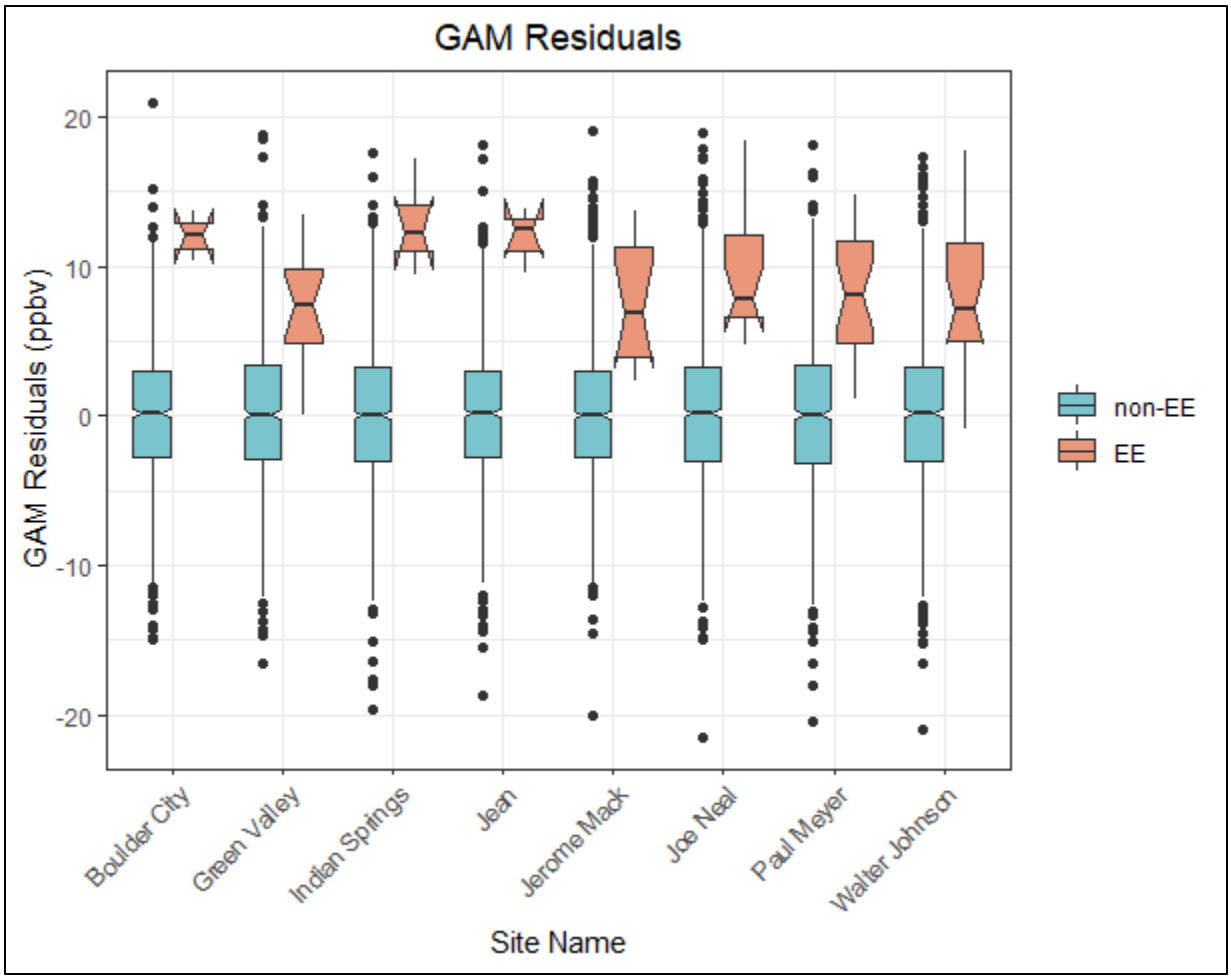

Figure 3-31. Exceptional event vs. non-exceptional event residuals. Non-exceptional events (non-EE in blue) and exceptional events (EE in orange) residuals are shown for each site modeled in Clark County. The notches for each box represent the 95th confidence interval. This figure illustrates the information in Table 3-14.

Overall, the GAM results show low bias and consistently significantly higher residuals on EE days compared with non-EE days. We also evaluated the GAM performance on verified high ozone, non-smoke days by looking at specific case studies. This was done to assess whether high-ozone days, such as the EE days, have a consistent bias that is not evident in the overall or high ozone day GAM performance. Out of the seven years used in the GAM model, four were high wildfire years in California (2015, 2017, 2018, and 2020). Since summer winds in Clark County are typically out of California (44% of trajectories originate in California according to the cluster analysis [not including transport through California in the Baja Mexico cluster]), wildfire smoke is likely to affect a large portion of summer days and influence ozone concentrations in Clark County. We identified specific case studies where most monitoring sites in Clark County had an MDA8 ozone concentration greater than or equal to 60 ppb and had no wildfire influence; "no wildfire influence" was determined by

inspecting HMS smoke plumes and HYSPLIT back trajectories for each day and confirming no smoke was over, near, or transported to Clark County. We found one to two examples from each year used in the GAM modeling, and required that at least half of the case study days needed to include an exceedance of the ozone NAAQS. **Table 3-15** shows the results of these case studies. Most case study days, including NAAQS exceedance days, show positive and negative residuals even when median ozone is greater than or equal to 65 ppb in Clark County, similar to the results for the entire multi-year dataset. GAM residuals on non-EE days when MDA8 is at or above 60 ppb have a median of 3.69 (95% confidence interval: 3.47, 3.88) (see Table 3-14). The high ozone, non-smoke case study days all show median residuals within or below the confidence interval of the high ozone residuals (from Table 3-14), meaning that the GAM model is able to accurately predict high ozone, non-smoke days within a reasonable range of error. Two additional factors indicate the GAM has good performance on normal, high ozone days: (1) the median residuals for the case studies are mostly lower than the 95% confidence interval of high ozone residuals (i.e., includes non-EE wildfire days), and (2) the case study days were verified as non-smoke days. Thus, residuals above the 95th confidence interval of the median residuals, such as those on the EE days, are statistically higher than on days with comparable high ozone concentrations, and not biased high because of the high ozone concentrations on these days.

Table 3-15. GAM high ozone, non-smoke case study results. Median GAM residuals for ten days in 2014-2020 are shown where most monitoring sites had MDA8 ozone concentrations of 60 ppb or greater. Sites used to calculate the MDA8 and GAM residual median/range are listed in the Clark County AQS Site Number column by site number.

Date	Clark County AQS Site Number	Median (Range) of Observed MDA8 Ozone (ppb)	Median (Range) GAM Residual (ppb)
5/17/2014	0601, 0075, 1019, 0540, 0043, 0071	66 (64-71)	1.66 (-0.53-4.28)
6/4/2014	0601, 0075, 0540, 1019, 0043, 0071	69 (66-72)	3.46 (1.70-4.80)
6/3/2015	1019, 0043, 0075, 0540, 7772, 0601, 0071	71 (65-72)	3.01 (-0.34-5.77)
6/20/2015	0601, 0298, 7772, 1019, 0540, 0075, 0043, 0071	65 (63-70)	1.40 (-6.20-5.28)
6/3/2016	0298, 1019, 0075, 0540, 0043, 0071	65 (63-71)	3.89 (1.89-5.26)
7/28/2016	0075, 0071, 0298, 0540, 0043	70 (63-72)	0.24 (-5.95-3.67)
6/17/2017	0601, 0075, 0071, 1019, 0540, 0298, 0043	66 (63-72)	1.85 (-1.94-7.01)
6/4/2018	0601, 0298, 7772, 1019, 0540, 0075, 0043, 0071	65 (60-67)	3.06 (-0.91-3.60)
5/5/2019	0601, 0298, 7772, 1019, 0540, 0075, 0043, 0071	65 (62-67)	1.28 (-2.00-3.42)
5/15/2020	0298, 0043, 0075, 0071	63 (63-65)	1.52 (1.09-3.49)

We also evaluate the bias of GAM residuals versus predicted MDA8 ozone concentrations in Figure 3-32. Residuals (i.e., observed ozone minus GAM-predicted MDA8 ozone) should be independent of the GAM-predicted ozone value, meaning that the difference between the actual ozone concentration on a given day and the GAM output should be due to outside influences and not well described by meteorological or seasonal values (i.e., variables used in the GAM prediction). Therefore, in a well-fit model, positive and negative residuals should be evenly distributed across all

GAM-predicted ozone concentrations and on average zero. In Figure 3-32, we see daily GAM residuals at all eight monitoring sites in Clark County from 2014-2020, the residuals are evenly distributed across all GAM-predicted ozone concentrations, with no pattern or bias at high or low MDA8 fit concentrations. This evaluation of bias in the model is consistent with established literature and other EE demonstrations (Gong et al., 2018; McVey et al., 2018; Texas Commission on Environmental Quality, 2021; Pernak et al., 2019), and indicate a well fit model. In **Figure 3-33**, we also provide a histogram of the residuals at each monitoring site modeled in Clark County. This analysis shows that residuals at each site are distributed normally around a median near zero, and none of the distributions shows significant tails at high or low residuals (median skew = 0.05 with 95% confidence interval [-0.03, 0.12]). This analysis of error in the model and our results are consistent with previously concurred EE demonstrations (Arizona Department of Environmental Quality, 2016) and previous literature (Jaffe et al., 2013; Alvarado et al., 2015; Gong et al., 2017; McClure and Jaffe, 2018; Pernak et al., 2019). **Appendix F** provides GAM residual analysis from the concurred ADEQ and submitted TCEQ demonstrations that compare well with our GAM residual results. Based on these analysis methods, bias in the model is low throughout the range of MDA8 prediction values and confirms that the GAM can be used to predict MDA8 ozone concentrations in Clark County.

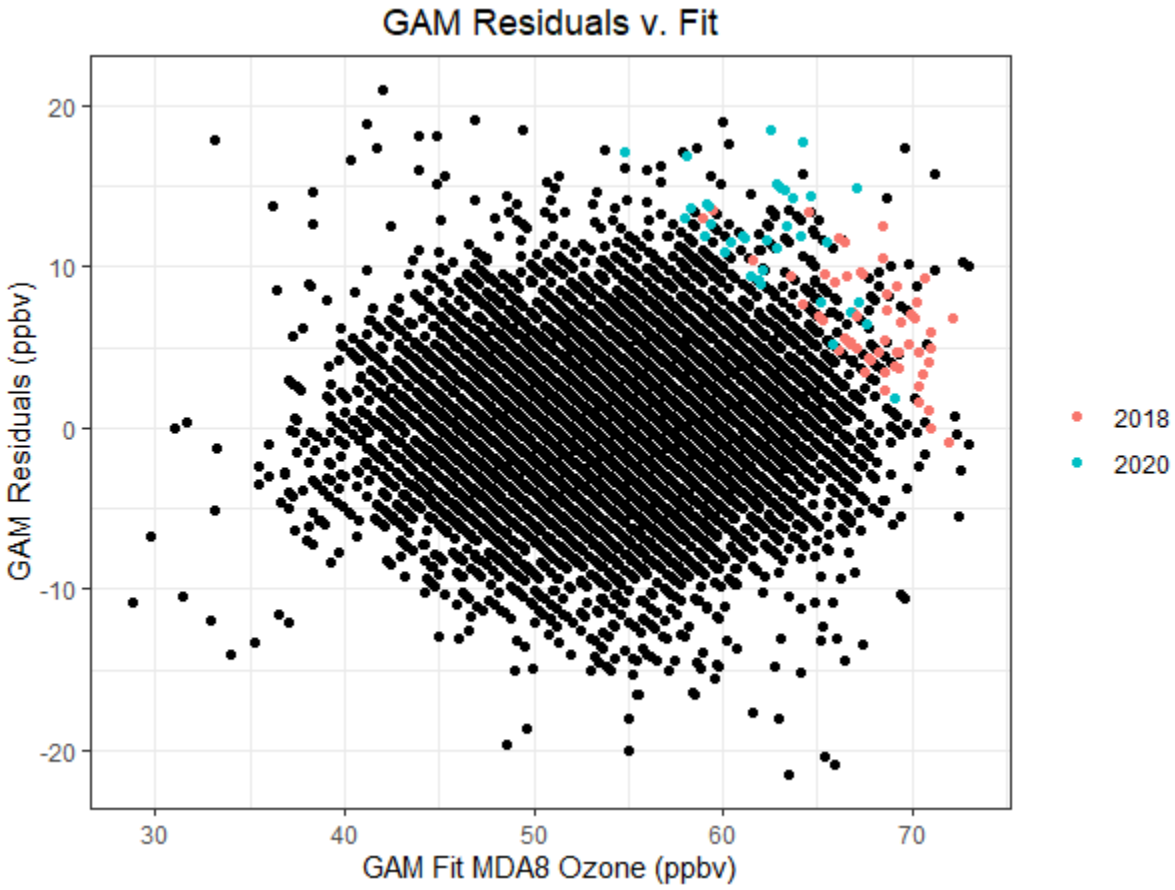

Figure 3-32. Daily GAM residuals for 2014-2020 vs GAM Fit (Predicted) MDA8 Ozone values. 2018 and 2020 exceptional events residuals are shown in red and blue.

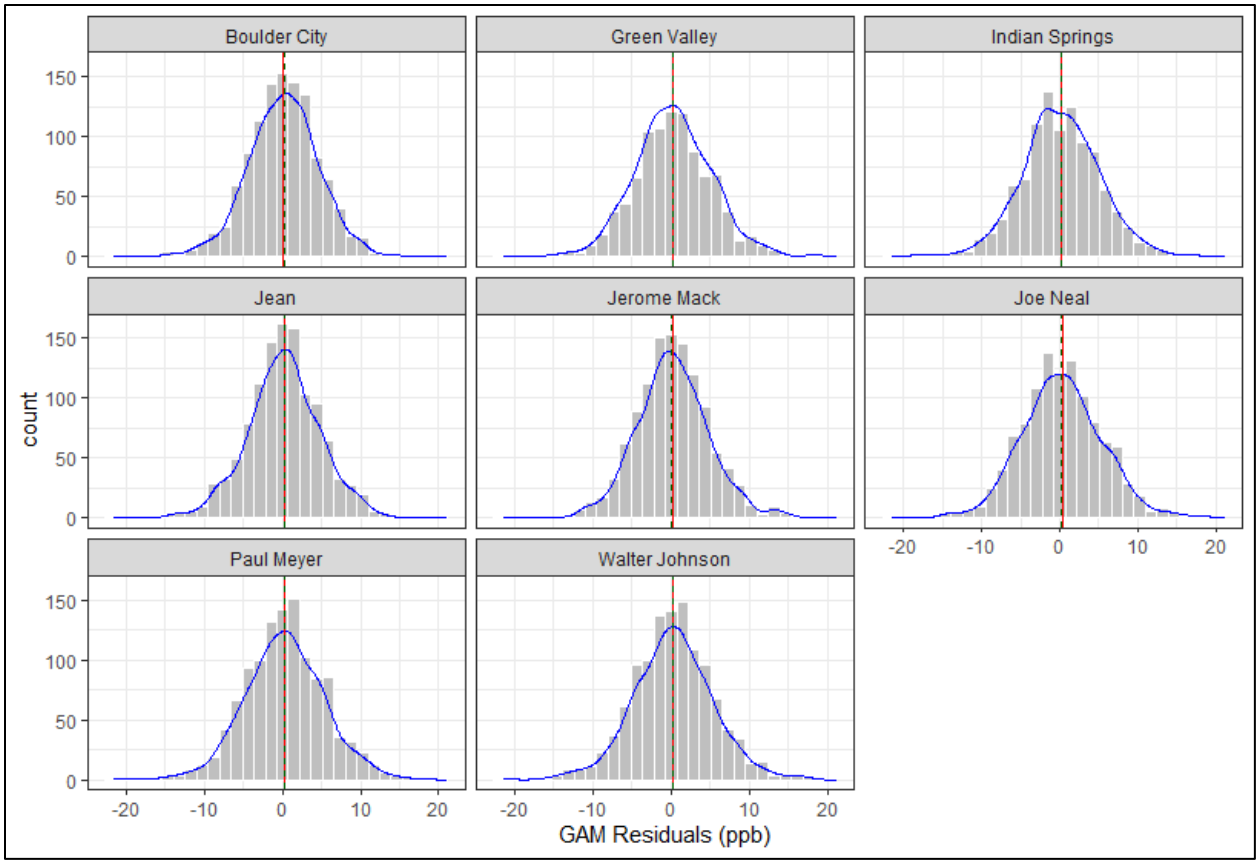

Figure 3-33. Histogram of GAM residuals at all modeled Clark County monitoring sites. The red line indicates the mean and the green dashed line indicates the median. The blue line provides the density distribution.

Within the GAM model, we include HYSPLIT 24-hour distance values, which are factored by cluster, to provide source region and stagnation information into the algorithm. A major upwind pollution source for Las Vegas is the Los Angeles Basin (see the Southern California cluster), which is around 400 km away. Since the GAM model uses source region and distance traveled information to help predict daily MDA8 ozone concentrations, contributions from LA should be accounted for in the algorithm. Based on this, we can assess whether GAM residuals on LA-source region days were significantly different from other source regions. In Figures 3-34 and 3-35, we subset the GAM results by removing any potential EE days. From these results, we find that both morning (18:00 UTC) and afternoon (22:00 UTC) trajectory data have similar distributions for all clusters. The notches in the box plots (representing the 95th confidence interval) provide an estimate of statistical difference and show that the median of residuals is near zero for all clusters. The Northwest U.S. cluster at 18:00 UTC shows slightly negative residuals, while the Long-Range Transport cluster shows slightly positive residuals for both 18:00 and 22:00 UTC. The Southern California cluster shows a median residual of around zero for both 18:00 and 22:00 UTC trajectories, with significant overlap between the 95th confidence intervals of most other clusters (not statistically different). Additionally, the number of data points per cluster (bottom of each figure) corresponds well with transport from California being

dominant for the April through September time frame. Overall, this analysis provides evidence that even when the Los Angeles Basin (Southern California cluster) is upwind of Las Vegas, the GAM model performs well (low median residuals), and the results are statistically similar to most of the other clusters. This implies that when residuals are large, the Los Angeles Basin's influence is unlikely to be the only contributor to enhancements in MDA8 ozone.

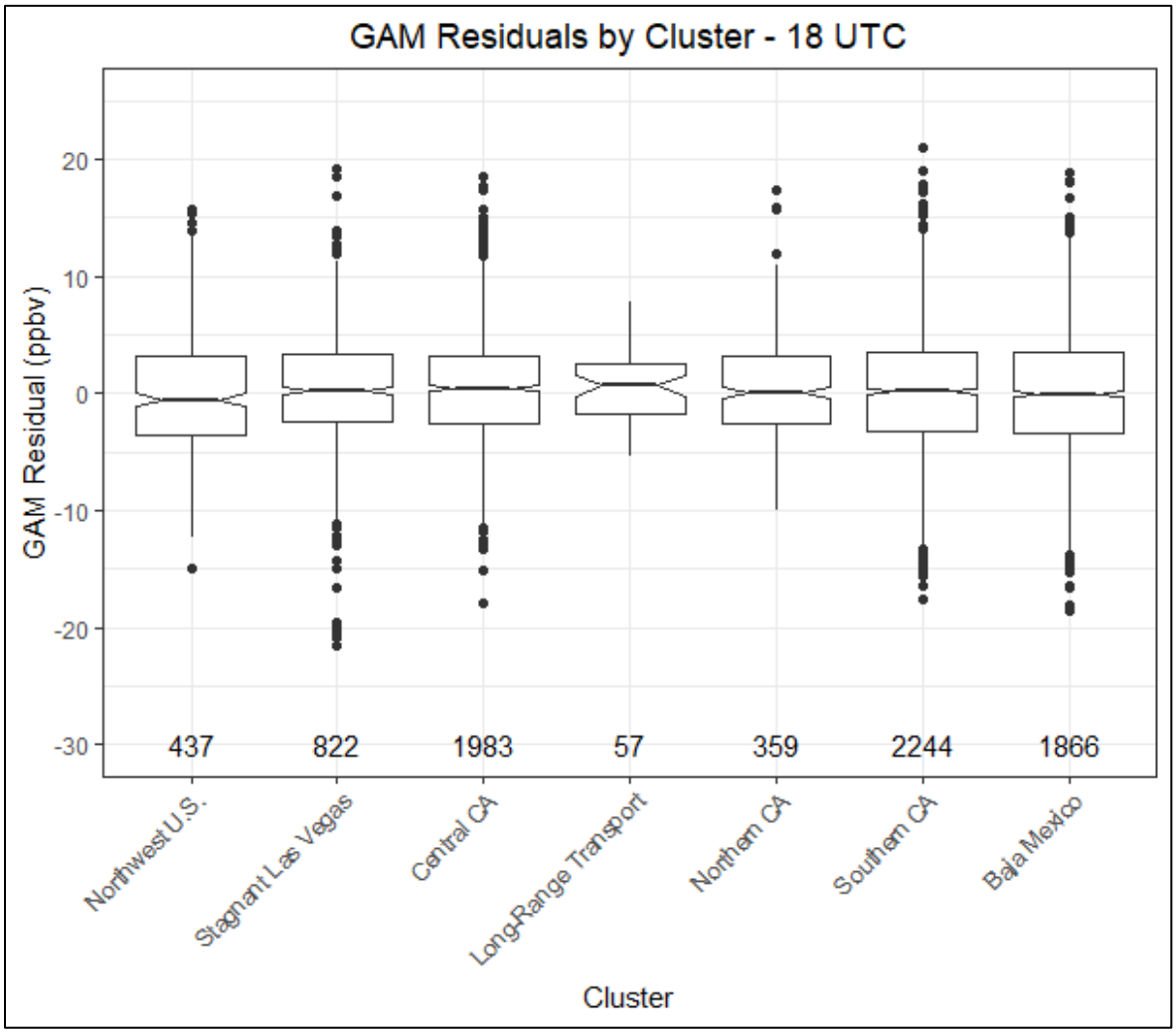

Figure 3-34. GAM cluster residual results for 18:00 UTC. The cluster is determined by grouping 24-hour back trajectories from Las Vegas based on their path. Clusters were created by using back trajectory results from Clark County between 2014 and 2020 (EE days were removed).

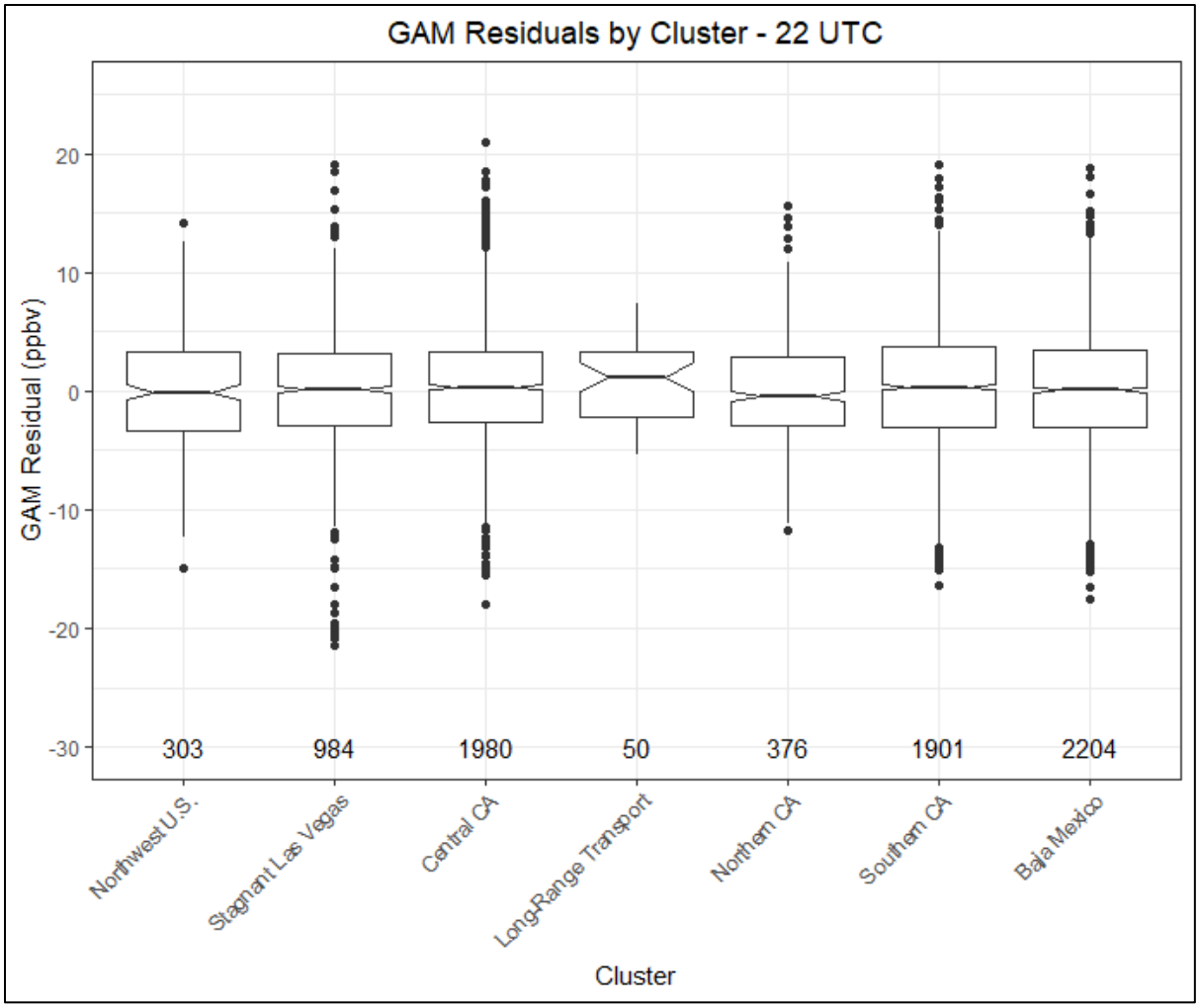

Figure 3-35. GAM cluster residual results for 22:00 UTC. The cluster is determined by grouping 24-hour back trajectories from Las Vegas based on their path. Clusters were created by using back trajectory results from Clark County between 2014 and 2020 (EE days were removed).

Mobile emissions sources decreased throughout the U.S. after COVID restrictions went into place in March 2020. Based on emission inventories from Las Vegas, on-road emissions make up a significant portion of the NO_x emissions inventory (see Section 2.3 for more details). Based on traffic data from the Nevada Department of Transportation, on-road traffic in Clark County in 2020 was significantly different than 2019 through early to mid-June (depending on the area where traffic volume was measured; see Appendix G for more details). Figure 3-36 provides a scatter plot of MDA8 ozone observed versus GAM fit for all eight monitoring sites, separated by year. The linear regression fit, slope, and intercept do not show large difference between 2020 and other modeled years. Figure 3-37 provides a more in-depth look at the most heavily affected months due to COVID restrictions and traffic changes (April–May 2020). The 95th confidence interval (shown as a notch in the box plots) show overlap between 2020 and most other years (except 2015 and 2016). The May 6, 9, and 28 EE days are included in the 2020 box. This analysis shows that there was not a statistically

different GAM response in 2020 compared with other years; this is confirmed in the COVID analysis section (Appendix G) where we show that MDA8 ozone during April–May 2020 in Las Vegas was not statistically different from previous years. While the reduction in traffic emissions due to COVID restrictions likely did not significantly affect the June 26 event, we thought it was important to address the effects of COVID restrictions on the 2020 GAM results. Overall, ozone in Clark County did not change significantly and, similarly, GAM results were not significantly affected.

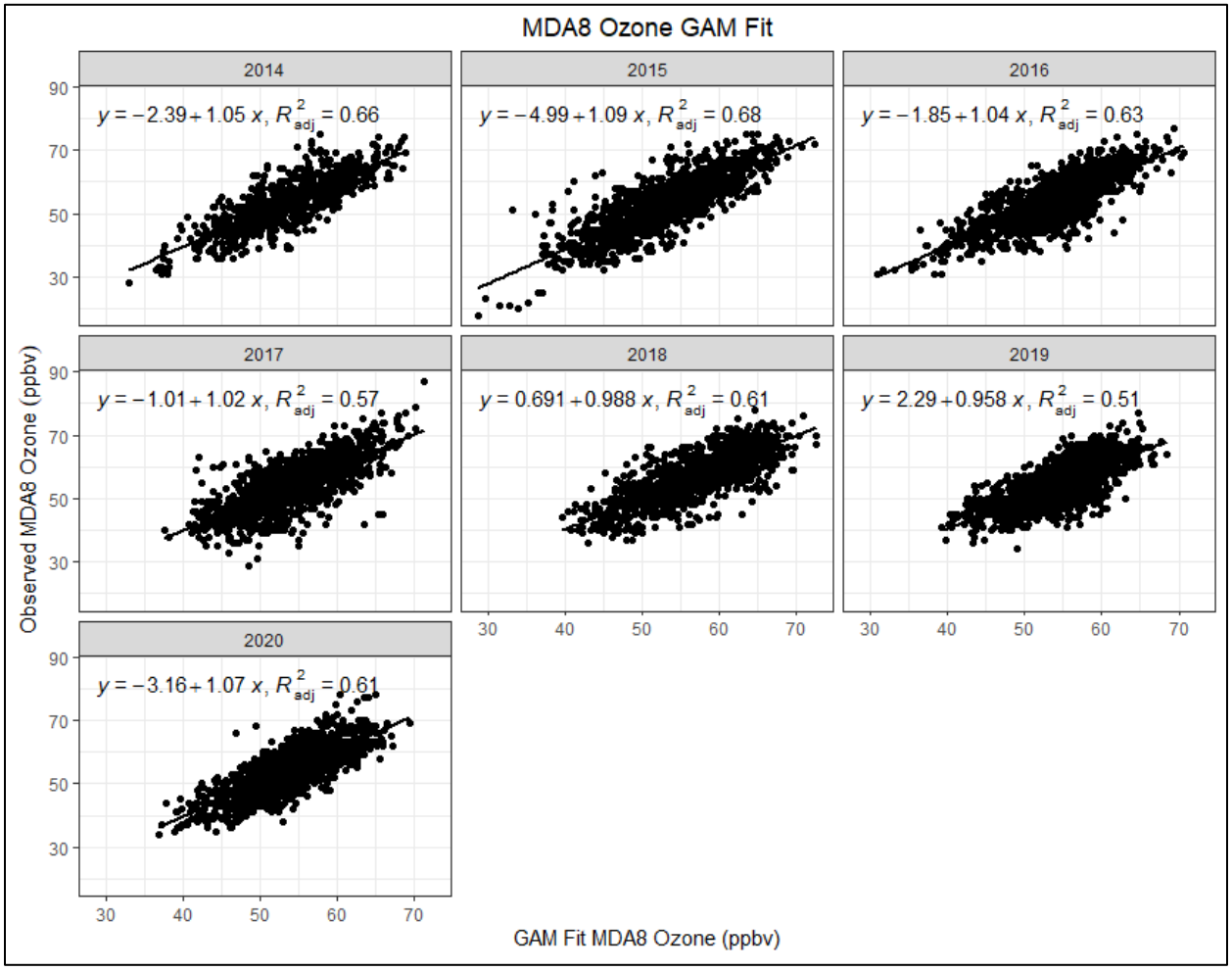

Figure 3-36. Observed MDA8 ozone vs. GAM fit ozone by year. The relationship between observed MDA8 ozone and GAM fit ozone at all eight modeled monitoring sites in Clark County is broken out by year, with linear regression and fit statistics shown (slope, intercept, and r^2). EE days are not included in the regression equations.

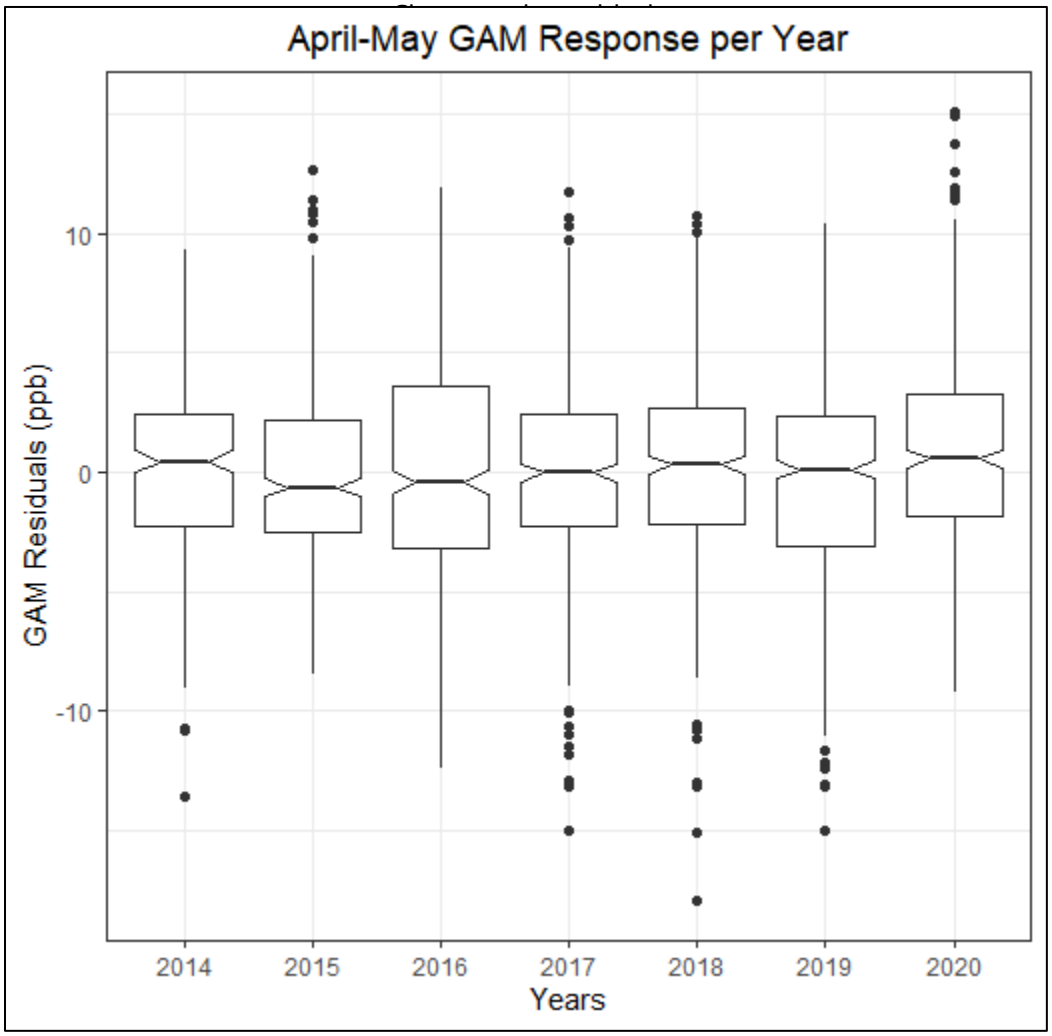

Figure 3-37. April–May Interannual GAM Response. April–May residuals per year from 2014-2020 are plotted for all eight modeled monitoring sites in Clark County. The potential EE days of May 6, 9, and 28 are included.

Figure 3-38 provides the observed MDA8 ozone versus GAM Fit MDA8 from 2014 through 2020 for Paul Meyer. We marked the possible 2020 (red), 2018 (blue), and other (purple) EE days to show that observed MDA8 ozone on these days is higher than those predicted by the GAM. The other (purple) points are from 2014-2016 and are suspected wildfire events, as indicated in EPA AQS record. We also highlight the June 26, 2020, EE day as a large red triangle in each figure. Linear regression statistics (slope, intercept, and r^2) are also provided for context. The linear regression shows a slope near unity, and a low intercept value (around 4 ppb) with a good fit r^2 value.

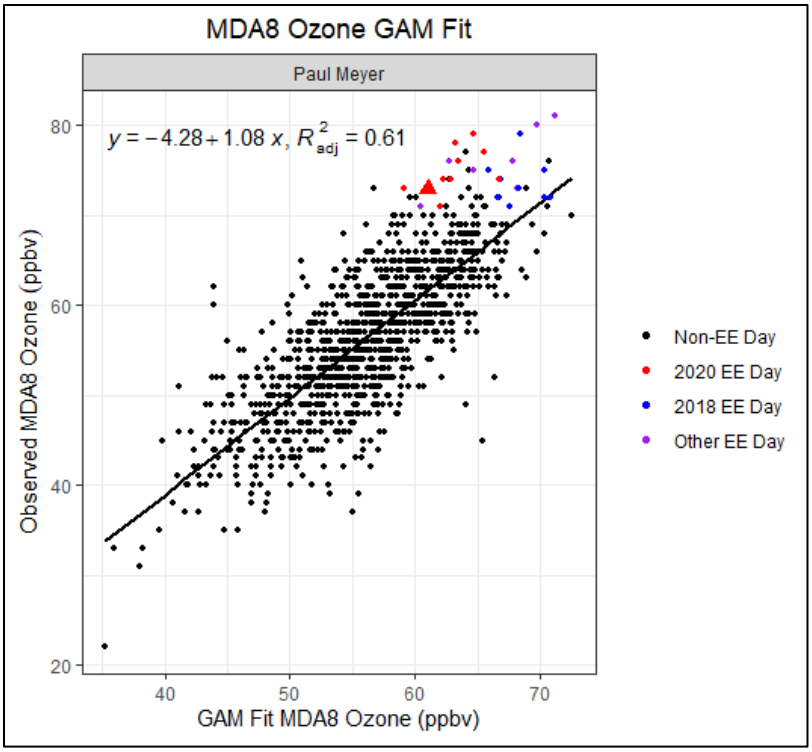

Figure 3-38. GAM MDA8 Fit versus Observed MDA8 ozone at the Paul Meyer site on June 26, 2020. Black circles indicate data not associated with the 2018 or 2020 EE days, red circles indicate 2020 EE days, blue circles indicate 2018 EE days, and purple circles indicate 2014-2016 EE days. June 26 is shown as a red triangle. The black line is the linear regression of the data and statistics (equation and r^2 value) are shown at the top of the figure.

Table 3-16 provides the GAM results for June 26, 2020, at the Paul Meyer monitoring site. GAM residuals show a modeled wildfire impact of 12 ppb, with the MDA8 GAM prediction value well below the 0.070 ppm standard. EPA guidance requires a further level of investigation; by adding the GAM MDA8 Prediction value and the Positive 95th quantile of residuals, we calculated the "No Fire" MDA8 ozone value. The difference between the observed and "No Fire" MDA8 ozone value is a conservative estimate of the influence of wildfire smoke at each site (2 ppb). Due to the large number of wildfires affecting Clark County during the seven-year modeling period, we also calculate the "No Fire" and minimum predicted fire influence given the 75th percentile (7 ppb). This provides a range of minimum smoke enhancement (2 to 7 ppb). The actual enhancement due to wildfire smoke likely lies between the minimum smoke enhancement estimate and the GAM residual. Previous studies and concurred EE demonstrations show and discuss the limitations of the 95th positive percentile evaluation (Miller et al., 2014; Arizona Department of Environmental Quality, 2016). Additionally, production of ozone is an extremely complex process that can only be predicted by meteorological variables in a GAM model with a 50-80% correlation based on previously cited papers (our GAM model shows a 55-61% correlation). In our case, this leaves exceptional events, wildfire influence during high wildfires years, stratospheric intrusions, non-normal emissions, non-normal meteorology, etc., which make up the other 39-45%. Due to the large number of high

wildfires years used in the GAM model, we assert that the minimum predicted fire influence value (as determined by the positive 95th quantile) should not be used as strict guideline for actual fire influence. Based on the values from the GAM model, we see a significant, non-typical enhancement in MDA8 ozone concentrations at the affected Clark County monitoring sites on June 26, 2020.

Table 3-16. June 26 GAM results and residuals for Paul Meyer. The GAM residual is the difference between observed MDA8 ozone and the GAM Prediction. We also estimate the minimum predicted fire influence based on the positive 95th quantile and GAM prediction value.

Site Name	MDA8 O_3 Concentration^{a} (ppm)	MDA8 GAM Prediction^{b} (ppm)	GAM Residual (ppm)	Positive 75th-95th Quantile^{c} (ppm)	"No Fire" MDA8^{b+c} (ppm)	Minimum Predicted Fire Influence$^{a-(b+c)}$ (ppm)
Paul Meyer	0.073	0.061	0.012	0.005-0.010	0.066-0.071	0.002-0.007

Finally, Figure 3-39 shows a two-week time series of observed MDA8 ozone values and the GAM prediction values at the Paul Meyer site. June 26, 2020 (and June 22, 2020, another EE day), shows a large gap between observed MDA8 ozone and the GAM-predicted values. Outside of the possible EE day, the GAM prediction values are close to the observed values, suggesting that immediately before and after the event, we are able to accurately predict typical fluctuations in ozone on non-event days.

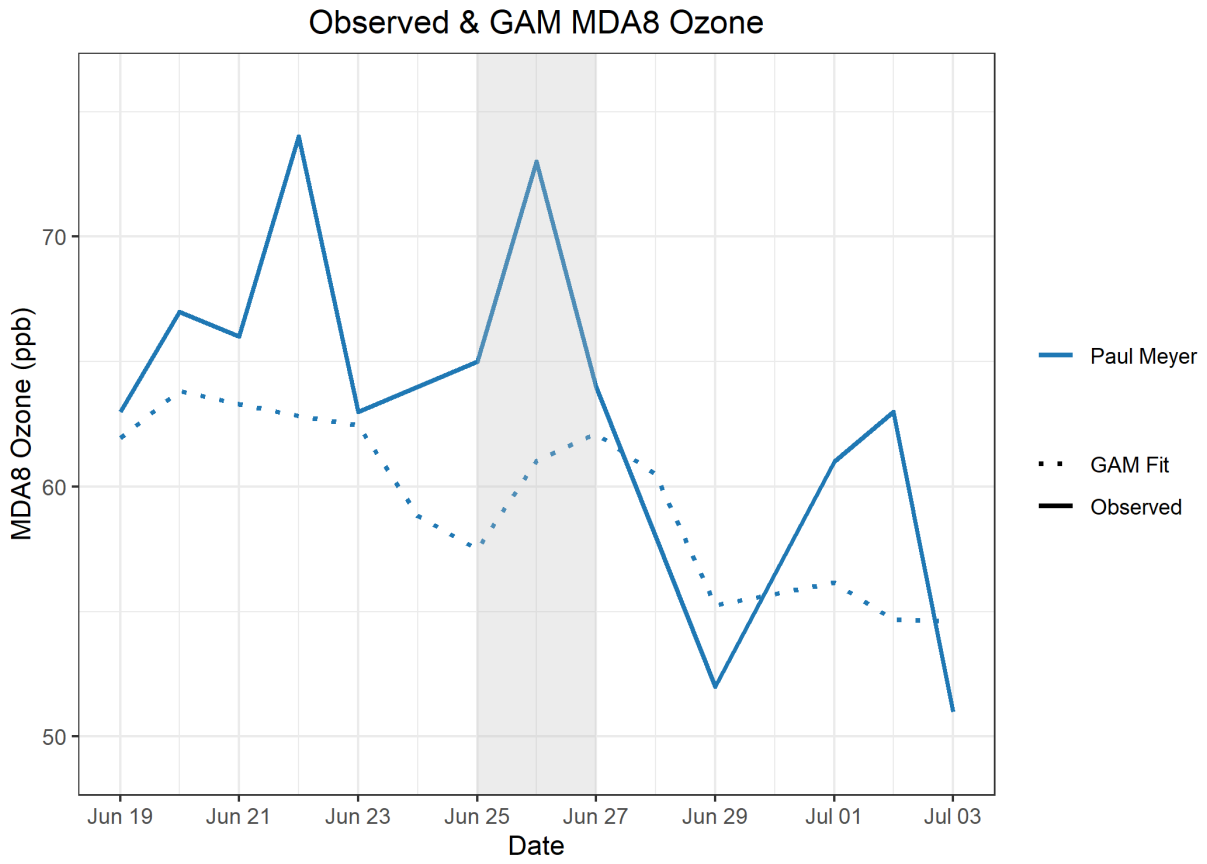

Figure 3-39. GAM time series showing observed MDA8 ozone for two weeks before and after the June 26 EE (solid lines). The GAM MDA8 ozone fit value is also shown for two weeks before and after June 26 (dotted line).

Overall, the GAM evidence clearly demonstrates that a non-typical source of ozone significantly impacted concentrations at the Paul Meyer monitoring site on June 26, 2020. Coupled with wildfire smoke evidence from all other tiers of analyses, we can conclude by weight of evidence that the enhancement in ozone concentrations was due the Miller, Twin, and Rock Path fires in Nevada and Utah that was transported into Clark County.

3.4 Clear Causal Relationship Conclusions

The analyses conducted in this report support the impact of smoke from the Rock Path Fire in Utah and the Twin and Miller fires in Nevada on ozone concentrations in Clark County, Nevada, on June 26, 2020. We find that:

1. Visible satellite imagery, news articles, webcam footage, forward trajectories, and back trajectories support the conclusion of smoke transport from the Rock Path, Twin, and Miller fires to Clark County.
2. A large mixing layer, back trajectories starting near the fire and ending at the surface in Clark County, and surface enhancements of wildfire-related pollutants ($PM_{2.5}$ and levoglucosan) in Clark County support the conclusion that smoke was mixed down to the surface in Clark County.
3. Comparisons with non-event concentrations, meteorologically similar day analyses, and GAM statistical modeling support the conclusion that the ozone concentrations seen in Clark County were well above typical summer concentrations.

The analyses presented in this report fulfill the requirements for a Tier 3 EE demonstration, and all conclusions for each type of analysis are summarized in Table 3-17. The effect of the Rock Path, Twin, and Miller fires on Clark County led to an ozone exceedance at the Paul Meyer monitoring station. Based on the evidence shown that the Rock Path, Twin, and Miller fires we provide a clear causal relationship between these wildfire events and the monitored exceedance on June 26, 2020, in Clark County, Nevada.

Table 3-17. Results for each tier analysis for the June 26 EE.

Tier	Requirements	Finding
1	• Comparison of fire-influenced exceedance with historical concentrations • Key factor: Evidence that fire and monitor meet one of the following criteria: – Seasonality differs from typical season, or – Ozone concentrations are 5-10 ppb higher than non-event related concentrations • Evidence of transport of fire emissions to monitor: – Trajectories of fire emissions (reaching ground level), or – Satellite images and supporting evidence from surface measurements – Media coverage and photographic evidence of smoke	• The June 26, 2020, ozone exceedance occurred during a typical ozone season, but event concentrations were significantly higher than non-event concentrations. • Forward and back trajectories, satellite images, media coverage, and ground images support smoke transport from the Rock Path, Miller, and Twin fires into Clark County.
2	• All Tier 1 requirements • Key Factor #1: Fire emissions and distance of fires • Key Factor #2: Comparison of the event-related ozone concentration with non-event-related high ozone concentrations (high percentile rank over five years/seasons) – Annual and seasonal comparison • Evidence that fire emissions affected the monitor (at least one of the following): – Visibility impacts – Changes in supporting measurements – Satellite enhancements of fire-related species (i.e., NO_x, CO, AOD, etc.) – Fire-related enhancement ratios and/or tracer species – Differences in spatial/temporal patterns	• Q/d values for the Nevada and Utah fires were well below 100. • Ozone concentrations at all sites showed high percentile rank over the past six years and ozone seasons. • Surface concentrations of supporting pollutants ($PM_{2.5}$ and NO_2) show enhanced concentrations and changes in typical diurnal profiles, consistent with smoke. • Satellite measurements also show enhanced levels of fire-related species near the fires. • Levoglucosan, a wildfire smoke tracer, showed a positive detection during this event.
3	• All Tier 2 requirements • Evidence of fire emissions effects on monitor: – Multiple analyses from those listed for Tier 2 • Evidence of fire emissions transport to the monitor: – Trajectory or satellite plume analysis, and – Additional discussion of meteorological conditions • Additional evidence such as: – Comparison to ozone concentrations on matching (meteorologically similar) days – Statistical regression modeling – Photochemical modeling of smoke contributions to ozone concentrations	• Meteorology patterns during this event show transport from the wildfires in Nevada and Utah to Clark County. • Vertical profiles show vertical mixing and transport to the surface. • Meteorologically similar day analysis shows that average MDA8 ozone concentrations across similar days were well below the ozone NAAQS and 10 ppb lower than the June 26 exceedance at Paul Meyer. • GAM statistical modeling predicts ozone concentrations lower than observed, suggesting an impact from non-typical sources on ozone concentrations in Clark County during this event.

4. Natural Event Unlikely to Recur

A wildfire is defined in 40 CFR 50.1(n) as "any fire started by an unplanned ignition caused by lightning; volcanoes; other acts of nature; unauthorized activity; or accidental, human-caused actions, or a prescribed fire that has developed into a wildfire. A wildfire that predominantly occurs on wildland is a natural event" Furthermore, a "wildland" is "an area in which human activity and development are essentially non-existent, except for roads, railroads, power lines, and similar transportation facilities. Structures, if any, are widely scattered." 40 CFR 50.1(o). As shown in Table 3-3, each fire that contributed to this event was cause by either lightning, or accidental, human-caused actions, and therefore meets the definition of wildfire. The fires predominately burned across wildland, as documented in incident reports and maps by either the National Wildfire Coordinating Group (https://utahfireinfo.gov/2020/07/01/rock-path-fires-update-7-1-2020/) or the Utah Wildfire Info website (https://inciweb.nwcg.gov/). Each fire in Table 3-3 is listed as burning across one or more designated wilderness areas, national forests, or tracts of BLM-managed land. Therefore, under 40 CFR §50.1, each wildfire listed in Table 3-3 can be classified as natural event that is unlikely to recur. Accordingly, the Clark County Department of Environment and Sustainability has shown in this submittal that smoke from these fires, which led to an ozone exceedance in Clark County on June 26, 2020, may be considered for treatment as an EE.

5. Not Reasonably Controllable or Preventable

As shown by the documentation provided in Section 3.2.1 of this submittal, each wildfire listed in Table 3-3 burned predominantly on wildland. The Exceptional Events rule stated in 40 CFR 50.1(j) indicate that a wildfire that occurs on wildland is not reasonably controllable or preventable. Previous sections of this report have shown that each fire referenced in this report was a wildfire that occurred on wildland. The Clark County Department of Environment and Sustainability is not aware of any evidence clearly demonstrating that prevention or control efforts beyond those actually made would have been reasonable. The National Wildfire Coordinating Group explicitly notes that the Twin Fire burned across "inaccessible terrain," thwarting firefighting efforts in this region (https://inciweb.nwcg.gov/incident/6808/?fbclid=IwAR0oARiXls2d7TEGdWIyiScABvisJ_6SaNunIIA-rsWMr0dkzms77mFYFTQ). Therefore, emissions from these wildfires were not reasonably controllable or preventable.

6. Public Comment

This exceptional event demonstration will undergo a 30-day public comment period concurrent with EPA's review beginning July 1, 2021. A copy of the public notice, along with any comments received and responses to those comments, will be submitted to EPA after the comment period has closed, consistent with the requirements of 40 CFR 50.14(c)(3)(v). **Appendix H** contains documentation of the public comment process.

7. Conclusions and Recommendations

The analyses conducted in this report support the conclusion that smoke from the Rock Path, Twin, and Miller fires impacted ozone concentrations in Clark County, Nevada, on June 26, 2020. This exceptional event demonstration has provided the following elements required by the EPA guidance for wildfire exceptional events (U.S. Environmental Protection Agency, 2016):

1. A narrative conceptual model that describes the Rock Path Fire in Utah and the Twin and Miller fires in Nevada and describes how the emissions from these wildfires led to ozone exceedances downwind in Clark County (Sections 1 and 2).
2. A clear causal relationship between the Rock Path, Twin, and Miller fires and the June 26 exceedance through ground and satellite-based measurements, trajectories, emission modeling, comparison with non-event concentrations, meteorologically similar day analyses, and statistical modeling (Section 3).
3. Event ozone concentrations at or above the 99th percentile when compared with the last six years of observations at the Paul Meyer site and among the four highest ozone days in 2020 (excluding other 2018 and 2020 EE events – Section 3).
4. The Rock Path and Twin fires were lightning-initiated (the cause of the Miller Fire is unknown, but likely also due to lightning) and grew rapidly on wildland beyond firefighting controls, which classifies this event as unlikely to recur (Section 4).
5. The emissions from the Rock Path, Twin, and Miller fires being transported to Clark County were neither reasonably controllable or preventable (Section 5).
6. This demonstration went through the public comment process via Clark County's Department of Environment and Sustainability (Section 6).

The major conclusions and supporting analyses found in this report are:

1. Visible satellite imagery, webcam footage, news articles, forward trajectories, and back trajectories support the conclusion of smoke transport from the Rock Path, Twin, and Miller fires to Clark County.
2. A large mixing layer, back trajectories starting near the fire and ending at the surface in Clark County, and surface enhancements of wildfire-related pollutants ($PM_{2.5}$ and levoglucosan) in Clark County support the conclusion that smoke was mixed down to the surface in Clark County.
3. Comparisons with meteorologically similar days, meteorologically similar day analyses, and GAM statistical modeling support the conclusion that the ozone concentrations seen in Clark County were well above typical summer concentrations.

The analyses presented in this report fulfill the requirements for a Tier 3 exceptional event demonstration, and conclusions for each type of analysis are summarized in Table 3-17. Emissions from the Rock Path, Twin, and Miller fires on Clark County caused an ozone exceedance at the Paul Meyer monitoring station. Based on the evidence shown that the Rock Path, Twin, and Miller fires were natural events and unlikely to recur, as well as the clear causal relationship between the wildfire events and the monitored exceedance, we conclude that the ozone exceedance event on June 26, 2020, in Clark County was not reasonably controllable or preventable.

8. References

Alvarado M., Lonsdale C., Mountain M., and Hegarty J. (2015) Investigating the impact of meteorology on O_3 and $PM_{2.5}$ trends, background levels, and NAAQS exceedances. Final report prepared for the Texas Commission on Environmental Quality, Austin, TX, by Atmospheric and Environmental Research, Inc., Lexington, MA, August 31.

Arizona Department of Environmental Quality (2016) State of Arizona exceptional event documentation for wildfire-caused ozone exceedances on June 20, 2015 in the Maricopa nonattainment area. Final report, September. Available at https://static.azdeq.gov/pn/1609_ee_report.pdf.

Arizona Department of Environmental Quality (2018) State of Arizona exceptional event documentation for wildfire-caused ozone exceedances on July 7, 2017 in the Maricopa Nonattainment Area. Final report, May. Available at https://static.azdeq.gov/pn/Ozone_2017ExceptionalEvent.pdf.

Bhattarai H., Saikawa E., Wan X., Zhu H., Ram K., Gao S., Kang S., Zhang Q., Zhang Y., Wu G., Wang X., Kawamura K., Fu P., and Cong Z. (2019) Levoglucosan as a tracer of biomass burning: recent progress and perspectives. *Atmospheric Research*, 220, 20-33, doi: 10.1016/j.atmosres.2019.01.004. Available at http://www.sciencedirect.com/science/article/pii/S0169809518311098.

Brey S.J. and Fischer E.V. (2016) Smoke in the city: how often and where does smoke impact summertime ozone in the United States? *Environ. Sci. Technol.*, 50(3), 1288-1294, doi: 10.1021/acs.est.5b05218, 2016/02/02.

Burton S.P., Ferrare R.A., Vaughan M.A., Omar A.H., Rogers R.R., Hostetler C.A., and Hair J.W. (2013) Aerosol classification from airborne HSRL and comparisons with the CALIPSO vertical feature mask. *Atmos. Meas. Tech.*, 6(5), 1397-1412. Available at https://amt.copernicus.org/articles/6/1397/2013/.

Bytnerowicz A., Cayan D., Riggan P., Schilling S., Dawson P., Tyree M., Wolden L., Tissell R., and Preisler H. (2010) Analysis of the effects of combustion emissions and Santa Ana winds on ambient ozone during the October 2007 southern California wildfires. *Atmospheric Environment*, 44, 678-687, doi: 10.1016/j.atmosenv.2009.11.014.

Camalier L., Cox W., and Dolwick P. (2007) The effects of meteorology on ozone in urban areas and their use in assessing ozone trends. *Atmospheric Environment*, 41, 7127-7137, doi: 10.1016/j.atmosenv.2007.04.061.

Clark County Department of Air Quality (2019) Ozone Advance program progress report update. August.

Clark County Department of Environment and Sustainability (2020) Revision to the Nevada state implementation plan for the 2015 Ozone NAAQS: emissions inventory and emissions statement requirements. September. Available at https://files.clarkcountynv.gov/clarknv/Environmental%20Sustainability/SIP%20Related%20Documents/O3/20200901_2015_O3%20EI-ES_SIP_FINAL.pdf?t=1617690564073&t=1617690564073.

Draxler R.R. (1991) The accuracy of rrajectories during ANATEX calculated using dynamic model analyses versus rawinsonde observations. *Journal of Applied Meteorology*, 30, 1446-1467, doi: 10.1175/1520-0450(1991)030<1446:TAOTDA>2.0.CO;2, February 25. Available at https://journals.ametsoc.org/doi/abs/10.1175/1520-0450%281991%29030%3C1446%3ATAOTDA%3E2.0.CO%3B2.

Finlayson-Pitts B.J. and Pitts Jr J.N. (1997) Tropospheric air pollution: Ozone, airborne toxics, polycyclic aromatic hydrocarbons, and particles. *Science*, 276, 1045-1051, (5315).

Gong X., Kaulfus A., Nair U., and Jaffe D.A. (2017) Quantifying O_3 impacts in urban areas due to wildfires using a generalized additive model. *Environ. Sci. Technol.*, 51(22), 13216-13223, doi: 10.1021/acs.est.7b03130.

Gong X., Hong S., and Jaffe D.A. (2018) Ozone in China: spatial distribution and leading meteorological factors controlling O_3 in 16 Chinese cities. *Aerosol and Air Quality Research*, 18(9), 2287-2300. Available at http://dx.doi.org/10.4209/aaqr.2017.10.0368.

Hennigan C.J., Sullivan A.P., Collett J.L., Jr., and Robinson A.L. (2010) Levoglucosan stability in biomass burning particles exposed to hydroxyl radicals. *Geophysical Research Letters*, 37(L09806), doi: 10.1029/2010GL043088. Available at https://www.firescience.gov/projects/09-1-03-1/project/09-1-03-1_hennigan_etal_grl_2010.pdf.

Hoffmann D., Tilgner A., Iinuma Y., and Herrmann H. (2009) Atmospheric stability of levoglucosan: a detailed laboratory and modeling study. *Environ. Sci. Technol.*, 44, 694–699.

Jaffe D., Chand D., Hafner W., Westerling A., and Spracklen D. (2008) Influence of fires on O_3 concentrations in the western U.S. *Environ. Sci. Technol.*, 42(16), 5885-5891, doi: 10.1021/es800084k.

Jaffe D.A., Bertschi I., Jaegle L., Novelli P., Reid J.S., Tanimoto H., Vingarzan R., and Westphal D.L. (2004) Long-range transport of Siberian biomass burning emissions and impact on surface ozone in western North America. *Geophys. Res. Let.*, 31(L16106).

Jaffe D.A., Wigder N., Downey N., Pfister G., Boynard A., and Reid S.B. (2013) Impact of wildfires on ozone exceptional events in the western U.S. *Environ. Sci. Technol.*, 47(19), 11065-11072, doi: 10.1021/es402164f, October 1. Available at http://pubs.acs.org/doi/abs/10.1021/es402164f.

Kim M.H., Omar A.H., Tackett J.L., Vaughan M.A., Winker D.M., Trepte C.R., Hu Y., Liu Z., Poole L.R., Pitts M.C., Kar J., and Magill B.E. (2018) The CALIPSO version 4 automated aerosol classification and lidar ratio selection algorithm. *Atmos. Meas. Tech.*, 11(11), 6107-6135, doi: 10.5194/amt-11-6107-2018. Available at https://amt.copernicus.org/articles/11/6107/2018/.

Kimbrough S., Hays M., Preston B., Vallero D.A., and Hagler G.S.W. (2016) Episodic impacts from California wildfires identified in Las Vegas near-road air quality monitoring. *Environ. Sci. Technol.*, 50(1), 18-24. Available at https://doi.org/10.1021/acs.est.5b05038.

Lai C., Liu Y., Ma J., Ma Q., and He H. (2014) Degradation kinetics of levoglucosan initiated by hydroxyl radical under different environmental conditions. *Atmospheric Environment*, 91, 32-39, doi: 10.1016/j.atmosenv.2014.03.054, 2014/07/01/. Available at http://www.sciencedirect.com/science/article/pii/S1352231014002398.

Langford A.O., Senff C.J., Alvarez R.J., Brioude J., Cooper O.R., Holloway J.S., Lin M.Y., Marchbanks R.D., Pierce R.B., Sandberg S.P., Weickmann A.M., and Williams E.J. (2015) An overview of the 2013 Las Vegas Ozone Study (LVOS): impact of stratospheric intrusions and long-range transport on surface air quality. *Atmospheric Environment*, 109, 305-322, doi: 10.1016/j.atmosenv.2014.08.040, 2015/05/01/. Available at http://www.sciencedirect.com/science/article/pii/S1352231014006426.

Louisiana Department of Environmental Quality (2018) Louisiana exceptional event of September 14, 2017: analysis of atmospheric processes associated with the ozone exceedance and supporting data. Report submitted to the U.S. EPA Region 6, Dallas, TX, March. Available at https://www.epa.gov/sites/production/files/2018-08/documents/ldeq_ee_demonstration_final_w_appendices.pdf.

Lu X., Zhang L., Yue X., Zhang J., Jaffe D., Stohl A., Zhao Y., and Shao J. (2016) Wildfire influences on the variability and trend of summer surface ozone in the mountainous western United States. *Atmospheric Chemistry & Physics*, 16, 14687-14702, doi: 10.5194/acp-16-14687-2016.

McClure C.D. and Jaffe D.A. (2018) Investigation of high ozone events due to wildfire smoke in an urban area. *Atmospheric Environment*, 194, 146-157, doi: 10.1016/j.atmosenv.2018.09.021, 2018/12/01/. Available at http://www.sciencedirect.com/science/article/pii/S1352231018306137.

McVey A., Pernak R., Hegarty J., and Alvarado M. (2018) El Paso ozone and $PM_{2.5}$ background and totals trend analysis. Final report prepared for the Texas Commission on Environmental Quality, Austin, Texas, by Atmospheric and Environmental Research, Inc., Lexington, MA, June. Available at

https://www.tceq.texas.gov/assets/public/implementation/air/am/contracts/reports/da/582188176307-20180629-aer-ElPasoOzonePMBackgroundTotalsTrends.pdf.

Miller D., DeWinter J., and Reid S. (2014) Documentation of data portal and case study to support analysis of fire impacts on ground-level ozone concentrations. Technical memorandum prepared for the U.S. Environmental Protection Agency, Research Triangle Park, NC by Sonoma Technology, Inc., Petaluma, CA, STI-910507-6062, September 5.

National Weather Service Forecast Office (2020) Las Vegas, NV: general climatic summary. Available at https://www.wrh.noaa.gov/vef/lassum.php.

Pernak R., Alvarado M., Lonsdale C., Mountain M., Hegarty J., and Nehrkorn T. (2019) Forecasting surface O_3 in Texas urban areas using random forest and generalized additive models. *Aerosol and Air Quality Research*, 19, 2815-2826, doi: 10.4209/aaqr.2018.12.0464.

Sacramento Metropolitan Air Quality Management District (2011) Exceptional events demonstration for 1-hour ozone exceedances in the Sacramento regional nonattainment area due to 2008 wildfires. Report to the U.S. Environmental Protection Agency, March 30.

Simon H., Baker K.R., and Phillips S. (2012) Compilation and interpretation of photochemical model performance statistics published between 2006 and 2012. *Atmospheric Environment*, 61, 124-139, doi: 10.1016/j.atmosenv.2012.07.012.

Simoneit B.R.T., Schauer J.J., Nolte C.G., Oros D.R., Elias V.O., Fraser M.P., Rogge W.F., and Cass G.R. (1999) Levoglucosan, a tracer for cellulose in biomass burning and atmospheric particles. *Atmospheric Environment*, 33, 173-182.

Simoneit B.R.T. (2002) Biomass burning - a review of organic tracers for smoke from incomplete combustion. *Applied Geochemistry*, 17, 129-162.

Solberg S., Walker S.-E., Schneider P., Guerreiro C., and Colette A. (2018) Discounting the effect of meteorology on trends in surface ozone: development of statistical tools. Technical paper by the European Topic Centre on Air Pollution and Climate Change Mitigation, Bilthoven, the Netherlands, ETC/ACM Technical Paper 2017/15, August. Available at https://www.eionet.europa.eu/etcs/etc-atni/products/etc-atni-reports/etcacm_tp_2017_15_discount_meteo_on_o3_trends.

Solberg S., Walker S.-E., Guerreiro C., and Colette A. (2019) Statistical modelling for long-term trends of pollutants: use of a GAM model for the assessment of measurements of O_3, NO_2 and PM. Report by the European Topic Centre on Air pollution, transport, noise and industrial pollution, Kjeller, Norway, ETC/ATNI 2019/14, December. Available at https://www.eionet.europa.eu/etcs/etc-atni/products/etc-atni-reports/etc-atni-report-14-2019-statistical-modelling-for-long-term-trends-of-pollutants-use-of-a-gam-model-for-the-assessment-of-measurements-of-o3-no2-and-pm-1.

Texas Commission on Environmental Quality (2021) Dallas-Fort Worth area exceptional event demonstration for ozone on August 16, 17, and 21, 2020. April. Available at https://www.tceq.texas.gov/assets/public/airquality/airmod/docs/ozoneExceptionalEvent/2020-DFW-EE-Ozone.pdf.

U.S. Census Bureau (2010) State & County QuickFacts. Available at http://quickfacts.census.gov/qfd/states/.html.

U.S. Environmental Protection Agency (2016) Guidance on the preparation of exceptional events demonstrations for wildfire events that may influence ozone concentrations. Final report, September. Available at www.epa.gov/sites/production/files/2016-09/documents/exceptional_events_guidance_9-16-16_final.pdf.

U.S. Environmental Protection Agency (2020) Green Book: 8-hour ozone (2015) area information. Available at https://www.epa.gov/green-book/green-book-8-hour-ozone-2015-area-information.

Wigder N.L., Jaffe D.A., and Saketa F.A. (2013) Ozone and particulate matter enhancements from regional wildfires observed at Mount Bachelor during 2004–2011. *Atmospheric Environment*, 75, 24-31, doi: 10.1016/j.atmosenv.2013.04.026, August. Available at http://www.sciencedirect.com/science/article/pii/S1352231013002719.

Wood S. (2020) Mixed GAM computation vehicle with automatic smoothness estimation. Available at https://cran.r-project.org/web/packages/mgcv/mgcv.pdf.

Wood S.N. (2017) *Generalized additive models: an introduction with R*, 2nd edition, CRC Press, Boca Raton, FL.

Zhang L., Lin M., Langford A.O., Horowitz L.W., Senff C.J., Klovenski E., Wang Y., Alvarez R.J., II, Petropavlovskikh I., Cullis P., Sterling C.W., Peischl J., Ryerson T.B., Brown S.S., Decker Z.C.J., Kirgis G., and Conley S. (2020) Characterizing sources of high surface ozone events in the southwestern US with intensive field measurements and two global models. *Atmospheric Chemistry & Physics*, 20, 10379-10400, doi: 10.5194/acp-20-10379-2020. Available at https://acp.copernicus.org/articles/20/10379/2020/acp-20-10379-2020.pdf.